TUFTS UNIVERSITY

Modeling of Soft Materials and Structures

by

Touhid Ahamed

A thesis submitted in partial fulfillment of the requirements
for the degree of

Master of Science

in

Civil and Environmental Engineering

ADVISOR: Luis Dorfmann

August 2015

Abstract

The thesis deals with the modeling of soft materials and structures. Attentions is confined to (i) constitutive modeling of time-dependent passive skeletal muscle and (ii) modeling of residually stressed materials. In constitutive modeling, a new three-dimensional constitutive material model is presented to capture time-dependent material responses, i.e. rate-dependence response, stress recovery and relaxation at constant stretch, of passive skeletal muscle in loading–unloading cycle. The proposed model, consists of dissipative components in parallel with elastic component, is capable of modeling rate-dependent and rate-independent response of muscle with no finite range. A robust, strongly objective numerical integration algorithm is used to solve the evolution equations concerning the proposed model. The proposed model can closely match experimental response with specialized material parameters. In modeling of residually stressed materials, numerical framework is presented to incorporate three-dimensional residual stress in stress analysis of soft materials and structures. General formulation, derivation of required tensor quantities for numerical implementation of the method is summarized. Verification and validation is performed by evaluating stress of residually stressed patient specific Abdominal Aortic Aneurysm (AAA) considering material anisotropy.

Dedicated to my parents and my wife

Acknowledgements

It is my immense pleasure to express my sincere gratitude to all without whose support and contribution this thesis would not have been possible.

First, I like to convey deepest appreciation to my thesis advisor and committee chair, Luis Dorfmann, to be my all time motivation and inspiration, and providing me with continued guidance, support and feedback throughout the research. He has made all this work possible and enjoyable with his compassionate and experienced mentorship.

I would like to extent my gratitude to Miles B. Rubin, Barry Trimmer and Robert Peattie for their support and collaborations. I really appreciate contribution and input from them in the study.

I would also like to thank Robert Viesca, James H. Adler and Jeffrey S. Guasto for serving on my thesis committee. I am grateful to the committee members for their time and feedback.

The research was funded by the National Science Foundation[Grant numbers CMMI-1031366, CMMI-1352955, ISO-1050908], Faculty Research Award provided by Tufts University, and partly by MB Rubin's Gerard Swope Chair in Mechanics.

Contents

List of Figures

List of Tables

Chapter 1

Introduction

Soft materials and structures are characterized by its ability to undergo large deformation in response to applied loading. Polymers, gels, soft biological tissues are the most common example of soft materials. Structures or components of structure composed with soft materials, for instances human organs, components of automobile and aerospace, isolation system of infrastructure, prosthetic devices etc., are termed as soft structures. Material and geometric nonlinearity, stability, hysteretic behavior are the most fundamental challenges of modeling soft materials and structures. In this research, we mainly focus our attention to the modeling soft biological tissue and human organ. However, the same approach is appropriate to many of the cases with other soft materials and structures.

Continued development of biomechanics, now, enable us to model and analysis of mechanical response of complex biological system. Which has exciting possible applications in medical treatment of disease, development of artificial organ, future use of biometerials as structural/mechanical components and so on. In mechanical point of view, the biological systems are nothing but an arrangement of different biological tissues, broadly known as biomaterial which is very complex in structure and highly nonlinear in response, in a setup of boundary valued problem. Two major requirements to solve such boundary valued problem, using numerical tool like finite element method, are to have the constitutive model of the material to capture the behaviors of interest and the finite element mesh of the problem geometry.

During the last three decades, a considerable progress has been made in formulating numerical model for different muscle tissues with the discovery of different mechanical responses. The complexity of model has increased substantially, from most simple isotropic model to complex anisotropic model possibly capable of transition from passive to active state, with the understanding of functional mechanism and mechanical

structure of different muscle tissues. Even though, the development still remains mainly within theories and simulations. Moreover, with the ongoing extensive attempts in simulation and testing, our research being on of them, and extended computing capabilities it is now just matter of time biomechanics will find its way to widespread practical applications.

The dissertation is divided into four main chapters. This chapter provides the brief introduction and background of the research. Second and third chapters, presented in form of manuscript in an intention to publish in scientific journal, present constitutive modeling of muscle tissue and numerical modeling of residually stressed materials respectively. Each of these two chapters is complete with corresponding sections presenting main ideal, result, discussion and bibliography. The mathematical notation used in this two chapters are different but throughly described and remain consistent within each chapter. The overall conclusion of the thesis is provided in Chapter four.

Appendices are included for supplementing materials regarding modeling of residually stressed materials. All the sections and subsections, figures, tables are summarized in contents, list of figures, list of tables respectively.

Chapter 2

Time-dependent behavior of passive skeletal muscle

T. Ahamed[1], M.B. Rubin[2], B.A. Trimmer[3], L. Dorfmann[1]

[1]Department of Civil and Environmental Engineering
Tufts University, Medford, MA

[2]Faculty of Mechanical Engineering
Technion−Israel Institute of Technology, Haifa, Israel

[3]Department of Biology
Tufts University, Medford, MA

Abstract

An isotropic three-dimensional nonlinear viscoelastic model is developed to simulate the time-dependent behavior of passive skeletal muscle. The development of the model is stimulated by experimental data that characterize the response during simple uniaxial stress cyclic loading and unloading. Of particular interest is the rate dependent response, the recovery of muscle properties from the preconditioned to the unconditioned state and stress relaxation at constant stretch during loading and unloading. The model considers the material to be a composite of a nonlinear hyperelastic component in parallel with a nonlinear dissipative component. The strain energy and the corresponding stress measures are separated additively into hyperelastic and dissipative parts. In

contrast to standard nonlinear inelastic models, here the dissipative component is modeled using an evolution equation that combines rate-independent and rate-dependent responses smoothly with no finite elastic range. Large deformation evolution equations for the distortional deformations in the elastic and in the dissipative component are presented. A robust, strongly objective numerical integration algorithm is used to model rate-dependent and rate-independent inelastic responses. The constitutive formulation is specialized to simulate the experimental data. The nonlinear viscoelastic model accurately represents the time-dependent passive response of skeletal muscle.

Keywords: passive muscle, finite deformation, rate-dependent response, stress relaxation

2.1 Introduction

Mathematical and numerical modeling of bioactive materials requires the use of constitutive equations, which in their simplest form must account for the passive, active and transitioning states [1–3]. The challenge is to select or develop an appropriate constitutive law and to experimentally determine the values of associated model parameters. In this paper, the biological model, *Manduca sexta*, is used to examine the time-dependent mechanical properties of the ventral interior lateral muscle (VIL) of the third abdominal segment (A3) under passive conditions. Attention is focused on the A3 VIL skeletal muscle since it is one of the largest larval muscles comprising 14 muscle fibers [4]. Time independent data of the passive and active states are given in Dorfmann et al. [4] and the transitioning state is discussed in Paetsch et al. [1]. A general representation of the theory of time-dependent materials is given by, for example, Wineman and Rajagopal [5] and Christensen [6].

Unlike either amorphous or crystalline materials, muscles are complex composites. Each muscle fiber contains aligned actin and myosin filaments within an amorphous matrix material composed of proteins, lipids and polysaccharides. Many studies focus on the active state; however, there is a growing appreciation of the importance of the passive properties of these materials for their roles as brakes and dampers.

An outstanding issue in muscle properties is the mechanism by which passive force changes with the deformation rate and how they recover after unloading [7, 8]. Different molecular mechanisms are responsible for these time-dependent processes. Both actin/myosin cross-bridge breakage and reformation, and the unfolding of gap-filament proteins (e.g., titin) have been proposed as likely mechanisms [9–13]. Intramuscular collagenous structural elements [14] and muscle junctions [15] may also contribute to

properties observed in experimental muscle preparations. At the molecular level, active force production is generated through conformational changes in proteins (specifically myosin heads) and the making and breaking of chemical bonds between aligned proteins. Thus, active shortening is produced by enzymatic processes that consume the chemical energy of phosphate bonds in ATP, a process that even occurs at low levels in inactive muscle and contributes to energy loses. Muscles cannot reverse this metabolic process directly so the muscle must be re-lengthened by external forces. Re-lengthening involves another structural rearrangement of the protein complexes which contribute to the dissipation of mechanical energy during strain cycling. Both the shortening and lengthening appear to have rate dependent and independent components as a result of the hierarchical cascade of molecular and mechanical interactions [16]. The distribution of mechanical stresses by each of the components is complex and poorly understood [17, 18] but the goal of this paper is to develop a model that better accounts for the overall time-dependent properties of passive muscle. These different molecular mechanisms are important because they influence the assumptions and validity of most mechanical models used to describe muscle behavior.

A seminal contribution to characterize viscoelasticity of skeletal muscle is due to Hill [19]. His experimental data showed that the amount of damping depends on the speed of shortening, conversely on the speed of lengthening. They are used by Hill [19] to define a phenomenological approach to describe the muscle-force and force-velocity relationships. Hill's two-component model consists of an undamped, purely elastic element in series with an energy dissipating element. The classic two-component model is arranged parallel to a purely elastic spring element, which provides the time-independent response and is known as the three-element Hill model. Hill's model has been extended to formulate three-dimensional stress-strain formulations, see, for example, Martins et al. [20], Parente et al. [21], Tang et al. [22].

Limited amount of data is available that characterize the viscoelastic properties of skeletal muscles [23, 24]. Meyer et al. [25] characterize stress relaxation of single passive muscle fibers and propose a three-element Hill model to simulate the observed response. The viscoelastic properties of passive skeletal muscle are investigated in Rehorn et al. [26]. Specifically, the change of the passive properties of single muscle fibers as a function of the lengthening velocity is evaluated. The data are then used to develop a uniaxial, quasi-linear viscoelastic model with the relaxation function expressed as a three-term Prony series. The authors attribute the viscoelastic behavior during tensile loading to the passive properties of the protein titan.

Experimental data and finite element modeling of passive rat tibias anterior muscle during compressive loading are given in Bosboom et al. [27]. A one-term Ogden model

combined with a Prony series expansion is used to account for the viscoelastic behavior. More recently, the nonlinear anisotropic properties of passive skeletal muscle have been addressed in Van Loocke et al. [28]. Attention is placed on the unconfined compressive behavior of porcine, bovine and ovine muscle samples. A strain-dependent Young's modulus is included in the model to account for the nonlinear behavior. Experimental characterization and a quasi-linear viscoelastic model of muscle tissue in compression is given in Van Loocke et al. [24]. Specifically, the model by Van Loocke et al. [28] is extended by introducing a relaxation function with the viscoelastic properties being transversely isotropic. The behavior of passive skeletal porcine muscle during cyclic compressive loading at different loading rates is characterized in Van Loocke et al. [29] and a nonlinear viscoelastic model to simulate this behavior is given.

Three-dimensional constitutive formulations of skeletal muscles using nonlinear solid mechanics have recently been developed. A hyperelastic, incompressible and transversely isotropic formulation to model the passive and active responses of the left and right masseter muscles is proposed by Röhrle and Pullan [30]. The model given by Ito et al. [31] accounts for viscoelasticity, material anisotropy, damage and failure due to excessive stretch. It is validated in uniaxial tension and compression by comparing numerical results to experimental data. An energy function comprised of an isochoric neo-Hookean part combined with an additional fiber contribution is used in [32] to characterize the behavior under tensile load. The fiber response is described using Hill's three-element formulation. A finite-strain anisotropic constitutive law to describe the viscoelastic response of abdominal rat muscles in the passive state is proposed by Calvo et al. [33]. A decoupled volumetric-isochoric representation of the energy function, augmented by an inelastic contribution expressed in terms of internal variables, is used to account for the nonlinear viscoelastic response of muscles in the anterior abdominal wall.

In previous work [4, 34], stress-strain relations for loading and unloading of transversely isotropic passive and active muscles were developed using the theory of hyperelasticity. The theory has been modified to account for the hysteretic response of a preconditioned muscle during loading-unloading. Phenomenological relations were included in the model to account for the molecular mechanisms responsible for energy dissipation and rate-dependent material behavior. The pseudo-elastic model in Dorfmann et al. [4, 34] did not account for the viscoelastic stress relaxation during loading and the time dependent recovery at constant elongation from the preconditioned to the unconditioned state.

The objective of this paper is to develop a three-dimensional constitutive model that accounts for the time-dependent behavior of skeletal muscle in the passive state. Hunter et al. [35] model the passive response of cardiac muscle using a hyperelastic orthotropic strain energy function and the incompressibility constraint. In particular, the response

to uniaxial stress in the principal directions of orthotropy is consistent with that of an incompressible isotropic material, but with different responses for each direction. In this paper, attention is limited to uniaxial stress in the muscle fiber direction so it is sufficient to use an isotropic model. Experimental data are used to justify the formulation and to validate the implementation of the numerical integration algorithm. The model considers the material to be a composite of a nonlinear hyperelastic component in parallel with a nonlinear dissipative component (see Figure 2.1). Standard models of viscoelasticity are typically formulated in terms of hereditary integrals of the history of deformation and rate of deformation. In contrast, here the dissipative component is based on the model by Hollenstein et al. [36], which exhibits smooth behavior and can be considered as a generalization of a viscoplastic overstress model [37], a generalized plasticity model [38, 39] and a generalized hyperplastic model [40]. Specifically, the dissipative component used here models combined rate-independent and rate-dependent inelastic responses with no finite elastic range.

An outline of the paper is as follows. Section 2.2 presents experimental data of unstimulated *Manduca* muscle subject to simple uniaxial tension. The data quantify the rate-dependent response, the recovery of muscle properties from the preconditioned state towards the unconditioned state and stress relaxation at constant stretch during loading and unloading. Section 2.3 summarizes the kinematics of finite deformation, the theories of hyperelasticity and rate-dependent and rate-independent inelasticity. Section 2.4 describes a robust, strongly objective numerical integration algorithm. Then, in Section 2.5, the general framework is specialized to soft tissue that experience large distortional deformations and exhibit exponential stiffening when loaded in tension. In Section 2.6 the model developed is formulated to simulate experimental data in simple uniaxial tension and the corresponding numerical results are included in Section 2.7.

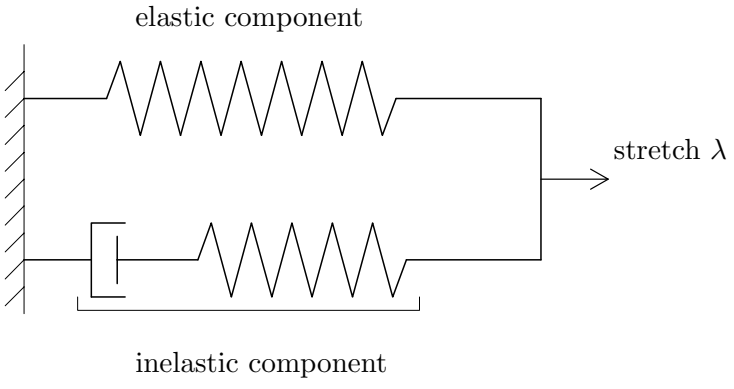

FIGURE 2.1: Schematic representation of the model.

2.2 Experimental results

Experimental data of the rate-dependent response of an unstimulated muscle of *Manduca sexta* for stretch rates of $\dot{\lambda} = 0.0144, 0.072, 0.36$ and $1.8\ \mathrm{s}^{-1}$ are summarized in Dorfmann et al. [34]. The data were used to formulate a pseudo-elastic constitutive model for the mechanical response of the *Manduca* muscle at finite strains. The model accounts for the energy dissipated with each loading-unloading cycle but does not address the effect of recovery time during which a preconditioned muscle returns to the reference configuration upon unloading [34]. In this paper the rate-dependent response of this material is revisited and a systematic evaluation of time-dependent processes is presented.

During each of the tests, the unstimulated muscle was subjected to five cycles of preconditioning with constant strain rate $\dot{\lambda}$ up to a pre-selected extension with stretch $\lambda = 1.24$. The experiments started at the prestressed resting length (denoted by point A in Figure 2.2), and cycles of loading to point B and unloading to point C were performed at different rates of stretch. The resting length of the muscle, equal to the initial distance of the pinned connections at each end of the muscle, was found to be 5.5 mm and used to determine the corresponding prestressed resting stretch $\lambda_\mathrm{r} = 1.05$. Changes in the distance between these connections were measured with an accuracy of $1\,\mu$m. The tensile force was measured using an Aurora 300B-LR lever-arm ergometer with an accuracy of less than 0.3 mN. Finally, following the methods summarized in Dorfmann et al. [34], the reference cross-sectional area was found to be $0.4\ \mathrm{mm}^2$. This information was used to determine the nominal stress as the ratio of the axial force to the reference cross-sectional area. Pre-conditioning was performed in order to monitor the progression of stress softening and to determine the ultimate stress–deformation response for stretches up to $\lambda = 1.24$. Figure 2.2 shows the nominal stress versus stretch λ for the muscle in an unstimulated state with stretch rates of $\dot{\lambda} = 0.0144, 0.072, 0.36$ and $1.8\ \mathrm{s}^{-1}$. The data show dependence on the loading rate, large nonlinear elastic deformations, a hysteretic response during loading-unloading and preconditioning (stress-softening) during the first few cycles of repeated loading. Recovery, during which the stress increased towards the prestressed resting state, was observed when the muscle was left at its resting length for several minutes. The results in Figure 2.2 also show that the reference configuration, corresponding to the resting length of the animal, is not stress-free.

To quantify the recovery of muscle properties from the preconditioned state towards the prestressed resting state, simple uniaxial tension tests were performed on two muscles with a resting length of 4.5 mm and a cross-sectional area of $0.265\ \mathrm{mm}^2$. For each test, a total of three loading-unloading cycles were performed from the prestressed resting stretch $\lambda_\mathrm{r} = 1.05$ to a maximum stretch $\lambda = 1.24$ at a constant strain rate of $\dot{\lambda} = 0.18$

s^{-1}. At the end of each loading-unloading cycle the muscles were held at the resting length for 3 minutes to allow recovery towards the prestressed resting state. The data in Figure 2.3 show that the muscles at resting length are not stress-free and that almost complete recovery occurs during the three minute intervals. Preconditioning occurs, which is noted when the first and second loading paths are compared.

To evaluate stress relaxation, simple uniaxial tension tests were performed on two muscle specimens having a resting length of 4.5 mm and a cross-sectional area of 0.265 mm^2. For each muscle stress-deformation data of a single loading-unloading cycle with constant strain rate $\dot{\lambda} = 0.2\ s^{-1}$ and with maximum elongation $\lambda = 1.26$ were collected. During both the loading and unloading portions of the cycle, interrupted relaxation tests were performed by holding the stretch constant ($\dot{\lambda} = 0$) for 30 seconds at the stretches $\lambda = 1.12$ and $\lambda = 1.19$. The data in Figure 2.4 show that the stress decreases during the relaxation tests from the loading portion of the cycle and that recovery with increasing stress occurs during the relaxation tests from the unloading portion of the cycle. Notice that the values of stress after relaxation from the loading portion of the cycle do not equal the values of stress after recovery from the unloading portion of the cycle for the

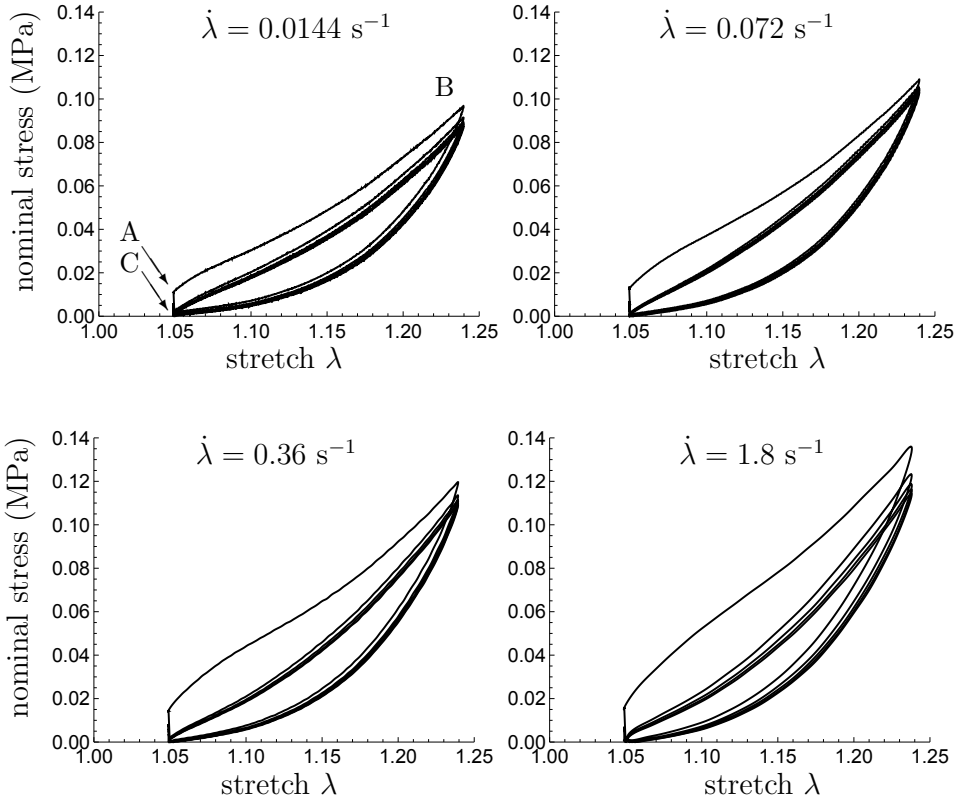

FIGURE 2.2: The nominal stress versus stretch of a passive *Manduca* muscle in simple uniaxial tension with prestressed resting stretch $\lambda_r = 1.05$, maximum extension $\lambda = 1.24$ and stretch rates of $\dot{\lambda} = 0.0144\ s^{-1}$, $\dot{\lambda} = 0.072\ s^{-1}$, $\dot{\lambda} = 0.36\ s^{-1}$ and $\dot{\lambda} = 1.8\ s^{-1}$. Reproduced from [34].

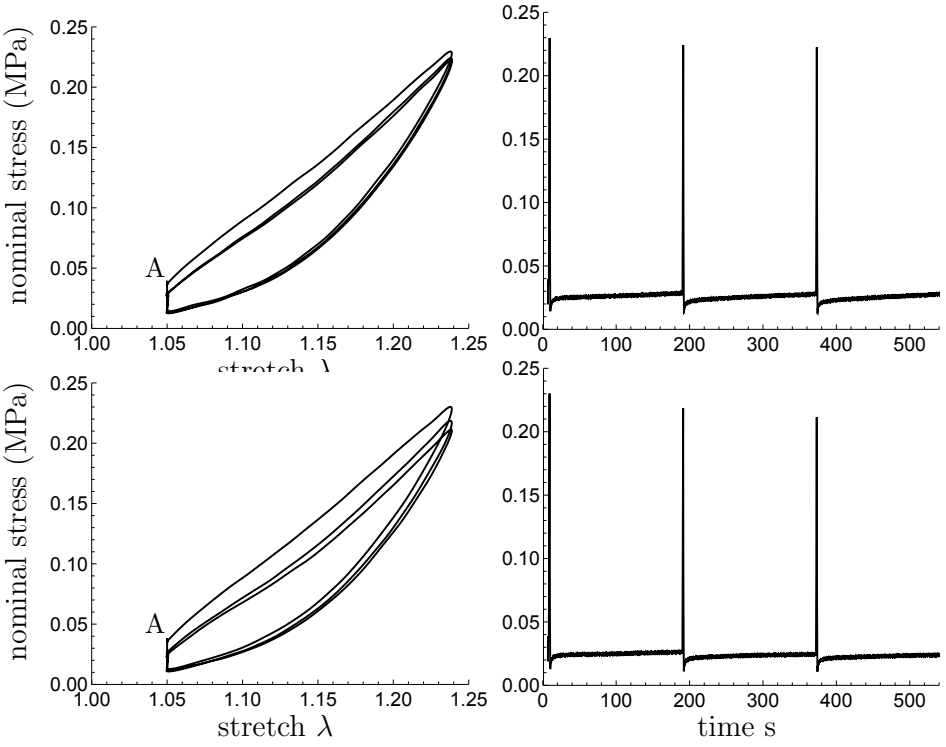

FIGURE 2.3: The stress-deformation responses of two unstimulated muscles in simple uniaxial tension during 3 loading-unloading cycles. At the end of each unloading the muscles are held at the resting length for 3 minutes during which recovery occurs from the preconditioned state to the prestressed resting state (point A). The left graphs show the nominal stress as a function of the stretch λ. The graphs on the right show the nominal stress as a function of time.

same value of λ. It is not known if these values of stress would coincide for the same values of λ if more time were allowed for the relaxation tests (as suggested by the model discussed in the next section).

The data reported in this section will be used to formulate a constitutive model for the time-dependent response of the *Manduca* muscle at finite strain. The theory of hyperelasticity is used to characterize the elastic response and a dissipative component to account for the inelastic response of the material. For simplicity it is assumed that stress relaxation at constant stretch during loading and during unloading approach the same equilibrium state.

2.3 Constitutive modeling

The data in Figures 2.2-2.4 suggest that the mechanical behavior of the material can be characterized by a composite model of an elastic component in parallel with a dissipative component. This model is shown schematically in Figure 2.1 where the single

elastic spring represents the time-independent nonlinear hyperelastic component and the spring element in series with a dashpot represents a nonlinear inelastic response similar to a Maxwell element. In the model discussed below the dashpot is generalized to include both rate-dependent and rate-independent inelastic responses. Since soft biological tissues undergo finite deformations, the model is formulated for arbitrarily large deformations.

By way of background, it is recalled that a material point in a fixed reference configuration is located by the vector $\mathbf{X}$ relative to a fixed origin. The same material point is located by the vector $\mathbf{x}$ (relative to the same origin) in the present configuration at time t. The velocity $\mathbf{v}$, velocity gradient $\mathbf{L}$ and the rate of deformation tensor $\mathbf{D}$ are defined by

$$\mathbf{v} = \dot{\mathbf{x}}, \quad \mathbf{L} = \frac{\partial \mathbf{v}}{\partial \mathbf{x}}, \quad \mathbf{D} = \frac{1}{2}\left(\mathbf{L} + \mathbf{L}^{\mathrm{T}}\right), \tag{2.1}$$

where a superposed $(\dot{})$ denotes material time differentiation holding $\mathbf{X}$ fixed. Since the proposed model includes hysteretic dissipation it is also recalled that the rate of material

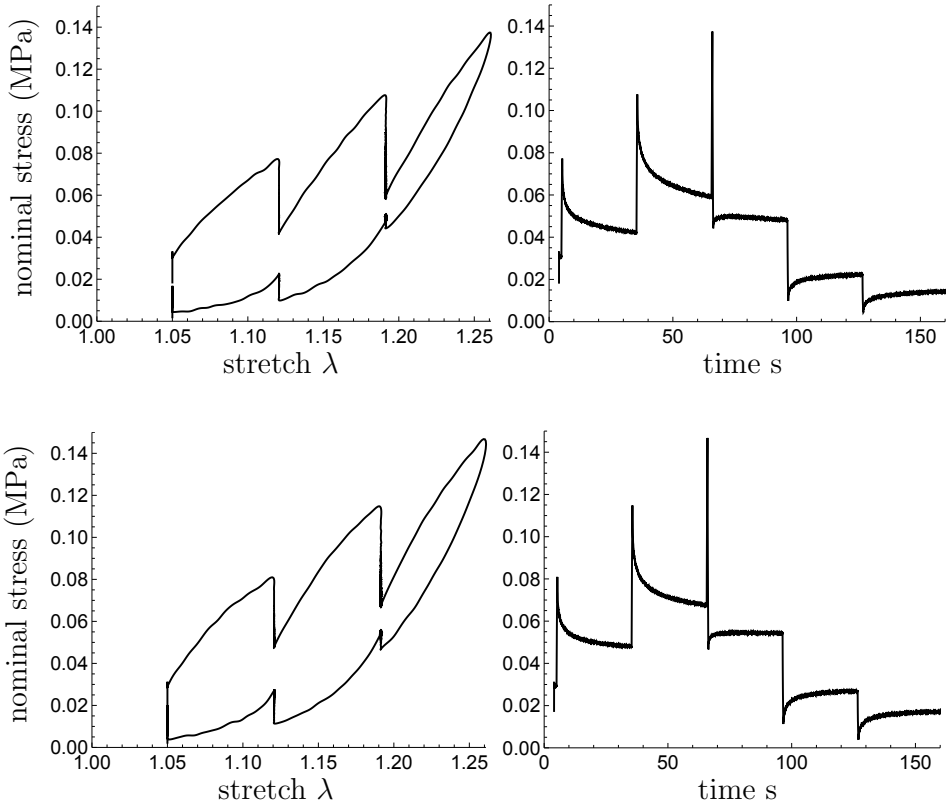

FIGURE 2.4: Experimental data showing the mechanical responses of two unstimulated muscles in simple uniaxial tension during loading and unloading. The graphs on the left show the nominal stress versus stretch λ. The graphs on the right depict the nominal stress versus time.

dissipation $\mathscr{D}$ can be expressed in the form

$$\mathscr{D} = \boldsymbol{\sigma} \cdot \mathbf{D} - \rho\dot{\Sigma} \geqslant 0, \tag{2.2}$$

where $\boldsymbol{\sigma}$ is the Cauchy stress, $\mathbf{A} \cdot \mathbf{B} = \mathrm{tr}\left(\mathbf{A}\mathbf{B}^{\mathrm{T}}\right)$ denotes the inner product between two second order tensors $\{\mathbf{A}, \mathbf{B}\}$, ρ is the current mass density and Σ is the strain energy per unit mass.

Specifically, for the composite model the strain energy is separated additively into a hyperelastic part Σ_{e} and a dissipative part Σ_{d}

$$\Sigma = \Sigma_{\mathrm{e}} + \Sigma_{\mathrm{d}}, \tag{2.3}$$

where the latter characterizes the elastic strain energy in the dissipative element. Similarly, the Cauchy stress $\boldsymbol{\sigma}$ separates additively into a hyperelastic part $\boldsymbol{\sigma}_{\mathrm{e}}$ and a dissipative part $\boldsymbol{\sigma}_{\mathrm{d}}$

$$\boldsymbol{\sigma} = \boldsymbol{\sigma}_{\mathrm{e}} + \boldsymbol{\sigma}_{\mathrm{d}}, \tag{2.4}$$

with the hyperelastic component being non-dissipative such that

$$\boldsymbol{\sigma}_{\mathrm{e}}\text{text in equation} \cdot \mathbf{D} = \rho\dot{\Sigma}_{\mathrm{e}}. \tag{2.5}$$

It then follows that the rate of material dissipation is due solely to the dissipative component which must satisfy the restriction

$$\mathscr{D} = \boldsymbol{\sigma}_{\mathrm{d}} \cdot \mathbf{D} - \rho\dot{\Sigma}_{\mathrm{d}} \geqslant 0. \tag{2.6}$$

2.3.1 Hyperelastic component

In general, hyperelastic materials experience both volumetric and distortional deformations. The volumetric deformation is characterized by the total dilatation J, which is determined by integrating the evolution equation

$$\dot{J} = J\mathbf{D} \cdot \mathbf{I}, \tag{2.7}$$

where $\mathbf{I}$ is the second order unit tensor. Using the theories in Flory [14] and Ogden [24] it is possible to define a symmetric second order unimodular tensor $\mathbf{B}'$ which is a pure measure of total distortional deformation by integrating the evolution equation

$$\dot{\mathbf{B}}' = \mathbf{L}\mathbf{B}' + \mathbf{B}'\mathbf{L}^{\mathrm{T}} - \frac{2}{3}\left(\mathbf{D} \cdot \mathbf{I}\right)\mathbf{B}'. \tag{2.8}$$

It can easily be shown that $\mathbf{B}'$ is the unimodular part of the standard left Cauchy-Green deformation tensor. Since $\mathbf{B}'$ is unimodular [$\det(\mathbf{B}') = 1$] it has only two independent invariants. These can be specified by the scalars β_1 and β_2 defined by

$$\beta_1 = \mathbf{B}' \cdot \mathbf{I}, \quad \beta_2 = \mathbf{B}'^2 \cdot \mathbf{I}, \tag{2.9}$$

which satisfy the equations

$$\dot{\beta}_1 = 2\,\mathrm{dev}\left(\mathbf{B}'\right) \cdot \mathbf{D}, \quad \dot{\beta}_2 = 4\,\mathrm{dev}\left(\mathbf{B}'^2\right) \cdot \mathbf{D}, \tag{2.10}$$

where the deviatoric operator dev ( ) of a second order tensor $\mathbf{A}$ is defined by

$$\mathrm{dev}\,(\mathbf{A}) = \mathbf{A} - \frac{1}{3}\,(\mathbf{A} \cdot \mathbf{I})\,\mathbf{I}. \tag{2.11}$$

For elastically isotropic materials the strain energy Σ_e is a function of the invariants $\{J, \beta_1, \beta_2\}$ expressed as

$$\Sigma_\mathrm{e} = \Sigma_\mathrm{e}\,(J, \beta_1, \beta_2)\,. \tag{2.12}$$

The hyperelastic part $\boldsymbol{\sigma}_\mathrm{e}$ of the Cauchy stress is then given by

$$\boldsymbol{\sigma}_\mathrm{e} = -p_\mathrm{e}\mathbf{I} + \mathrm{dev}\,(\boldsymbol{\sigma}_\mathrm{e})\,, \quad p_\mathrm{e} = -\rho_0 \frac{\partial \Sigma_\mathrm{e}}{\partial J}, \tag{2.13}$$

$$\mathrm{dev}\,(\boldsymbol{\sigma}_\mathrm{e}) = 2\rho \frac{\partial \Sigma_\mathrm{e}}{\partial \beta_1} \mathrm{dev}\left(\mathbf{B}'\right) + 4\rho \frac{\partial \Sigma_\mathrm{e}}{\partial \beta_2} \mathrm{dev}\left(\mathbf{B}'^2\right), \tag{2.14}$$

where use has been made of the conservation of mass which connects the mass density ρ in the present configuration to its value ρ_0 in the reference configuration

$$\rho J = \rho_0. \tag{2.15}$$

2.3.2 Dissipative component

The work in Rubin and Attia [43] proposes that the elastic distortional deformation of the dissipative component, which is insensitive to volume changes, can be characterized by the symmetric unimodular tensor $\mathbf{B}'_\mathrm{d}$, which is determined by integrating the evolution equation

$$\dot{\mathbf{B}}'_\mathrm{d} = \mathbf{L}\mathbf{B}'_\mathrm{d} + \mathbf{B}'_\mathrm{d}\mathbf{L}^\mathrm{T} - \frac{2}{3}\,(\mathbf{D} \cdot \mathbf{I})\,\mathbf{B}'_\mathrm{d} - \Gamma\mathbf{A}_\mathrm{d}, \tag{2.16}$$

where the function Γ controls the rate of inelastic distortional deformation and is specified by a constitutive equation. Its direction is controlled by $\mathbf{A}_{\mathrm{d}}$, which is given by

$$\mathbf{A}_{\mathrm{d}} = \mathbf{B}'_{\mathrm{d}} - \left(\frac{3}{\mathbf{B}'^{-1}_{\mathrm{d}} \cdot \mathbf{I}} \right) \mathbf{I}, \quad \mathbf{A}_{\mathrm{d}} \cdot \mathbf{B}'^{-1}_{\mathrm{d}} = 0. \tag{2.17}$$

This functional form for $\mathbf{A}_{\mathrm{d}}$ causes inelastic relaxation of $\mathbf{B}'_{\mathrm{d}}$ towards the unit tensor $\mathbf{I}$, with the restriction $(2.17)_2$ ensuring that $\mathbf{B}'_{\mathrm{d}}$ remains unimodular. Moreover, comparison of (2.16) with (2.8) shows that when the rate of inelasticity $\Gamma \mathbf{A}_{\mathrm{d}}$ vanishes, $\mathbf{B}'_{\mathrm{d}}$ satisfies the same evolution equation as that for the total elastic distortional deformation $\mathbf{B}'$. However, $\mathbf{B}'_{\mathrm{d}}$ can still differ from $\mathbf{B}'$ if the material experienced any inelastic deformation during its history of loading, since $\mathbf{B}'_{\mathrm{d}}$ does not retain permanent memory of a specific reference configuration.

Two independent invariants of $\mathbf{B}'_{\mathrm{d}}$ can be specified by the scalars $\{\alpha_1, \alpha_2\}$ as

$$\alpha_1 = \mathbf{B}'_{\mathrm{d}} \cdot \mathbf{I}, \quad \alpha_2 = \mathbf{B}'^{2}_{\mathrm{d}} \cdot \mathbf{I}, \tag{2.18}$$

which satisfy the equations

$$\begin{aligned} \dot{\alpha_1} &= 2\,\mathrm{dev}\left(\mathbf{B}'_{\mathrm{d}}\right) \cdot \mathbf{D} - \Gamma \mathbf{A}_{\mathrm{d}} \cdot \mathbf{I}, \\ \dot{\alpha_2} &= 4\,\mathrm{dev}\left(\mathbf{B}'^{2}_{\mathrm{d}}\right) \cdot \mathbf{D} - 2\Gamma \mathbf{A}_{\mathrm{d}} \cdot \mathbf{B}'_{\mathrm{d}}. \end{aligned} \tag{2.19}$$

The strain energy Σ_{d}, for elastically isotropic materials, is specified to be a function of $\{\alpha_1, \alpha_2\}$

$$\Sigma_{\mathrm{d}} = \Sigma_{\mathrm{d}}\left(\alpha_1, \alpha_2\right), \tag{2.20}$$

and the dissipative part $\boldsymbol{\sigma}_{\mathrm{d}}$ of the Cauchy stress is taken in the form

$$\boldsymbol{\sigma}_{\mathrm{d}} = \mathrm{dev}\left(\boldsymbol{\sigma}_{\mathrm{d}}\right) = 2\rho \frac{\partial \Sigma_{\mathrm{d}}}{\partial \alpha_1} \mathrm{dev}\left(\mathbf{B}'_{\mathrm{d}}\right) + 4\rho \frac{\partial \Sigma_{\mathrm{d}}}{\partial \alpha_2} \mathrm{dev}\left(\mathbf{B}'^{2}_{\mathrm{d}}\right). \tag{2.21}$$

Moreover, the rate of material dissipation (2.6) requires

$$\mathscr{D} = \Gamma \rho \left[\frac{\partial \Sigma_{\mathrm{d}}}{\partial \alpha_1} \mathbf{A}_{\mathrm{d}} \cdot \mathbf{I} + 2 \frac{\partial \Sigma_{\mathrm{d}}}{\partial \alpha_2} \mathbf{A}_{\mathrm{d}} \cdot \mathbf{B}'_{\mathrm{d}} \right] \geqslant 0. \tag{2.22}$$

A model with a smooth elastic-inelastic transition which can be either rate-independent or rate-dependent, with and without a yield function is given by Hollenstein et al. [36]. For the model here considered, the value of Γ depends on the effective rate of total

distortional deformation $\dot{\varepsilon}$ defined by

$$\dot{\varepsilon} = \sqrt{\frac{2}{3}\text{dev}\,(\mathbf{D}) \cdot \text{dev}\,(\mathbf{D})}. \tag{2.23}$$

The experimental data of the *Manduca* muscle suggest that the functional form of Γ depends on the state of the dissipative component. In particular, a model is proposed for which the parameters $\{a, b\}$ have different values when the material is being loaded $\{a_{\text{l}}, b_{\text{l}}\}$ with the dissipative component being in a state of triaxial extension and when the material is being unloaded $\{a_{\text{u}}, b_{\text{u}}\}$ with the dissipative component being in a state of triaxial compression. Since data are only available for uniaxial stress it is not possible to quantify a three-dimensional formulation that models all states of the dissipative component. Nevertheless, since the present model is developed for three-dimensional deformations it is desirable to suggest a theoretical structure that can be used. To this end, it is recalled from Rubin [44] that simple isotropic functions can be developed using a Lode angle to distinguish between different states of the material. Motivated by this work, it is convenient to introduce a Lode angle γ based on the deviatoric part of the elastic distortional deformation of the dissipative component by

$$\sin(3\gamma) = -\frac{27\det\left[\text{dev}\,(\mathbf{B}'_{\text{d}})\right]}{2\left[\frac{3}{2}\text{dev}\,\left(\mathbf{B}'_{\text{d}}\right) \cdot \text{dev}\,\left(\mathbf{B}'_{\text{d}}\right)\right]^{3/2}}, \quad -\frac{\pi}{6} \leqslant \gamma \leqslant \frac{\pi}{6}. \tag{2.24}$$

Different functional forms of Γ were considered in [44], but here attention is limited to a Mohr-Coulomb type model with Γ being specified by

$$\Gamma = a\,(a_{\text{l}}, a_{\text{u}}, \gamma) + b\,(b_{\text{l}}, b_{\text{u}}, \gamma)\,\dot{\varepsilon}, \tag{2.25}$$

where

$$a\,(a_{\text{l}}, a_{\text{u}}, \gamma) = \frac{\sqrt{3}\,a_{\text{l}}\,a_{\text{u}}}{(a_{\text{l}} + a_{\text{u}})\cos\gamma + \sqrt{3}\,(a_{\text{l}} - a_{\text{u}})\sin\gamma} > 0, \tag{2.26}$$

and

$$b\,(b_{\text{l}}, b_{\text{u}}, \gamma) = \frac{\sqrt{3}\,b_{\text{l}}\,b_{\text{u}}}{(b_{\text{l}} + b_{\text{u}})\cos\gamma + \sqrt{3}\,(b_{\text{l}} - b_{\text{u}})\sin\gamma} > 0, \tag{2.27}$$

and with $\{a_{\text{l}}, a_{\text{u}}, b_{\text{l}}, b_{\text{u}}\}$ being positive constants. This functional dependence of Γ on the Lode angle γ can be modified once multi-axial data become available.

For the simple case of uniaxial stress in the fixed unit $\mathbf{s}$ direction, starting from zero stress in the dissipative component, the distortional deformation tensor $\mathbf{B}'_{\text{d}}$ can be written as a function of the stretch $\lambda_{\text{d}} > 0$ in the form

$$\mathbf{B}'_{\text{d}} = \lambda_{\text{d}}^2\,\mathbf{s}\otimes\mathbf{s} + \frac{1}{\lambda_{\text{d}}}\,(\mathbf{I} - \mathbf{s}\otimes\mathbf{s}), \quad \mathbf{s}\cdot\mathbf{s} = 1. \tag{2.28}$$

It can be shown that

$$\gamma = -\frac{\pi}{6}, \quad a\left(a_{\mathrm{l}}, a_{\mathrm{u}}, -\frac{\pi}{6}\right) = a_{\mathrm{l}}, \quad b\left(b_{\mathrm{l}}, b_{\mathrm{u}}, -\frac{\pi}{6}\right) = b_{\mathrm{l}} \quad \text{for} \quad \lambda_{\mathrm{d}} > 1, \tag{2.29}$$

$$\gamma = \frac{\pi}{6}, \quad a\left(a_{\mathrm{l}}, a_{\mathrm{u}}, \frac{\pi}{6}\right) = a_{\mathrm{u}}, \quad b\left(b_{\mathrm{l}}, b_{\mathrm{u}}, \frac{\pi}{6}\right) = b_{\mathrm{u}} \quad \text{for} \quad \lambda_{\mathrm{d}} < 1. \tag{2.30}$$

Thus, the values $\{a_{\mathrm{l}}, b_{\mathrm{l}}\}$ characterize loading with the dissipative component being in triaxial extension $\{\lambda_{\mathrm{d}} > 1\}$ and the values $\{a_{\mathrm{u}}, b_{\mathrm{u}}\}$ characterize unloading with the dissipative component in triaxial compression $\{\lambda_{\mathrm{d}} < 1\}$.

2.4 Robust, strongly objective numerical integration algorithm

A robust, strongly objective numerical integration algorithm was developed in Hollenstein et al. [36], which can be applied to the evolution equations (2.7), (2.8) and (2.16). This algorithm is briefly summarized in this section with reference to the proposed model. Specifically, it is assumed that at time $t = t_1$ the values $\{J(t_1), \mathbf{B}'(t_1), \mathbf{B}'_{\mathrm{d}}(t_1)\}$ of $\{J, \mathbf{B}', \mathbf{B}'_{\mathrm{d}}\}$ are known and the objective is to find the values $\{J(t_2), \mathbf{B}'(t_2), \mathbf{B}'_{\mathrm{d}}(t_2)\}$ of these quantities at the end of the time step at $t = t_2$ with $\Delta t = t_2 - t_1$.

Following the work in [45–47] it is convenient to define the relative deformation gradient $\mathbf{F}_{\mathrm{r}}$, the relative dilatation J_{r} and the unimodular part $\mathbf{F}'_{\mathrm{r}}$ of $\mathbf{F}_{\mathrm{r}}$ by the evolution equations

$$\dot{\mathbf{F}}_{\mathrm{r}} = \mathbf{L}\mathbf{F}_{\mathrm{r}}, \quad \dot{J}_{\mathrm{r}} = J_{\mathrm{r}}\mathbf{D} \cdot \mathbf{I}, \quad \dot{\mathbf{F}}'_{\mathrm{r}} = \mathbf{L}\mathbf{F}'_{\mathrm{r}} - \frac{1}{3}\left(\mathbf{D} \cdot \mathbf{I}\right)\mathbf{F}'_{\mathrm{r}}, \tag{2.31}$$

with the initial conditions

$$\mathbf{F}_{\mathrm{r}}\left(t_1\right) = \mathbf{I}, \quad J_{\mathrm{r}}\left(t_1\right) = 1, \quad \mathbf{F}'_{\mathrm{r}}\left(t_1\right) = \mathbf{I}, \tag{2.32}$$

where

$$J_{\mathrm{r}} = \det\left(\mathbf{F}_{\mathrm{r}}\right), \quad \mathbf{F}'_{\mathrm{r}} = J_{\mathrm{r}}^{-1/3}\mathbf{F}_{\mathrm{r}}. \tag{2.33}$$

For finite element programs the value $\mathbf{F}_{\mathrm{r}}\left(t_2\right)$ can be determined directly in terms of the nodal displacements during the time step so that the evolution equations (2.31) and (2.32) do not need to be integrated explicitly.

Now, the exact solutions of (2.7) and (2.8) can be written in the forms

$$J\left(t_2\right) = J_{\mathrm{r}}\left(t_2\right) J\left(t_1\right), \quad \mathbf{B}'\left(t_2\right) = \mathbf{F}'_{\mathrm{r}}\left(t_2\right) \mathbf{B}'\left(t_1\right) \mathbf{F}'^{\mathrm{T}}_{\mathrm{r}}\left(t_2\right). \tag{2.34}$$

Also, the elastic trial value of $\mathbf{B}'_{\mathrm{d}}$, denoted by $\mathbf{B}'^{\star}_{\mathrm{d}}$, determined by the solution of (2.16) with vanishing rate of inelastic deformation $\Gamma = 0$, can be expressed in the form

$$\mathbf{B}'^{\star}_{\mathrm{d}} = \mathbf{F}'_{\mathrm{r}}\left(t_2\right)\mathbf{B}'_{\mathrm{d}}\left(t_1\right)\mathbf{F}'^{\mathrm{T}}_{\mathrm{r}}\left(t_2\right). \tag{2.35}$$

Using an implicit backward Euler integrated approximation, the auxiliary tensor $\bar{\mathbf{B}}'_{\mathrm{d}} \approx \mathbf{B}'_{\mathrm{d}}\left(t_2\right)$ associated with the evolution equation (2.16) is given by

$$\bar{\mathbf{B}}'_{\mathrm{d}} = \mathbf{B}'^{\star}_{\mathrm{d}} - \Delta t\Gamma\left(t_2\right)\left[\bar{\mathbf{B}}'_{\mathrm{d}} - \left(\frac{3}{\bar{\mathbf{B}}'^{-1}_{\mathrm{d}}\cdot\mathbf{I}}\right)\mathbf{I}\right], \tag{2.36}$$

where $\Gamma\left(t_2\right)$ is the value of Γ at the end of the time step. Next, taking the deviatoric part of (2.36) and requiring that $\operatorname{dev}\left[\mathbf{B}'_{\mathrm{d}}\left(t_2\right)\right] = \operatorname{dev}\left(\bar{\mathbf{B}}'_{\mathrm{d}}\right)$ it follows that

$$\operatorname{dev}\left[\mathbf{B}'_{\mathrm{d}}\left(t_2\right)\right] = \frac{1}{1+\Delta t\Gamma\left(t_2\right)}\operatorname{dev}\left(\mathbf{B}'^{\star}_{\mathrm{d}}\right). \tag{2.37}$$

In order to determine the value of $\Gamma\left(t_2\right)$ in (2.37) it is recalled from Papes [48] that the value $\bar{\mathbf{D}}$ of $\mathbf{D}\left(t_2\right)$ at the end of the time step can be approximated by

$$\mathbf{D}\left(t_2\right) \approx \bar{\mathbf{D}} = \frac{1}{2\Delta t}\left[\mathbf{F}_{\mathrm{r}}\left(t_2\right)\mathbf{F}^{\mathrm{T}}_{\mathrm{r}}\left(t_2\right) - \mathbf{I}\right], \tag{2.38}$$

so that the average increment of the effective total rate of deformation, defined in (2.23), can be approximated by

$$\Delta\varepsilon = \Delta t\,\dot{\varepsilon}\left(t_2\right) \approx \Delta t\sqrt{\frac{2}{3}\operatorname{dev}\left(\bar{\mathbf{D}}\right)\cdot\operatorname{dev}\left(\bar{\mathbf{D}}\right)} \tag{2.39}$$

and the Lode angle γ in (2.24) is given by

$$\sin(3\gamma) = -\frac{27\det\left[\operatorname{dev}\left(\bar{\mathbf{D}}\right)\right]}{2\left[\frac{3}{2}\operatorname{dev}\left(\bar{\mathbf{D}}\right)\cdot\operatorname{dev}\left(\bar{\mathbf{D}}\right)\right]^{3/2}}, \quad -\frac{\pi}{6} \leqslant \gamma \leqslant \frac{\pi}{6}. \tag{2.40}$$

Thus, $\Delta t\Gamma\left(t_2\right)$ becomes

$$\Delta t\Gamma\left(t_2\right) = \Delta t\, a\left(a_{\mathrm{l}}, a_{\mathrm{u}}, \gamma\right) + b\left(b_{\mathrm{l}}, b_{\mathrm{u}}, \gamma\right)\Delta\varepsilon. \tag{2.41}$$

Finally, using (2.41) in (2.37), the value of $\mathbf{B}'_{\mathrm{d}}$ at the end of the time step can be expressed in the form

$$\mathbf{B}'_{\mathrm{d}}\left(t_2\right) = \operatorname{dev}\left[\mathbf{B}'_{\mathrm{d}}\left(t_2\right)\right] + \frac{1}{3}\alpha\left(t_2\right)\mathbf{I}, \tag{2.42}$$

where the scalar $\alpha\left(t_2\right)$ is determined by solving the cubic equation

$$\det\left[\mathbf{B}'_{\mathrm{d}}\left(t_2\right)\right] = 1. \tag{2.43}$$

For details see Eq. (49a) in Rubin and Attia [43].

2.5 Specific constitutive equations

Since many soft tissues experience large distortional deformations relative to volumetric deformations it is convenient to consider them to be incompressible by introducing the volumetric constraint

$$J = 1. \tag{2.44}$$

The constraint response which enforces the incompressibility condition (2.44) effectively replaces the pressure p_{e} in (2.13) by an arbitrary function that is determined by the balance of linear momentum and boundary conditions. It follows that only the distortional response of the strain energy function Σ_e needs to be specified. Specifically, here Σ_e is taken in the form

$$\rho_0\Sigma_{\mathrm{e}} = \frac{\mu_{\mathrm{e}}}{2\beta_{\mathrm{e}}}\left\{\exp\left[\beta_{\mathrm{e}}(\beta_1 - 3)\right] - 1\right\}, \tag{2.45}$$

where μ_e is a non-negative, constant shear modulus and β_e is a positive material constant that controls the nonlinearity of the elastic response. Then, using (2.14) the elastic part $\boldsymbol{\sigma}_{\mathrm{e}}$ of the stress is given by

$$\boldsymbol{\sigma}_{\mathrm{e}} = -p_{\mathrm{e}}\mathbf{I} + \mu_{\mathrm{e}}\exp\left[\beta_{\mathrm{e}}\left(\beta_1 - 3\right)\right]\operatorname{dev}\left(\mathbf{B}'\right). \tag{2.46}$$

The constitutive equation for the elastic strain energy of the dissipative component is taken in a similar form to (2.45) with

$$\rho_0\Sigma_{\mathrm{d}} = \frac{\mu_{\mathrm{d}}}{2\alpha_{\mathrm{d}}}\left\{\exp\left[\alpha_{\mathrm{d}}(\alpha_1 - 3)\right] - 1\right\}, \tag{2.47}$$

where μ_{d} is a non-negative, constant shear modulus and α_{d} is a positive material constant that controls nonlinearity of the elastic response of the dissipative component. It then follows from (2.21) that the dissipative part $\boldsymbol{\sigma}_{\mathrm{d}}$ of the stress is given by

$$\boldsymbol{\sigma}_{\mathrm{d}} = \operatorname{dev}\left(\boldsymbol{\sigma}_{\mathrm{d}}\right) = \mu_{\mathrm{d}}\exp\left[\alpha_{\mathrm{d}}\left(\alpha_1 - 3\right)\right]\operatorname{dev}\left(\mathbf{B}'_{\mathrm{d}}\right). \tag{2.48}$$

Also, the rate of material dissipation (2.22) requires

$$\mathscr{D} = \frac{1}{2}\Gamma\mu_{\mathrm{d}}\exp\left[\alpha_{\mathrm{d}}\left(\alpha_1 - 3\right)\right]\left(\mathbf{A}_{\mathrm{d}}\cdot\mathbf{I}\right) \geqslant 0. \tag{2.49}$$

It can be shown that by expressing $\mathbf{B}'_{\mathrm{d}}$ in its spectral form that the expression $\mathbf{A}_{\mathrm{d}} \cdot \mathbf{I}$ is non-negative so that (2.49) is satisfied by the functional form (2.25) for Γ.

2.6 Simulation

The model developed in the previous sections is used here to simulate the experimental data for simple uniaxial tension of the *Manduca* muscle. To this end, λ is taken to be the axial stretch in the fixed $\mathbf{s}$ direction with the material being stress-free in its initial state with

$$\lambda(0) = 1, \quad \mathbf{B}'(0) = \mathbf{I}, \quad \mathbf{B}'_{\mathrm{d}}(0) = \mathbf{I}. \tag{2.50}$$

Moreover, the velocity gradient $\mathbf{L}$ is specified by (2.28) so that the solutions of the evolution equations (2.8) and (2.16) give

$$\mathbf{B}' = \lambda^2 \mathbf{s} \otimes \mathbf{s} + \frac{1}{\lambda} (\mathbf{I} - \mathbf{s} \otimes \mathbf{s}), \quad \beta_1 = \frac{\lambda^3 + 2}{\lambda}, \tag{2.51}$$

$$\mathbf{B}'_{\mathrm{d}} = \lambda_{\mathrm{d}}^2 \mathbf{s} \otimes \mathbf{s} + \frac{1}{\lambda_{\mathrm{d}}} (\mathbf{I} - \mathbf{s} \otimes \mathbf{s}), \quad \alpha_1 = \frac{\lambda_{\mathrm{d}}^3 + 2}{\lambda_{\mathrm{d}}}, \tag{2.52}$$

where λ_{d} is the stretch associated with the dissipative component. Thus, for uniaxial stress in the $\mathbf{s}$ direction, the pressure p_e is determined by the condition that the lateral stress vanishes. The total stress is represented in the form

$$\boldsymbol{\sigma} = \sigma \mathbf{s} \otimes \mathbf{s}, \tag{2.53}$$

where the explicit expression for σ, using (2.4), (2.46) and (2.48), is given by

$$\sigma = \mu_{\mathrm{e}} \exp\left[\beta_{\mathrm{e}} (\beta_1 - 3)\right] \left(\lambda^2 - \frac{1}{\lambda}\right) + \mu_{\mathrm{d}} \exp\left[\alpha_{\mathrm{d}} (\alpha_1 - 3)\right] \left(\lambda_{\mathrm{d}}^2 - \frac{1}{\lambda_{\mathrm{d}}}\right). \tag{2.54}$$

Furthermore, for incompressible material subject to simple uniaxial tension, the nominal axial stress Π (stress per unit reference area) is given by

$$\Pi = \frac{\sigma}{\lambda}. \tag{2.55}$$

Now, using the numerical procedure described in Section 2.4, it follows that the value of the unimodular part of the relative deformation gradient at the end of a typical time step, $\mathbf{F}'_{\mathrm{r}}(t_2)$, is given by

$$\mathbf{F}'_{\mathrm{r}}(t_2) = \frac{\lambda(t_2)}{\lambda(t_1)} \mathbf{s} \otimes \mathbf{s} + \sqrt{\frac{\lambda(t_1)}{\lambda(t_2)}} (\mathbf{I} - \mathbf{s} \otimes \mathbf{s}), \tag{2.56}$$

and the elastic trial value $\lambda_d^\star$ of λ_d can be expressed by

$$\lambda_{\mathrm{d}}^\star = \left[\frac{\lambda\left(t_2\right)}{\lambda\left(t_1\right)}\right] \lambda_d\left(t_1\right). \tag{2.57}$$

Then, equation (2.37) yields a cubic equation for $\lambda_{\mathrm{d}}\left(t_2\right)$ in the form

$$\lambda_{\mathrm{d}}^2\left(t_2\right) - \frac{1}{\lambda_{\mathrm{d}}\left(t_2\right)} = \left[\frac{1}{1+\Delta t \Gamma\left(t_2\right)}\right]\left(\lambda_{\mathrm{d}}^{\star 2} - \frac{1}{\lambda_{\mathrm{d}}^\star}\right). \tag{2.58}$$

Moreover, in determining the value of $\Gamma\left(t_2\right)$ in (2.41) use has been made of the expression (2.38), which yields

$$\operatorname{dev}\left(\bar{\mathbf{D}}\right) = \frac{1}{2\Delta t}\left[\frac{\lambda^2\left(t_2\right)}{\lambda^2\left(t_1\right)} - \frac{\lambda\left(t_1\right)}{\lambda\left(t_2\right)}\right]\left(\mathbf{s}\otimes\mathbf{s} - \frac{1}{3}\mathbf{I}\right). \tag{2.59}$$

Then, using the values $\left\{\lambda\left(t_2\right), \lambda_{\mathrm{d}}\left(t_2\right)\right\}$ together with (2.51) - (2.55) gives the value of the nominal stress $\Pi\left(t_2\right)$ at the end of the time step.

2.7 Model predictions

The rate-dependent response of an unstimulated muscle, the recovery of muscle properties from the preconditioned state and stress relaxation for constant stretches are now evaluated using the formulation presented in Section 2.5. Recordings of experimental data were initiated when the stretch $\lambda = \lambda_{\mathrm{r}}$ corresponding to the resting length of the muscle. For completeness, the numerical computation includes the stress-free initial state and a quasi-static extension from $\lambda(0) = 1$ to $\lambda_{\mathrm{r}} = 1.05$, which ensures zero stress in the dissipative component. At $\lambda = \lambda_{\mathrm{r}}$, the stretch rate changes and assumes values equivalent to those used in the experimental characterization. The data shown in Figures 2.2, 2.3 and 2.4 are obtained from different muscles so that, due to the variability of biological tissue, a change in the material parameters should be expected. This is shown by comparing values of corresponding parameters in Tables 2.1, 2.2 and 2.3. Trial and error estimates are used to determine the parameters μ_{e} and β_{e} of the elastic energy function (2.45). The remaining parameters, $\{\mu_{\mathrm{d}}, \alpha_{\mathrm{d}}\}$ used to define the energy Σ_{d} in (2.47) and $\{a_{\mathrm{l}}, b_{\mathrm{l}}, a_{\mathrm{u}}, b_{\mathrm{u}}\}$ to define Γ in (2.25), are determined by a least square optimization routine using the data shown in Section 2.2.

2.7.1 Rate-dependent response

Figure 2.2 summarizes experimental data of the rate-dependent response of an unstimulated *Manduca* muscle for stretch rates $\dot{\lambda} = 0.0144, 0.072, 0.36$ and $1.8\ \mathrm{s}^{-1}$. These

data are used to determine the corresponding material model parameters, which are summarized in Table 2.1 and used to obtain the numerical results depicted in Figure 2.5. Specifically, the numerical results show the nominal stress Π as a function of the stretch λ for two loading-unloading cycles in simple tension with maximum extension $\lambda = 1.24$ for $\dot{\lambda} = 0.0144, 0.072, 0.36$ and $1.8\ \mathrm{s}^{-1}$. The results also show a change in material response when transitioning from quasi-static loading to the specified stretch rate at $\lambda = \lambda_\mathrm{r}$. The inelastic behavior is characterized by the permanent set of the material at completion of the first loading-unloading cycle. Reloading differs from the primary loading path indicating preconditioning of the material similar to the Mullins effect observed in rubberlike materials [49–51]. For convenience of comparison, experimental behavior for loading-unloading cycles of the preconditioned material are included as dashed curves in Figure 2.5. Comparing the numerical results with the experimental data validates the formulation of the proposed model to simulate the rate-dependent response of *Manduca* muscle.

μ_e	β_e	μ_d	α_d	a_l	b_l	a_u	b_u
0.06	5	0.16	6	0.16	8	0.6	60

TABLE 2.1: Model parameters used to simulate the rate dependent response of an unstimulated muscle. The values of a_l and a_u are in s^{-1} and μ_e and μ_d are given in MPa.

2.7.2 Recovery from preconditioned state

The material model is now used to describe the time-dependent recovery of a *Manduca* muscle from the preconditioned state. The experimental data in Figure 2.3 show three loading-unloading cycles at constant strain rate and maximum extension $\lambda = 1.24$. At the end of each unloading, the muscle is held at the resting length for three minutes during which the material nearly recovers its prestressed resting state. These data are now used to determine material parameters, which are summarized in Table 2.2 with the corresponding numerical results given in Figure 2.6. The graph on the left starts from the stress-free configuration $\lambda(0) = 1$ and shows the nominal stress Π as a function of λ for three loading-unloading cycles. The transition from quasi-static loading to the stretch rate $\dot{\lambda} = 0.18\ \mathrm{s}^{-1}$ is again visible during primary loading when $\lambda = \lambda_\mathrm{r}$. During unloading the material does not return to the initial stress-free state clearly showing the inelastic component of the deformation. During the recovery time, at constant stretch $\lambda = \lambda_\mathrm{r}$, the stress increases but does not reach the primary loading state. Therefore, the reloading again differs from primarily loading. The nominal stress Π as a function of time is shown in the graph on the right in Figure 2.6. Experimental behavior, depicted by dashed curves, are included to assess the accuracy of the model prediction.

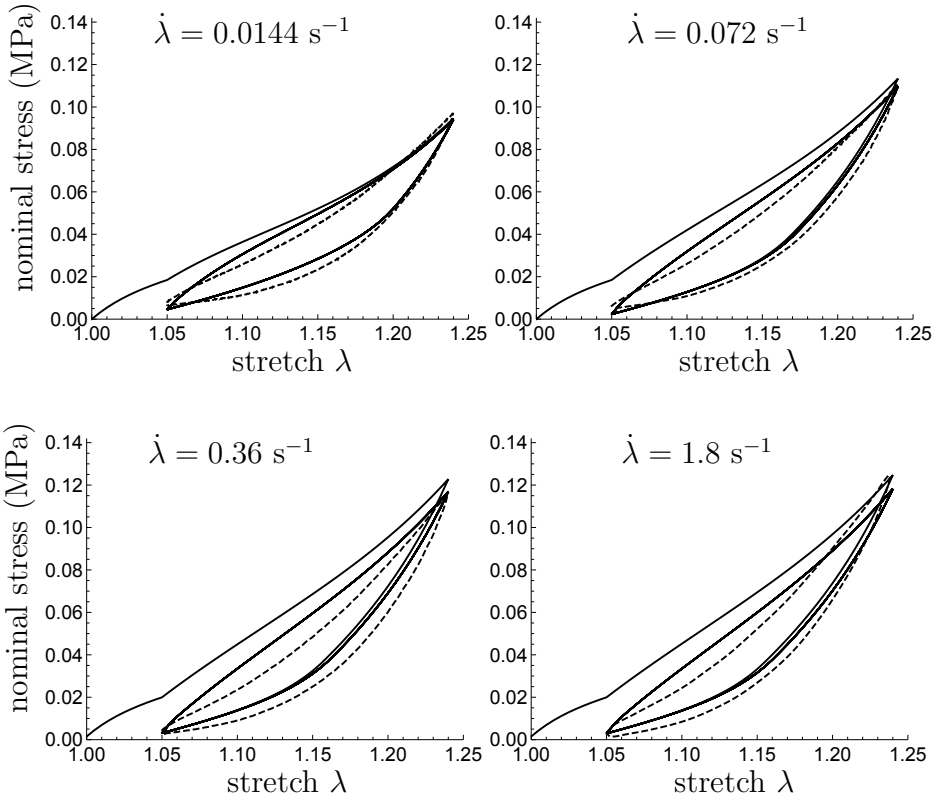

FIGURE 2.5: Numerical results showing two loading-unloading cycles of an unstimulated *Manduca* muscle in simple tension with maximum extension $\lambda = 1.24$ and stretch rates of $\dot{\lambda} = 0.0144$ s^{-1}, $\dot{\lambda} = 0.072$ s^{-1}, $\dot{\lambda} = 0.36$ s^{-1} and $\dot{\lambda} = 1.8$ s^{-1}. The dashed curves represent the experimental behavior of the preconditioned material. All graphs depict the nominal stress as a function of the stretch λ.

μ_e	β_e	μ_d	α_d	a_l	b_l	a_u	b_u
0.17	3.9	0.31	2.3	0.25	12	0.3	40

TABLE 2.2: Magnitudes of the material model parameters used to simulate the recovery of passive muscle properties from a preconditioned state. The values of a_l and a_u are in s^{-1} and the μ_e and μ_d are given in MPa.

2.7.3 Stress relaxation

The data in Figure 2.4 are used to determine a set of material parameters that represent the time-dependent response of the *Manduca* muscle used in this study. These are listed in Table 2.3 and are used to simulate stress relaxation at constant stretch during loading and unloading portions of a cycle of simple uniaxial tension. Figure 2.7 shows the numerical results of an unstimulated muscle in simple tension from the stress-free configuration $\lambda(0) = 1$ to a maximum stretch $\lambda \approx 1.26$. The loading rate changes from quasi-static to $\dot{\lambda} = 0.2$ s^{-1} at $\lambda_r = 1.05$. During loading and unloading portions of the cycle the stretch is held constant for 30 seconds at $\lambda = 1.12$ and $\lambda = 1.19$ and the change in stress as a function of time is evaluated numerically. The change of the

nominal stress Π with time, depicted in the graph on the right in Figure 2.7, differs from that during loading and unloading portions of the cycle. Specifically, during loading the stress decays with relaxation not completed after 30 seconds, during unloading the stress increases reaching a constant value in less than 30 seconds. This requires different values of the material parameters $\{a, b\}$ to define Γ during loading and unloading, see Equation (2.25). The graph on the right shows a change in slope at $t = 5$ s indicating the change in loading rate at $\lambda = \lambda_{\rm r}$. The dashed curves in Figure 2.7 represent the observed behavior and are used to quantify the accuracy of the numerical prediction.

$\mu_{\rm e}$	$\beta_{\rm e}$	$\mu_{\rm d}$	$\alpha_{\rm d}$	$a_{\rm l}$	$b_{\rm l}$	$a_{\rm u}$	$b_{\rm u}$
0.06	5.5	0.22	11	0.04	6.5	1	80

TABLE 2.3: Summary of material model parameters describing stress relaxation of an unstimulated muscle during loading and unloading in simple tension. The values of $a_{\rm l}$ and $a_{\rm u}$ are in $\rm s^{-1}$ and the $\mu_{\rm e}$ and $\mu_{\rm d}$ are given in MPa.

2.8 Discussion and concluding remarks

Motivated by the need to characterize the time-dependent response of skeletal muscle, this paper presents new experimental data and a phenomenological constitutive model that captures the observed behavior with reasonable accuracy. The data, from the unstimulated ventral interior lateral muscle of the third abdominal segment of *Manduca*

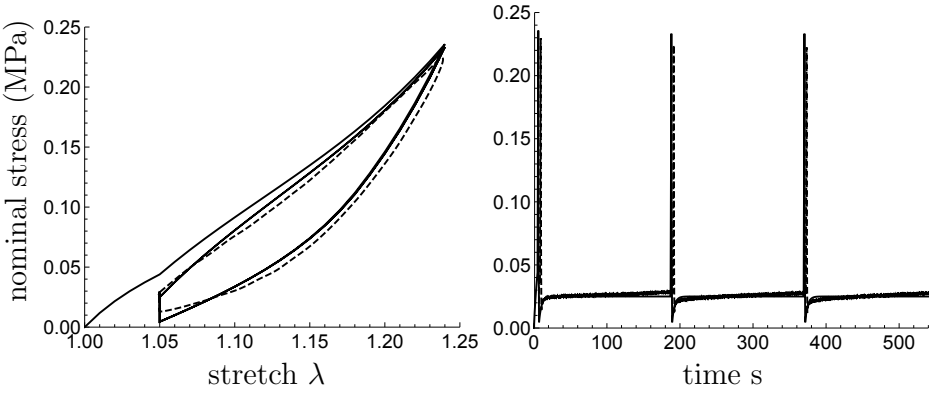

FIGURE 2.6: Numerical results representing three loading-unloading cycles of an unstimulated muscle in simple tension. At the end of each cycle, at the resting length $\lambda_{\rm r} = 1.05$, a 180 seconds recovery period is included to allow recovery of muscle properties from the preconditioned state. The graph on the left shows the loading-unloading response, the graph on the right depicts the change in nominal stress as a function of time. The dashed curves represent the experimental behavior of the preconditioned material. Experimental data in Figure 2.3 show that the stress-stretch response of the preconditioned muscle coincides during the second and third loading cycles. Therefore, for clarity of representation, only one loading-unloading cycle is included in the graph on the left.

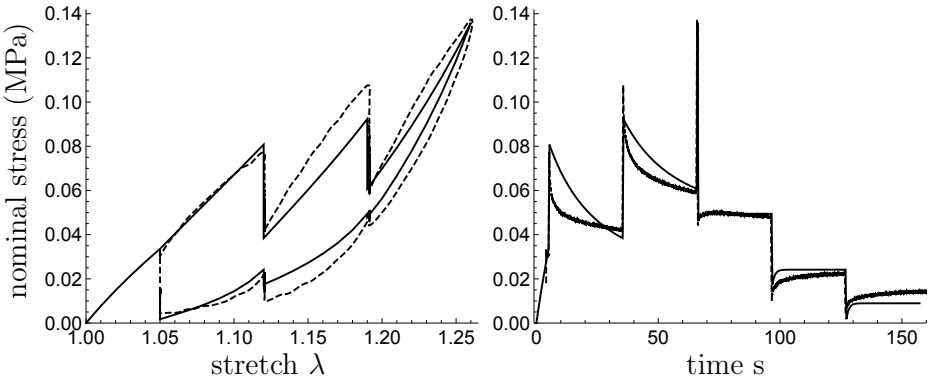

FIGURE 2.7: Numerical results showing the response of the unstimulated *Manduca* muscle in simple tension. The graph on the left shows the nominal stress versus stretch during loading and unloading. The graph on the right depicts stress relaxation as a function of time for constant values of λ. Experimental behavior, depicted by the dashed curves, are included to assess the accuracy of the model prediction

.

sexta, are limited to simple uniaxial tensile loading-unloading in the fiber direction. The experimental characterization quantifies the inelastic rate-dependent behavior, the recovery of muscle properties from the preconditioned response towards the prestressed resting state and stress relaxation at constant stretch during loading and unloading.

The proposed model considers the material as a composite of a nonlinear hyperelastic component in parallel with a dissipative component. In contrast with standard nonlinear inelastic models, here the dissipative component is modeled using an evolution equation that combines rate-independent and rate-dependent behavior, which exhibits smooth response with no finite elastic range. The three-dimensional constitutive model is specialized to simple uniaxial tension in the preferred direction, hence an isotropic formulation provides sufficient flexibility to capture the mechanical response. As such, the structure of the proposed formulation is not muscle specific, i.e. a change in the material parameters fully accounts for the variability of biological tissue. The restriction imposed by the current isotropic formulation is that the principal direction of the uniaxial stress component and the preferred direction of the material coincide.

Acknowledgement

This research was supported by the National Science Foundation [Grant numbers CMMI-1031366, CMMI-1352955, IOS-1050908] and by a Faculty Research Award provided by Tufts University. This research was partially supported by MB Rubin's Gerard Swope Chair in Mechanics.

Bibliography

[1] Paetsch, C., Trimmer, B.A., Dorfmann, A.: A constitutive model for active-passive transition of muscle fibers. Int. J. Nonlinear Mech. **47**, 377–387 (2012)

[2] Paetsch, C., Dorfmann, A.: Non-linear modeling of active biohybrid materials. Int. J. Nonlin. Mech. **56**, 105–114 (2013)

[3] Paetsch, C., Dorfmann, L.: Stability of active muscle tissue. J. Eng. Math. in press (2015)

[4] Dorfmann, A., Trimmer, B.A., Woods, W.A.: A constitutive model for muscle properties in a soft-bodied arthropod. J. Roy. Soc. Interface **4**, 257–269 (2007)

[5] Wineman A.S., Rajagopal K.R.: Mechanical response of polymers. Cambridge Press (2000)

[6] Christensen R.M.: Theory of viscoelasticty. Dover (1982)

[7] Proske, U., Morgan, D.L.: Do cross-bridges contribute to the tension during stretch of passive muscle? J. Muscle Res. Cell M. **20**, 433–442 (1999)

[8] Mutungi, G., Ranatunga, K.W.: Do cross-bridges contribute to the tension during stretch of passive muscle? A response. J. Muscle Res. Cell M. **21**, 301–302 (2000)

[9] Bagni, M.A., Colombini, B., Geiger, P., Berlinguer Palmini, R., Cecchi G.: Non-cross-bridge calcium-dependent stiffness in frog muscle fibers. J. Physiol.-London **286**, 1353–1357 (2004)

[10] Campbell, K.S., Lakie, M.: A cross-bridge mechanism can explain the thixotropic short-range elastic component of relaxed frog skeletal muscle. J. Physiol.-London **510**, 941–962 (1998)

[11] Granzier, H.L., Labeit, S.: The giant protein titin: a major player in myocardial mechanics, signaling, and disease. Circ. Res. **94**, 284–295 (2004)

[12] Granzier, H.L., Wang, K.: Interplay between passive tension and strong and weak binding cross-bridges in insect indirect flight muscle. A functional dissection by gelsolin-mediated thin filament removal. J. Gen. Physiol. **101**, 235–270 (1993a)

[13] Granzier, H.L., Wang, K.: Passive tension and stiffness of vertebrate skeletal and insect flight muscles: The contribution of weak cross-bridges and elastic filaments. Biophys. J. **65**, 2141–2159 (1993b)

[14] Gosline, J., Lillie, M., Carrington, E., Guerette, P., Ortlepp, C., Savage, K.: Elastic proteins: Biological roles and mechanical properties. Phil. Trans. R. Soc. London B **357**, 121–132 (2002)

[15] Lieber, R.L., Leonard, M.E., Brown-Maupin, C.G.: Effects of muscle contraction on the load-strain properties of frog aponeurosis and tendon. Cells Tissues Organs **166**, 48–54 (2000)

[16] Powers, K., Schappacher-Tilp, G., Jinha, A. Leonard, T., Nishikawa, K., Herzog, W.: Titin force is enhanced in actively stretched skeletal muscle. J. Exp. Biol. **217**, 3629–3636 (2014)

[17] Gautel M.: The sarcomeric cytoskeleton: who picks up the strain? Curr. Opin. Cell Biol. **23**, 39–46 (2011)

[18] Ortega, J.O., Lindstedt, S.L., Nelson, F.E., Jubrias, S.A., Kushmerick, M.J., Conley, K.E.: Muscle force, work and cost: a novel technique to revisit the Fenn effect. J. Exp. Biol. doi: 10.1242/jeb114512 (2015)

[19] Hill, A.V.: The heat of shortening and the dynamic constants of muscle. Proc. R. Soc. London B **126**, 136–195 (1938)

[20] Martins, J.A.C., Pires, E.B., Salvado, R., Dinis, P.B.: A numerical model of passive and active behavior of skeletal muscles. Comput. Methods Appl. Mech. Eng. **151**, 419–433 (1998)

[21] Parente, M.P.L., Natal Jorge, R.M., Mascarenhas, T., Fernandes, A.A., Martins, J.A.C.: The influence of the material properties on the biomechanical behavior of the pelvic floor muscles during vaginal delivery. J. Biomech. **42**, 1301–1306 (2009)

[22] Tang, C.Y., Zhang, G., Tsui, C.P.: A 3D skeletal muscle model coupled with active contraction of muscle fibres and hyperelastic behavior. J. Biomech. **126**, 865–872 (2009)

[23] Palevski, A., Glaich, I., Portnoy, S., Linder-Ganz, E., Gefen, A.: Stress relaxation of porcine gluteus muscle subjected to sudden transverse deformation as related to pressure sore modeling. J. Biomech. **128**, 782–787 (2006)

[24] Van Loocke, M., Lyons, C.G., Simms, C.K.: Viscoelastic properties of passive skeletal muscle in compression: Stress-relaxation behaviour and constitutive modelling. J. Biomech. **41**, 1555–1566 (2008)

[25] Meyer, G.A., McCulloch, A.D., Lieber, R.L.: A nonlinear model of passive muscle viscosity. J. Appl. Mech.-T. ASME **133(091007)**, 1–9 (2011)

[26] Rehorn, M.R., Schroer, A.K., Blemker, S.S.: The passive properties of muscle fibers are velocity dependent. J. Biomech. **47**, 687–693 (2014)

[27] Bosboom, E.M.H., Hesselink, M.K.C., Oomens, C.W.J. , Bouten, C.V.C., Drost, M.R., Baaijens, F.P.T.: Passive transverse mechanical properties of skeletal muscle under in vivo compression. J. Biomech. **34**, 1365–1368 (2001)

[28] Van Loocke, M., Lyons, C.G., Simms, C.K.: A validated model of passive muscle in compression. J. Biomech. **39**, 2999–3009 (2006)

[29] Van Loocke, M., Lyons, C.G., Simms, C.K.: Viscoelastic properties of passive skeletal muscle in compression: Cyclic behaviour. J. Biomech. **42**, 1038–1048 (2009)

[30] Röhrle, O., Pullan, A. J.: Three-dimensional finite element modelling of muscle forces during mastication. J. Biomech. **40**, 3363–3372 (2007)

[31] Ito, D., Tanaka, E., Yamamoto, S.: A novel constitutive model of skeletal muscle taking into account anisotropic damage. J. Mech. Behavior Biomed. Mat. **3**, 85–93 (2010)

[32] Lu, Y.T., Zhu, H.X., Richmond, S., Middleton, J.: A visco-hyperelastic model for skeletal muscle tissue under high strain rates. J. Biomech. **43**, 2629–2632 (2010)

[33] Calvo, B., Sierra, M., Grasa, J., Mu noz, M. J., Pe na, E.: Determination of passive viscoelastic response of the abdominal muscle and related constitutive modeling: Stress-relaxation behavior. J. Mech. Behavior Biomed. Mat. **36**, 47–58 (2014)

[34] Dorfmann, A.L., Woods, W.A., Trimmer, B.A.: Muscle performance in a soft-bodied terrestrial crawler: Constitutive modeling of strain-rate dependency. J. Roy. Soc. Interface **5**, 349–362 (2008)

[35] Hunter, P.J., McCulloch, A.D., ter Keurs, H.E.D.J.: Modelling the mechanical properties of cardiac muscle. Prog. Biophys. Mol. Bio. **69**, 289–331 (1998)

[36] Hollenstein, M., Jabareen, M., Rubin, M.B.: Modeling a smooth elastic-inelastic transition with a strongly objective numerical integrator needing no iteration. Comput. Mech. **52**, 649–667 (2013)

[37] Perzyna, P.: The constitutive equations for rate sensitive plastic materials. Q. Appl. Math. **20**, 321–332 (1963)

[38] Lubliner, L., Taylor, R.L., Auricchio, F.: A new model of generalized plasticity and its numerical implementation. Int. J. Solids Structures **30**, 3171–3184 (1993)

[39] Panoskaltsis, V.P., Polymenakos, L.C., Soldatos, D.: On large deformation generalized plasticity. J. Mech. Mater. Struct. **3**, 441–457 (2008)

[40] Einav, I.: The unification of hypoplastic and elasto-plastic theories. Int. J. Solids Struct. **49**, 1305–1315 (2012)

[14] Flory, P.J.: Thermodynamic relations for highly elastic materials. Trans. Faraday Soc. **57**, 829–838 (1961)

[24] Ogden, R.W.: Nearly isochoric elastic deformations: application to rubberlike solids. J. Mech. Phys. Solids **26**, 37–57 (1978)

[43] Rubin, M.B., Attia, A.: Calculation of hyperelastic response of finitely deformed elastic-viscoplastic materials. Int. J. Numer. Methods Eng. **39**, 309–320 (1996)

[44] Rubin, M.B.: A simple and convenient isotropic failure surface. ASCE J. Engineering Mechanics **117**, 348–369 (1991)

[45] Rubin, M.B., Papes, O.: Advantages of formulating evolution equations for elastic-viscoplastic materials in terms of the velocity gradient instead of the spin tensor. J. Mech. Mater. Struct. **6**, 529–543 (2011)

[46] Simo, J.C.: Algorithms for static and dynamic multiplicative plasticity that preserve the classical return mapping schemes of the infinitesimal theory. Comput. Methods Appl. Mech. Eng. **99**, 61–112 (1992)

[47] Simo, J.C., Hughes, T.J.R.: Computational inelasticity. Springer, New York (1998)

[48] Papes, O.: Nonlinear continuum mechanics in engineering applications. Ph. D. dissertation DISS ETH NO 19956, ETH Zurich (2012)

[49] Dorfmann, A., Ogden., R.W.: A pseudo-elastic model for loading, partial unloading and reloading of particle-reinforced rubber. Int. J. Solids Struct. **40**, 2699–2714 (2003)

[50] Dorfmann, A., Ogden, R.W.: A constitutive model for the Mullins effect with permanent set in particle-reinforced rubber. Int. J. Solids Struct. **41**, 1855–1878 (2004)

[51] Dorfmann, A., Pancheri, F.Q.: A constitutive model for the Mullins effect with changes in material symmetry. Int. J. Nonlin. Mech. **47**, 874–887 (2012)

Chapter 3

Modeling of residually stressed materials with application to AAA

T. Ahamed[1], L. Dorfmann[1]

[1]Department of Civil and Environmental Engineering
Tufts University, Medford, MA

Abstruct

Growth and adaptation generate residual stress in many living tissues and systems that need to be incorporated in the definition of constitutive equations. This paper summarizes the general formulation of residual stresses and specifies all tensor quantities necessary to implement the three-dimensional theory in a nonlinear finite element code. Verification and validation is performed by evaluating the wall stress distribution of an abdominal aortic aneurysm (AAA) using patient specific geometry and material model parameters. A number of human AAA specimens are characterized in biaxial extension and their responses averaged to obtain representative stress-stretch data. The material is anisotropic having two preferred directions representing the orientation of the collagen fibers in the aortic tissue. The numerical results show that the residual stress in the material modifies the wall stress distribution by reducing the stress gradient across the wall thickness. A large amount of published information is available to characterize the correlation between wall stress distribution and medical implications.

3.1 Introduction

Stresses in a body, in the absence of any applied loads, are defined as residual stresses. Experimental work by Holzapfel and Ogden [19], Nienhaus et al. [22], Tierney et al. [37], Vandiver and Goriely [39] show the presence of residual stress in plants, human tissues, insects and other animals. These are due to tissue growth and remodeling and we refer to [6, 33, 36, 39, 42, 43] and to references therein for a detailed discussion.

The presence of residual stress in biological materials has been known for a long time, but their implications and consequences on the behavior of the biological system, from a biomechanics point of view, are yet to be fully appreciated. This has created great interest during the last few years and many valuable publications followed.

To characterize the influence of residual stresses on the behavior of biological systems it is necessary to determine their actual spacial distribution. Fung [15] emphasized the influence of residual stress to explain the experimentally observed responses of tubular sections of arterial tissue and introduced the opening angle experiment to quantify the corresponding magnitude [8]. This technique was used by Vaishnav and Vossoughi [38] to estimate the residual stress distribution and the corresponding strains in bovine and porcine aortas. In a seminal publication, Holzapfel and Ogden [19] developed an analytical method to determine the layer specific residual stress distribution of the human aorta using the magnitude of the opening angle as an input parameter. Experimental techniques have been used by Costa et al. [9] and Wang et al. [41] to measure, respectively, the three-dimensional residual strain distribution of canine left ventricle and the residual deformation of ocular tissue, which were then used to determine the residual stress. The influence of tissue growth on generating residual stress in biological materials has been investigated by Olsson and Klarbring [27], Polzer et al. [30], Skalak et al. [33].

Fung [15], and Chuong and Fung [8] emphasized the need to include residual stress in any analysis to determining the actual stress distribution in the material. Holzapfel et al. [18], using appropriate constitutive equations, performed an analytical stress analyses of the arterial wall to compare the stress distribution with and without taking residual stress into account. Analytical methods to determine the arterial wall stress distributions assume, in general, a circular tube of incompressible material, with constant cross section and wall thickness subject to a constant pressure. Analytical methods must be replaced by numerical approximations if these calculations are to be applied to patient specific geometries.

The numerical approach proposed by Shams et al. [32] and Wang et al. [40] used a modified constitutive formulation to including residual stress of human left ventricle. Pierce et al. [29] used a finite element formulation to determine the wall stress distribution

of patient-specific AAA's including the effect of residual stress. The paper by Pierce et al. [29] presents results, but did not include derivations necessary to implement the constitutive formulation in a nonlinear finite element solution scheme.

In this study we summarize the main tensorial quantities that are required for a numerical solution of boundary value problems with arbitrary geometry and loading. Explicit expression are given when deemed necessary. The formulation is verified and validated by simulating the wall stress distribution in a patient specific AAA geometry using experimentally determine material parameters. The outline of the paper is as follows. We begin in Section 3.2 with an overview of the basic equations required to present a hyperelastic, invariant based anisotropic constitutive law that includes residual stresses. Section 3.3 contains the increments of the kinematic and energy expressions that are necessary to derive the fourth-order elasticity tensor. In Section 3.3.2 the general constitutive formulation is specialized and in Section 3.3.3 a simple form of residual stress estimation is given. Section 3.4 describes the patient specific finite element model, the patient based material parameters, fiber orientations and the numerical results.

3.2 Basic equations

3.2.1 Kinematic

The region $\mathcal{B}_\mathrm{r}$ occupied by an unloaded and residually stressed deformable body is chosen as reference configuration from which the deformation is measured. The location of any material particle in $\mathcal{B}_\mathrm{r}$ is identified by its position vector $\mathbf{X}$ relative to some origin. Let $\mathcal{B}$ denote the configuration of the body obtained by a continuous transformation $\mathbf{x} = \boldsymbol{\chi}(\mathbf{X})$, where the vector function $\boldsymbol{\chi}$ assigns to each point $\mathbf{X}$ a unique position $\mathbf{x}$ in $\mathcal{B}$ and vice versa. The deformation gradient tensor relative to the configuration $\mathcal{B}_\mathrm{r}$ is defined by

$$\mathbf{F} = \frac{\partial \boldsymbol{\chi}(\mathbf{X})}{\partial \mathbf{X}} = \frac{\partial \mathbf{x}}{\partial \mathbf{X}}, \tag{3.1}$$

with Cartesian components $F_{i\alpha} = \partial x_i / \partial X_\alpha$, where $i, \alpha \in \{1, 2, 3\}$. Roman indices are associated with the current configuration $\mathcal{B}$ and Greek indices with the reference configuration $\mathcal{B}_\mathrm{r}$. We also use the standard notation J to denote the volume ratio given by

$$J = \det \mathbf{F} = \frac{\mathrm{d}v}{\mathrm{d}V} > 0, \tag{3.2}$$

where $\mathrm{d}v$ and $\mathrm{d}V$ denote corresponding volume elements in $\mathcal{B}$ and $\mathcal{B}_\mathrm{r}$, respectively. Frequently, deformations of many biological materials are said to be isochoric such that $J = 1$ (volume-preserving), which is of course an idealization. In the following we

relax this constraint and assume the general case of compressible materials with $J \neq 1$. Following the developments given by Flory [14] and Ogden [23, 24] we adopt the multiplicative decomposition of the total deformation into volumetric and isochoric parts expressed by

$$\mathbf{F} = (J^{1/3})\bar{\mathbf{F}}, \tag{3.3}$$

where $\bar{\mathbf{F}}$ is the isochoric portion of the deformation with $\det \bar{\mathbf{F}} = 1$. For further details on decomposition of the deformation, refer to Holzapfel [17]. The isochoric right and left Cauchy-Green tensors are, respectively, given by

$$\bar{\mathbf{C}} = \bar{\mathbf{F}}^{\mathrm{T}}\bar{\mathbf{F}}, \qquad \bar{\mathbf{B}} = \bar{\mathbf{F}}\bar{\mathbf{F}}^{\mathrm{T}}, \tag{3.4}$$

with the principle invariants of $\bar{\mathbf{C}}$ (equivalently $\bar{\mathbf{B}}$) written

$$\bar{I}_1 = \mathrm{tr}\,\bar{\mathbf{C}}, \quad \bar{I}_2 = \frac{1}{2}\left[(\mathrm{tr}\,\bar{\mathbf{C}})^2 - \mathrm{tr}\left(\bar{\mathbf{C}}^2\right)\right], \quad \bar{I}_3 \equiv 1, \tag{3.5}$$

where tr denotes the trace of the second-order tensor.

Unit vectors $\mathbf{M}$ and $\mathbf{M}'$ are introduced to denote the two preferred directions of an anisotropic material in the reference configuration $\mathcal{B}_{\mathrm{r}}$ and, following the work by Ogden [25], define the structure tensors $\mathbf{M} \otimes \mathbf{M}$ and $\mathbf{M}' \otimes \mathbf{M}'$. Spencer and Rivlin [35] and Spencer [34] showed that the integrity bases for three 3×3 matrices, in addition to $\bar{I}_1, \bar{I}_2, \bar{I}_3$, include additional invariants that depend on $\mathbf{M} \otimes \mathbf{M}$ and $\mathbf{M}' \otimes \mathbf{M}'$. Since $\mathbf{M}$ and $\mathbf{M}'$ are unit vectors, these are calculated as

$$\bar{I}_4 = \mathbf{M} \cdot (\bar{\mathbf{C}}\mathbf{M}), \quad \bar{I}_5 = \mathbf{M} \cdot (\bar{\mathbf{C}}^2\mathbf{M}), \quad \bar{I}_6 = \mathbf{M}' \cdot (\bar{\mathbf{C}}\mathbf{M}'), \quad \bar{I}_7 = \mathbf{M}' \cdot (\bar{\mathbf{C}}^2\mathbf{M}'), \tag{3.6}$$

with the remaining invariant quantities a function of both fiber directions

$$\mathbf{M} \cdot (\bar{\mathbf{C}}\mathbf{M}'), \quad \mathbf{M} \cdot (\bar{\mathbf{C}}^2\mathbf{M}'). \tag{3.7}$$

Note that $(3.7)_2$ is not independent and can therefore be eliminated.

3.2.2 Residual stress

An initial stress in the unloaded reference configuration $\mathcal{B}_{\mathrm{r}}$ is defined as residual stress by Hoger [16], Shams et al. [32] and Ogden [26]. In the absence of body forces, surface traction and intrinsic couple stresses the residual stress, denoted by $\boldsymbol{\tau}$, is symmetric and satisfies the equilibrium equation

$$\mathrm{Div}\,\boldsymbol{\tau} = \mathbf{0}, \tag{3.8}$$

where Div denotes the divergence operator with respect to $\mathcal{B}_\mathrm{r}$. Since there are no surface traction applied to the boundary $\partial\mathcal{B}_\mathrm{r}$ the residual stress must also satisfy the boundary condition

$$\boldsymbol{\tau}\mathbf{N} = \mathbf{0}, \tag{3.9}$$

where $\mathbf{N}$ is the unit normal at $\mathbf{X}$, which implies that the residual stress in $\mathcal{B}_\mathrm{r}$ is non-uniform. When modeling the mechanical response of arterial tissue, specifically the response of abdominal aortic aneurysm, the residual stress is due to growth and remodeling and we refer to [19] and to the references therein for a detailed discussion.

The integrity bases for three 3×3 symmetric matrices, given by equation (3.5), (3.6) and (3.7), need to be expanded to four 3×3 matrices. Specifically, the matrices corresponding to the tensors $\mathbf{C}, \mathbf{M}\otimes\mathbf{M}, \mathbf{M}'\otimes\mathbf{M}'$ and $\boldsymbol{\tau}$. Again, following Spencer and Rivlin [35], the additional invariants are defined as

$$\bar{I}_8 = \mathrm{tr}(\bar{\mathbf{C}}\boldsymbol{\tau}), \quad \bar{I}_9 = \mathrm{tr}(\bar{\mathbf{C}}\boldsymbol{\tau}^2), \quad \bar{I}_{10} = \mathrm{tr}(\bar{\mathbf{C}}^2\boldsymbol{\tau}), \quad \bar{I}_{11} = \mathrm{tr}(\bar{\mathbf{C}}^2\boldsymbol{\tau}^2), \tag{3.10}$$

together with the invariant quantities

$$\mathbf{M}\cdot(\bar{\mathbf{C}}\boldsymbol{\tau}\mathbf{M}), \quad \mathbf{M}\cdot(\bar{\mathbf{C}}\boldsymbol{\tau}^2\mathbf{M}), \quad \mathbf{M}\cdot(\bar{\mathbf{C}}^2\boldsymbol{\tau}\mathbf{M}), \quad \mathbf{M}\cdot(\bar{\mathbf{C}}^2\boldsymbol{\tau}^2\mathbf{M}), \tag{3.11}$$

$$\mathbf{M}'\cdot(\bar{\mathbf{C}}\boldsymbol{\tau}\mathbf{M}'), \quad \mathbf{M}'\cdot(\bar{\mathbf{C}}\boldsymbol{\tau}^2\mathbf{M}'), \quad \mathbf{M}'\cdot(\bar{\mathbf{C}}^2\boldsymbol{\tau}\mathbf{M}'), \quad \mathbf{M}'\cdot(\bar{\mathbf{C}}^2\boldsymbol{\tau}^2\mathbf{M}'), \tag{3.12}$$

$$\mathbf{M}\cdot(\bar{\mathbf{C}}\boldsymbol{\tau}\mathbf{M}'), \quad \mathbf{M}\cdot(\bar{\mathbf{C}}\boldsymbol{\tau}^2\mathbf{M}'), \quad \mathbf{M}\cdot(\bar{\mathbf{C}}^2\boldsymbol{\tau}\mathbf{M}'), \quad \mathbf{M}\cdot(\bar{\mathbf{C}}^2\boldsymbol{\tau}^2\mathbf{M}'), \tag{3.13}$$

where the last two expressions in (3.13) are not independent. For an unconstrained material there are thus a total of 22 invariants, for an incompressible material $I_3 \equiv 1$ and the number reduces to 21.

3.2.3 Hyperelastic material

The theory of hyperelasticity describes the elastic response of a material using a strain energy function W defined per unit volume in the reference configuration $\mathcal{B}_\mathrm{r}$. For an isotropic material, in the absence of residual stress, the energy W depends only on the deformation gradient $\mathbf{F}$ and we write $W = W(\mathbf{F})$. For a residually stressed, anisotropic elastic solid with two preferred directions, W depends on $\mathbf{F}$, on the structure tensors $\mathbf{M}\otimes\mathbf{M}$, $\mathbf{M}'\otimes\mathbf{M}'$ and also on the residual stress $\boldsymbol{\tau}$. This is represented by

$$W = W\left(\mathbf{F}, \mathbf{M}\otimes\mathbf{M}, \mathbf{M}'\otimes\mathbf{M}', \boldsymbol{\tau}\right) \tag{3.14}$$

where $\boldsymbol{\tau} = \boldsymbol{\tau}(\mathbf{X})$. For a hyperelastic material the stress rate of working is associated entirely with stored energy. The energy balance equation, written in terms of the the

nominal stress tensor $\mathbf{S}$, leads to the connection

$$\mathbf{S} = \frac{\partial W}{\partial \mathbf{F}}, \quad S_{\alpha i} = \frac{\partial W}{\partial F_{i\alpha}}, \tag{3.15}$$

which identifies the convention for the order of the indices in the differentiation with respect to a non symmetric second-order tensor. Integration over a surface and the use of Nanson's formula [12] gives the Cauchy stress tensor

$$\boldsymbol{\sigma} = J^{-1}\mathbf{F}\frac{\partial W}{\partial \mathbf{F}}, \quad \sigma_{ij} = J^{-1}F_{i\alpha}\frac{\partial W}{\partial F_{j\alpha}}. \tag{3.16}$$

A strain energy function must be independent of superimposed rigid body deformations, which requires W to be an isotropic function of the four tensors $\mathbf{F}, \mathbf{M}\otimes\mathbf{M}, \mathbf{M}'\otimes\mathbf{M}', \boldsymbol{\tau}$. Then, the form of W is reduced to the dependence on the finite integrity bases of these quantities.

Following Bose and Dorfmann [7] we assume a decoupled energy function

$$W = \bar{W}\left(\bar{\mathbf{F}}, \mathbf{M}\otimes\mathbf{M}, \mathbf{M}'\otimes\mathbf{M}', \boldsymbol{\tau}\right) + U(J) \tag{3.17}$$

where $\bar{W}$ and $U(J)$ denote the volume-preserving (distortional) and volumetric (dilatational) contributions, respectively. In order to reduce the number of material parameters, we consider a reduced form of the integrity bases and write the energy in the form

$$W = \bar{W}\left(\bar{I}_1, \bar{I}_2, \bar{I}_4, \bar{I}_6, \bar{I}_8\right) + U(J) \tag{3.18}$$

where, for simplicity, we kept the same notation to denote the energy function W. The use of the decomposition (3.18) in (3.15) gives the isochoric and volumetric components of the nominal stress, denoted respectively by $\bar{\mathbf{S}}$ and $\mathbf{S}_{\text{vol}}$, as

$$\mathbf{S} = \bar{\mathbf{S}} + \mathbf{S}_{\text{vol}} = \sum_{i\in\mathcal{I}} \bar{W}_i \frac{\partial \bar{I}_i}{\partial \mathbf{F}} + \frac{\mathrm{d}U}{\mathrm{d}J}\frac{\mathrm{d}J}{\mathrm{d}\mathbf{F}}, \quad \boldsymbol{\sigma} = J^{-1}\mathbf{F}\mathbf{S}, \tag{3.19}$$

where the index set $\mathcal{I} = \{1, 2, 4, 6, 8\}$ is defined for notational convenience and $\bar{W}_i = \partial\bar{W}/\partial\bar{I}_i, i \in \mathcal{I}$. When the dependence on $\bar{I}_4, \bar{I}_6, \bar{I}_8$ is omitted from (3.19), the corresponding expression for an isotropic material is obtained. The derivatives of the invariants and of J with respect to the deformation gradient $\mathbf{F}$ are needed to derive the explicit expressions of the nominal stress components $\bar{\mathbf{S}}$ and $\mathbf{S}_{\text{vol}}$. For reference these

are summarized here in the form

$$\frac{\partial \bar{I}_1}{\partial \mathbf{F}} = 2J^{-1/3}\left[\bar{\mathbf{F}}^{\mathrm{T}} - \frac{1}{3}\bar{I}_1\bar{\mathbf{F}}^{-1}\right], \tag{3.20}$$

$$\frac{\partial \bar{I}_2}{\partial \mathbf{F}} = 2J^{-1/3}\left[\bar{I}_1\bar{\mathbf{F}}^{\mathrm{T}} - \bar{\mathbf{F}}^{\mathrm{T}}\bar{\mathbf{F}}\bar{\mathbf{F}}^{\mathrm{T}} - \frac{2}{3}\bar{I}_2\bar{\mathbf{F}}^{-1}\right], \tag{3.21}$$

$$\frac{\partial \bar{I}_4}{\partial \mathbf{F}} = 2J^{-1/3}\left[\mathbf{M}\otimes\bar{\mathbf{F}}\mathbf{M} - \frac{1}{3}\bar{I}_4\bar{\mathbf{F}}^{-1}\right], \tag{3.22}$$

$$\frac{\partial \bar{I}_6}{\partial \mathbf{F}} = 2J^{-1/3}\left[\mathbf{M}'\otimes\bar{\mathbf{F}}\mathbf{M}' - \frac{1}{3}\bar{I}_6\bar{\mathbf{F}}^{-1}\right], \tag{3.23}$$

$$\frac{\partial \bar{I}_8}{\partial \mathbf{F}} = 2J^{-1/3}\left[\boldsymbol{\tau}\bar{\mathbf{F}}^{\mathrm{T}} - \frac{1}{3}\bar{I}_8\bar{\mathbf{F}}^{-1}\right], \tag{3.24}$$

and

$$\frac{\mathrm{d}J}{\mathrm{d}\mathbf{F}} = J\mathbf{F}^{-1}. \tag{3.25}$$

Using equation (3.19) and substituting (3.20)-(3.25) gives the explicit expression of the Cauchy stress $\boldsymbol{\sigma}$ and its isochoric and volumetric components. These are denoted respectively by $\bar{\boldsymbol{\sigma}}$ and $\boldsymbol{\sigma}_{\mathrm{vol}}$ and have the forms

$$\begin{aligned}\bar{\boldsymbol{\sigma}} = 2J^{-1}\Bigg[&\bar{W}_1\left(\bar{\mathbf{B}} - \frac{1}{3}\bar{I}_1\mathbf{I}\right) + \bar{W}_2\left(\bar{I}_1\bar{\mathbf{B}} - \bar{\mathbf{B}}^2 - \frac{2}{3}\bar{I}_2\mathbf{I}\right) + \bar{W}_4\left(\bar{\mathbf{m}}\otimes\bar{\mathbf{m}} - \frac{1}{3}\bar{I}_4\mathbf{I}\right)\\ &+ \bar{W}_6\left(\bar{\mathbf{m}}'\otimes\bar{\mathbf{m}}' - \frac{1}{3}\bar{I}_6\mathbf{I}\right) + \bar{W}_8\left(\bar{\mathbf{F}}\boldsymbol{\tau}\bar{\mathbf{F}}^{\mathrm{T}} - \frac{1}{3}\bar{I}_8\mathbf{I}\right)\Bigg],\end{aligned} \tag{3.26}$$

and

$$\boldsymbol{\sigma}_{\mathrm{vol}} = \frac{\mathrm{d}U}{\mathrm{d}J}\mathbf{I}, \tag{3.27}$$

where $\bar{\mathbf{m}} = \bar{\mathbf{F}}\mathbf{M}$ and $\bar{\mathbf{m}}' = \bar{\mathbf{F}}\mathbf{M}'$.

Expressions (3.26) and (3.27) can be written more concisely by introducing the deviatoric operator defined as $\mathrm{dev}(\mathbf{A}) = \mathbb{P} : \mathbf{A}$, where the fourth-order projection tensor $\mathbb{P}$ has components $\mathbb{P}_{ijkl} = \delta_{ik}\delta_{jl} - (1/3)\delta_{ij}\delta_{kl}$ and $\mathbf{A}$ is a second-order symmetric tensor. The component form of $\mathbb{P} : \mathbf{A}$ is $\mathbb{P}_{ijkl}A_{kl}$. The total Cauchy stress $\boldsymbol{\sigma} = \bar{\boldsymbol{\sigma}} + \boldsymbol{\sigma}_{\mathrm{vol}}$ can then be written in a more compact form

$$\begin{aligned}\boldsymbol{\sigma} = 2J^{-1}\Big[&\bar{W}_1\,\mathrm{dev}\,\bar{\mathbf{B}} + \bar{W}_2\,\mathrm{dev}\left(\bar{I}_1\bar{\mathbf{B}} - \bar{\mathbf{B}}^2\right) + \bar{W}_4\,\mathrm{dev}\left(\bar{\mathbf{m}}\otimes\bar{\mathbf{m}}\right)\\ &+ \bar{W}_6\,\mathrm{dev}\left(\bar{\mathbf{m}}'\otimes\bar{\mathbf{m}}'\right) + \bar{W}_8\,\mathrm{dev}\,\bar{\boldsymbol{\Sigma}}\Big] + \frac{\mathrm{d}U}{\mathrm{d}J}\mathbf{I},\end{aligned} \tag{3.28}$$

where we used the notation $\bar{\boldsymbol{\Sigma}} = \bar{\mathbf{F}}\boldsymbol{\tau}\bar{\mathbf{F}}^{\mathrm{T}}$ used in, for example, [26, 32] and [21].

3.3 Numerical solution

Exact solutions are possible only for a limited number of problems restricting the use of a constitutive model to simple geometries and boundary conditions [21]. In this section we develop the tensor quantities required for implementing a nearly incompressible, anisotropic and residually stressed material in the finite element package ABAQUS [1].

Consider a small virtual incremental displacement superimposed on $\boldsymbol{\chi}(\mathbf{X})$, which we denote by $\delta\mathbf{u}$. Through the transformation $\mathbf{x} = \boldsymbol{\chi}(\mathbf{X})$ we define $\delta\mathbf{u}$ as an Eulerian quantity and write

$$\delta\mathbf{F} = \delta\mathbf{l}\mathbf{F}, \tag{3.29}$$

where $\delta\mathbf{l}$ is the virtual displacement gradient. This can be decomposed into the sum of a symmetric and an antisymmetric part as

$$\delta\mathbf{l} = \delta\mathbf{d} + \delta\mathbf{w}, \tag{3.30}$$

where $\delta\mathbf{d}$ is the first variation of the rate-of-deformation and $\delta\mathbf{w}$ the first variation of the continuum spin. These are give by

$$\delta\mathbf{d} = \frac{1}{2}\left(\delta\mathbf{l} + \delta\mathbf{l}^{\mathrm{T}}\right), \quad \delta\mathbf{w} = \frac{1}{2}\left(\delta\mathbf{l} - \delta\mathbf{l}^{\mathrm{T}}\right), \tag{3.31}$$

which are respectively symmetric and antisymmetric.

The numerical solution is based on a variational formulation of the boundary-value problem. For completeness, we recall the internal virtual work expression in the form

$$\int_{\mathcal{B}} \boldsymbol{\sigma} : \delta\mathbf{l}\,\mathrm{d}v = \int_{\mathcal{B}_{\mathrm{r}}} J\boldsymbol{\sigma} : \delta\mathbf{l}\,\mathrm{d}V, \tag{3.32}$$

where the transformation $\mathrm{d}v = J\mathrm{d}V$ is used to convert the integral from the current region $\mathcal{B}$ to the reference region $\mathcal{B}_{\mathrm{r}}$. For consistency with the notation used in ABAQUS [1], the operator : is used to define, for a pair of second order tensors $\mathbf{A}$ and $\mathbf{B}$, the double contraction $A_{ij}B_{ij}$. Since the Cauchy stress is symmetric the integrand $\boldsymbol{\sigma} : \delta\mathbf{l}$ may also be written as $\boldsymbol{\sigma} : \delta\mathbf{d}$.

Consider a small incremental displacement superimposed on the configuration $\mathcal{B}$, which for convenience, is treated as a function of $\mathbf{x}$ and denoted by $\mathrm{d}\mathbf{u}$. This leads to the important connection

$$\mathrm{d}\mathbf{F} = \mathrm{d}\mathbf{l}\,\mathbf{F}, \tag{3.33}$$

where $\mathrm{d}\mathbf{l}$ is the spatial gradient of $\mathrm{d}\mathbf{u}$, with components defined by $\mathrm{d}l_{ij} = \partial \mathrm{d}u_i/\partial x_j$. Following the same argument as in (3.30), the incremental displacement gradient $\mathrm{d}\mathbf{l}$ can

be additively decomposed into symmetric and antisymmetric parts denoted $\mathrm{d}\mathbf{d}$ and $\mathrm{d}\mathbf{w}$, respectively.

The use of Newton's method to solve the non-linear equilibrium equations requires linearization of the internal virtual work expression as

$$\mathrm{d}\delta W_{\mathrm{int}} = \int_{\mathcal{B}_{\mathrm{r}}} [\mathrm{d}(J\boldsymbol{\sigma}) : \delta\mathbf{d} + J\boldsymbol{\sigma} : \mathrm{d}\delta\mathbf{d}]\, \mathrm{d}V, \tag{3.34}$$

where here and henceforth the operator d is used to denote the increment of the quantity concerned. For an overview of variational formulations applicable to incompressible and nearly incompressible materials we refer to Holzapfel [17] and Adler et al. [2].

Constitutive equations in ABAQUS [1] must be given in rate form as a relation between the Kirchhoff stress rate, $\mathrm{d}(J\boldsymbol{\sigma})$, and the rate of deformation $\mathrm{d}\mathbf{d}$. Objectivity of the stress rate resulting from the evaluation of $\mathrm{d}(J\boldsymbol{\sigma})$ is not guaranteed and, using continuum elements, the Jaumann rate of the Kirchhoff stress is required. The notation defined by Prot and Skallerud [31] is used to write the Jaumann rate of $J\boldsymbol{\sigma}$ as

$$\mathrm{d}^{\nabla J}(J\boldsymbol{\sigma}) = \mathrm{d}(J\boldsymbol{\sigma}) - J(\mathrm{d}\mathbf{w}\boldsymbol{\sigma} - \boldsymbol{\sigma}\mathrm{d}\mathbf{w}), \tag{3.35}$$

$$= \mathbb{C}^{\nabla J} : \mathrm{d}\mathbf{d}, \tag{3.36}$$

where the operator $\mathrm{d}^{\nabla J}$ denotes the increment determined from the Jaumann rate and $\mathbb{C}^{\nabla J}$ is the corresponding symmetric fourth-order elasticity tensor. Equating the right-hand sides of equations (3.35) and (3.36) and solving for $\mathrm{d}(J\boldsymbol{\sigma})$ gives

$$\mathrm{d}\left(J\boldsymbol{\sigma}\right) = J\left(J^{-1}\mathbb{C}^{\nabla J} : \mathrm{d}\mathbf{d} + \mathrm{d}\mathbf{w}\boldsymbol{\sigma} - \boldsymbol{\sigma}\mathrm{d}\mathbf{w}\right). \tag{3.37}$$

ABAQUS [1] requires that the fourth-order elasticity tensor be implemented as

$$\mathbb{C} = J^{-1}\mathbb{C}^{\nabla J}, \tag{3.38}$$

as specified in Section 4.6 of the Abaqus Theory Manual. The Kirchhoff stress rate of the isochoric and volumetric components of the Cauchy stress tensor are denoted by $\mathrm{d}(J\bar{\boldsymbol{\sigma}})$ and $\mathrm{d}(J\boldsymbol{\sigma}_{\mathrm{vol}})$, respectively. Equation (3.37) is then additively decomposed as

$$\mathrm{d}(J\bar{\boldsymbol{\sigma}}) = J(J^{-1}\bar{\mathbb{C}}^{\nabla \mathrm{J}} : \mathrm{d}\mathbf{d} + \mathrm{d}\mathbf{w}\bar{\boldsymbol{\sigma}} - \bar{\boldsymbol{\sigma}}\mathrm{d}\mathbf{w}), \tag{3.39}$$

and

$$\mathrm{d}(J\boldsymbol{\sigma}_{\mathrm{vol}}) = J(J^{-1}\mathbb{C}_{\mathrm{vol}}^{\nabla \mathrm{J}} : \mathrm{d}\mathbf{d}), \tag{3.40}$$

where $\bar{\mathbb{C}}^{\nabla \mathrm{J}}$ is the isochoric part of the elasticity tensor and $\mathbb{C}_{\mathrm{vol}}^{\nabla \mathrm{J}}$ is the volumetric part. The final form of the elasticity tensor is then given by

$$\mathbb{C} = J^{-1}(\bar{\mathbb{C}}^{\nabla \mathrm{J}} + \mathbb{C}_{\mathrm{vol}}^{\nabla \mathrm{J}}). \tag{3.41}$$

3.3.1 Fourth-order elasticity tensor

This subsection summarizes the derivation of the fourth-order elasticity tensor of a hyperelastic, anisotropic and residually stressed material. An energy function with a reduced number of invariants is used to keep the derivation simple and concise. Thus, the formulation (3.18) is replaced by

$$W = \bar{W}(\bar{I}_1, \bar{I}_4, \bar{I}_6, \bar{I}_8) + U(J), \tag{3.42}$$

which allows to rewrite equation (3.28) as

$$\begin{aligned} \boldsymbol{\sigma} = 2J^{-1} \big[& \bar{W}_1 \mathrm{dev}\, \bar{\mathbf{B}} + \bar{W}_4 \mathrm{dev}\,(\bar{\mathbf{m}} \otimes \bar{\mathbf{m}}) \\ & + \bar{W}_6 \mathrm{dev}\,(\bar{\mathbf{m}}' \otimes \bar{\mathbf{m}}') + \bar{W}_8 \mathrm{dev}\, \bar{\boldsymbol{\Sigma}} \big] + \frac{\mathrm{d}U}{\mathrm{d}J} \mathbf{I}. \end{aligned} \tag{3.43}$$

The increment of the isochoric part of equation (3.43) can be written as

$$\begin{aligned} \mathrm{d}(J\bar{\boldsymbol{\sigma}}) = 2 \big[& \mathrm{d}\bar{W}_1 \mathrm{dev}\, \bar{\mathbf{B}} + \bar{W}_1\ \mathrm{d}(\mathrm{dev}\, \bar{\mathbf{B}}) \\ & + \mathrm{d}\bar{W}_4 \mathrm{dev}\,(\bar{\mathbf{m}} \otimes \bar{\mathbf{m}}) + \bar{W}_4\ \mathrm{d}(\mathrm{dev}\,(\bar{\mathbf{m}} \otimes \bar{\mathbf{m}})) \\ & + \mathrm{d}\bar{W}_6 \mathrm{dev}\,(\bar{\mathbf{m}}' \otimes \bar{\mathbf{m}}') + \bar{W}_6\ \mathrm{d}(\mathrm{dev}\,(\bar{\mathbf{m}}' \otimes \bar{\mathbf{m}}')) \\ & + \mathrm{d}\bar{W}_8 \mathrm{dev}\, \bar{\boldsymbol{\Sigma}} + \bar{W}_8 \mathrm{d}(\mathrm{dev}\, \bar{\boldsymbol{\Sigma}}) \big]. \end{aligned} \tag{3.44}$$

For convenience, the expression of the increments $\mathrm{d}\bar{W}_i$, $i \in \{1, 4, 6, 8\}$ are written as

$$\begin{aligned} \mathrm{d}\bar{W}_1 &= \bar{W}_{11}\mathrm{d}\bar{I}_1 + \bar{W}_{14}\mathrm{d}\bar{I}_4 + \bar{W}_{16}\mathrm{d}\bar{I}_6 + \bar{W}_{18}\mathrm{d}\bar{I}_8, \\ \mathrm{d}\bar{W}_4 &= \bar{W}_{14}\mathrm{d}\bar{I}_1 + \bar{W}_{44}\mathrm{d}\bar{I}_4 + \bar{W}_{46}\mathrm{d}\bar{I}_6 + \bar{W}_{48}\mathrm{d}\bar{I}_8, \\ \mathrm{d}\bar{W}_6 &= \bar{W}_{16}\mathrm{d}\bar{I}_1 + \bar{W}_{46}\mathrm{d}\bar{I}_4 + \bar{W}_{66}\mathrm{d}\bar{I}_6 + \bar{W}_{68}\mathrm{d}\bar{I}_8, \\ \mathrm{d}\bar{W}_8 &= \bar{W}_{18}\mathrm{d}\bar{I}_1 + \bar{W}_{48}\mathrm{d}\bar{I}_4 + \bar{W}_{68}\mathrm{d}\bar{I}_6 + \bar{W}_{88}\mathrm{d}\bar{I}_8, \end{aligned} \tag{3.45}$$

where $\bar{W}_{ij} = \partial^2 \bar{W} / \partial \bar{I}_i \partial \bar{I}_j$, $\{i, j\} \in \{1, 4, 6, 8\}$. The increment of the invariants are given, respectively, by

$$\begin{aligned} \mathrm{d}\bar{I}_1 &= 2\mathrm{dev}\, \bar{\mathbf{B}} : \mathrm{d}\mathbf{d}, \quad \mathrm{d}\bar{I}_4 = 2\mathrm{dev}\,(\bar{\mathbf{m}} \otimes \bar{\mathbf{m}}) : \mathrm{d}\mathbf{d}, \\ \mathrm{d}\bar{I}_6 &= 2\mathrm{dev}\,(\bar{\mathbf{m}}' \otimes \bar{\mathbf{m}}') : \mathrm{d}\mathbf{d}, \quad \mathrm{d}\bar{I}_8 = 2\mathrm{dev}\, \bar{\boldsymbol{\Sigma}} : \mathrm{d}\mathbf{d}, \end{aligned} \tag{3.46}$$

where, $\mathrm{d}\mathbf{d}$ is the symmetric part of incremental displacement gradient $\mathrm{d}\mathbf{l}$. The increment of $\mathrm{dev}\,\bar{\mathbf{B}}$, which can be obtained by

$$\mathrm{d}(\mathrm{dev}\,\bar{\mathbf{B}}) = \mathrm{d}(\mathbb{P} : \bar{\mathbf{B}}) = \mathbb{P} : \mathrm{d}\bar{\mathbf{B}} = \mathrm{dev}\,(\mathrm{d}\bar{\mathbf{B}}), \tag{3.47}$$

where, $\mathbb{P}$ is the fourth-order projection tensor defined in Section 3.2.3. The increment of $\bar{\mathbf{B}}$ can be written as

$$\mathrm{d}\bar{\mathbf{B}} = \mathbb{H} : \mathrm{d}\mathbf{e} + \mathrm{d}\mathbf{w}\,\bar{\mathbf{B}} - \bar{\mathbf{B}}\,\mathrm{d}\mathbf{w}, \tag{3.48}$$

where the fourth-order tensor $\mathbb{H}$ has the form $\mathbb{H}_{ijkl} = 1/2(\delta_{ik}\bar{B}_{jl}+\delta_{il}\bar{B}_{jk}+\bar{B}_{ik}\delta_{jl}+\bar{B}_{il}\delta_{jk})$ and $\mathrm{d}\mathbf{e} = \mathrm{dev}\,(\mathrm{d}\mathbf{d})$ denotes the increment of the deviatoric strain rate. Equation (3.47) can now be written in an alternative forms

$$\mathrm{d}(\mathrm{dev}\,\bar{\mathbf{B}}) = \mathrm{dev}\,(\mathbb{H} : \mathrm{d}\mathbf{e}) + \mathrm{d}\mathbf{w}\,\bar{\mathbf{B}} - \bar{\mathbf{B}}\,\mathrm{d}\mathbf{w}, \tag{3.49}$$

and

$$\mathrm{d}(\mathrm{dev}\,\bar{\mathbf{B}}) = \left[\mathbb{H} - \frac{2}{3}(\mathbf{I}\otimes\bar{\mathbf{B}} + \bar{\mathbf{B}}\otimes\mathbf{I}) + \frac{2}{9}I_1\mathbf{I}\otimes\mathbf{I}\right] : \mathrm{d}\mathbf{d} + \mathrm{d}\mathbf{w}\bar{\mathbf{B}} - \bar{\mathbf{B}}\mathrm{d}\mathbf{w}. \tag{3.50}$$

Following a similar process that leads to equation (3.50), the increments of $\mathrm{dev}\,(\bar{\mathbf{m}}\otimes\bar{\mathbf{m}})$, $\mathrm{dev}\,(\bar{\mathbf{m}}'\otimes\bar{\mathbf{m}}')$ and $\mathrm{dev}\,\bar{\mathbf{\Sigma}}$ can be written as

$$\begin{aligned}\mathrm{d}[\mathrm{dev}\,(\bar{\mathbf{m}}\otimes\bar{\mathbf{m}})] = &\left[\mathbb{A}_1 - \frac{2}{3}(\mathbf{I}\otimes\bar{\mathbf{m}}\otimes\bar{\mathbf{m}} + \bar{\mathbf{m}}\otimes\bar{\mathbf{m}}\otimes\mathbf{I}) + \frac{2}{9}I_4\mathbf{I}\otimes\mathbf{I}\right] : \mathrm{d}\mathbf{d} \\ &+ \mathrm{d}\mathbf{w}(\bar{\mathbf{m}}\otimes\bar{\mathbf{m}}) - (\bar{\mathbf{m}}\otimes\bar{\mathbf{m}})\mathrm{d}\mathbf{w},\end{aligned} \tag{3.51}$$

$$\begin{aligned}\mathrm{d}[\mathrm{dev}\,(\bar{\mathbf{m}}'\otimes\bar{\mathbf{m}}')] = &\left[\mathbb{A}_2 - \frac{2}{3}(\mathbf{I}\otimes\bar{\mathbf{m}}'\otimes\bar{\mathbf{m}}' + \bar{\mathbf{m}}'\otimes\bar{\mathbf{m}}_2'\otimes\mathbf{I}) + \frac{2}{9}I_6\mathbf{I}\otimes\mathbf{I}\right] : \mathrm{d}\mathbf{d} \\ &+ \mathrm{d}\mathbf{w}(\bar{\mathbf{m}}'\otimes\bar{\mathbf{m}}') - (\bar{\mathbf{m}}'\otimes\bar{\mathbf{m}}')\mathrm{d}\mathbf{w},\end{aligned} \tag{3.52}$$

$$\mathrm{d}(\mathrm{dev}\,\bar{\mathbf{\Sigma}}) = \left[\mathbb{A}_3 - \frac{2}{3}(\mathbf{I}\otimes\bar{\mathbf{\Sigma}} + \bar{\mathbf{\Sigma}}\otimes\mathbf{I}) + \frac{2}{9}I_8\mathbf{I}\otimes\mathbf{I}\right] : \mathrm{d}\mathbf{d} + \mathrm{d}\mathbf{w}\bar{\mathbf{\Sigma}} - \bar{\mathbf{\Sigma}}\mathrm{d}\mathbf{w}, \tag{3.53}$$

where $\mathbb{A}_1, \mathbb{A}_2$ and $\mathbb{A}_3$ are given in component form, respectively, by

$$\begin{aligned}\mathbb{A}_{1ijkl} &= 1/2(\delta_{ik}\bar{m}_j\bar{m}_l + \bar{m}_i\bar{m}_k\delta_{jl} + \delta_{il}\bar{m}_j\bar{m}_k + \bar{m}_i\bar{m}_l\delta_{jk}), \\ \mathbb{A}_{2ijkl} &= 1/2(\delta_{ik}\bar{m}_j'\bar{m}_l' + \bar{m}_i'\bar{m}_k'\delta_{jl} + \delta_{il}\bar{m}_j'\bar{m}_k' + \bar{m}_i'\bar{m}_l'\delta_{jk}), \\ \mathbb{A}_{3ijkl} &= 1/2(\delta_{ik}\bar{\Sigma}_{jl} + \bar{\Sigma}_{ik}\delta_{jl} + \delta_{il}\bar{\Sigma}_{jk} + \bar{\Sigma}_{il}\delta_{jk}).\end{aligned} \tag{3.54}$$

By first substituting (3.46) into (3.45) and then (3.45), (3.50)-(3.53), into (3.44) and comparing with equation (3.39) gives the explicit expression of the isochoric tangent

stiffness related to Jaumann rate

$$
\begin{aligned}
\bar{\mathbb{C}}^{\nabla J} = 2[2(&\bar{W}_{11}\mathrm{dev}\,\bar{\mathbf{B}}\otimes\mathrm{dev}\,\bar{\mathbf{B}} + \bar{W}_{14}\mathrm{dev}\,\bar{\mathbf{B}}\otimes\mathrm{dev}\,(\bar{\mathbf{m}}\otimes\bar{\mathbf{m}})\\
&+ \bar{W}_{14}\mathrm{dev}\,(\bar{\mathbf{m}}\otimes\bar{\mathbf{m}})\otimes\mathrm{dev}\,\bar{\mathbf{B}} + \bar{W}_{16}\mathrm{dev}\,\bar{\mathbf{B}}\otimes\mathrm{dev}\,(\bar{\mathbf{m}}'\otimes\bar{\mathbf{m}}')\\
&+ \bar{W}_{16}\mathrm{dev}\,(\bar{\mathbf{m}}'\otimes\bar{\mathbf{m}}')\otimes\mathrm{dev}\,\bar{\mathbf{B}} + \bar{W}_{18}\mathrm{dev}\,\bar{\mathbf{B}}\otimes\mathrm{dev}\,\bar{\mathbf{\Sigma}}\\
&+ \bar{W}_{18}\mathrm{dev}\,\bar{\mathbf{\Sigma}}\otimes\mathrm{dev}\,\bar{\mathbf{B}} + \bar{W}_{44}\mathrm{dev}\,(\bar{\mathbf{m}}\otimes\bar{\mathbf{m}})\otimes\mathrm{dev}\,(\bar{\mathbf{m}}\otimes\bar{\mathbf{m}})\\
&+ \bar{W}_{46}\mathrm{dev}\,(\bar{\mathbf{m}}\otimes\bar{\mathbf{m}})\otimes\mathrm{dev}\,(\bar{\mathbf{m}}'\otimes\bar{\mathbf{m}}') + \bar{W}_{46}\mathrm{dev}\,(\bar{\mathbf{m}}'\otimes\bar{\mathbf{m}}')\otimes\mathrm{dev}\,(\bar{\mathbf{m}}\otimes\bar{\mathbf{m}})\\
&+ \bar{W}_{48}\mathrm{dev}\,(\bar{\mathbf{m}}\otimes\bar{\mathbf{m}})\otimes\mathrm{dev}\,\bar{\mathbf{\Sigma}} + \bar{W}_{48}\mathrm{dev}\,\bar{\mathbf{\Sigma}}\otimes\mathrm{dev}\,(\bar{\mathbf{m}}\otimes\bar{\mathbf{m}})\\
&+ \bar{W}_{66}\mathrm{dev}\,(\bar{\mathbf{m}}'\otimes\bar{\mathbf{m}}')\otimes\mathrm{dev}\,(\bar{\mathbf{m}}'\otimes\bar{\mathbf{m}}') + \bar{W}_{68}\mathrm{dev}\,(\bar{\mathbf{m}}'\otimes\bar{\mathbf{m}}')\otimes\mathrm{dev}\,\bar{\mathbf{\Sigma}}\\
&+ \bar{W}_{68}\mathrm{dev}\,\bar{\mathbf{\Sigma}}\otimes\mathrm{dev}\,(\bar{\mathbf{m}}'\otimes\bar{\mathbf{m}}') + W_{88}\mathrm{dev}\,\bar{\mathbf{\Sigma}}\otimes\mathrm{dev}\,\bar{\mathbf{\Sigma}})\\
&+ \bar{W}_1(\mathbb{H} - \frac{2}{3}(\mathbf{I}\otimes\bar{\mathbf{B}} + \bar{\mathbf{B}}\otimes\mathbf{I}) + \frac{2}{9}I_1\mathbf{I}\otimes\mathbf{I})\\
&+ \bar{W}_4(\mathbb{A}_1 - \frac{2}{3}(\mathbf{I}\otimes\bar{\mathbf{m}}\otimes\bar{\mathbf{m}} + \bar{\mathbf{m}}\otimes\bar{\mathbf{m}}\otimes\mathbf{I}) + \frac{2}{9}I_4\mathbf{I}\otimes\mathbf{I})\\
&+ \bar{W}_6(\mathbb{A}_2 - \frac{2}{3}(\mathbf{I}\otimes\bar{\mathbf{m}}'\otimes\bar{\mathbf{m}}' + \bar{\mathbf{m}}'\otimes\bar{\mathbf{m}}'\otimes\mathbf{I}) + \frac{2}{9}I_6\mathbf{I}\otimes\mathbf{I})\\
&+ \bar{W}_8(\mathbb{A}_3 - \frac{2}{3}(\mathbf{I}\otimes\bar{\mathbf{\Sigma}} + \bar{\mathbf{\Sigma}}\otimes\mathbf{I}) + \frac{2}{9}I_8\mathbf{I}\otimes\mathbf{I})].
\end{aligned}
\tag{3.55}
$$

The increment of volumetric part of the Cauchy stress $J\boldsymbol{\sigma}_{\mathrm{vol}}$ is given by

$$
\mathrm{d}(J\boldsymbol{\sigma}_{\mathrm{vol}}) = \mathrm{d}J\left(\frac{\mathrm{d}U}{\mathrm{d}J} + J\frac{\mathrm{d}^2U}{\mathrm{d}^2J}\right)\mathbf{I}, \tag{3.56}
$$

where the increment of J is given by $\mathrm{d}J = J\,\mathrm{tr}\,(\mathrm{d}\mathbf{d})$. Comparing with equation (3.40), $\mathbb{C}_{\mathrm{vol}}^{\nabla J}$ can be expressed in the form

$$
\mathbb{C}_{\mathrm{vol}}^{\nabla J} = J\left(\frac{\mathrm{d}U}{\mathrm{d}J} + J\frac{\mathrm{d}^2U}{\mathrm{d}^2J}\right)\mathbf{I}\otimes\mathbf{I}. \tag{3.57}
$$

The elasticity tensor $\mathbb{C}$, which is defined in (3.41), is obtained by the terms given in (3.55) and (3.57).

3.3.2 Constitutive model

There are many examples, both in biological and engineered systems, where residual stresses have a significant influence on the overall mechanical response [29, 39]. To validate and verify the equations derived in Sections 3.2 and 3.3 a physiologic abdominal aortic aneurysm wall stress analysis is perfumed. Specifically, a patient-specific geometry, combined with a non-uniform distribution of wall pressure is used to evaluate the associated wall stress field in the presence of residual stress. Details on wall pressure measurements and the corresponding data are given in [13].

A finite element model is developed by Wang et al. [40] to evaluate the response of a residually stressed ventricular myocardium. A simple and extended approach is developed that differ in the number of terms used in the energy function to incorporate the effect of residual stress. In their simple approach, for example, it is shown that for consistency with the reference configuration is sufficient to assume $\bar{W}_8$ constant. We follow this argument and assume in what follows that $\bar{W}_8 = 1/2$.

The isochoric part of the energy function $\bar{W}$ includes the contributions from the isotropic base matrix, from the two families of oriented fibers and from the residual stress. In particular, the response of the isotropic base matrix is given by the exponential strain energy function by Demiray [11], the anisotropic character is included using the formulation developed by Holzapfel et al. [18] and the residual stress is accounted for using a constant term. Therefore, the energy function $\bar{W}$ has the form

$$\bar{W} = \frac{\mu_{\text{iso}}}{2\alpha}\left\{\exp\left[\alpha\left(\bar{I}_1 - 3\right)\right] - 1\right\} + \frac{\mu_{\text{fib}}}{2k}\sum_{i=4,6}\left\{\exp\left[k\left(\bar{I}_i - 1\right)^2\right] - 1\right\} + \frac{1}{2}\bar{I}_8, \tag{3.58}$$

where μ_{iso} denotes the shear stiffness of the matrix, μ_{fib} describes the degree of anisotropy and α and k are dimensionless parameters. Finally, the volumetric portion of the strain energy is taken as the penalty function

$$U(J) = \frac{\kappa}{2}\left(J - 1\right)^2, \tag{3.59}$$

where κ is known as the penalty parameter [2]. For nearly incompressible materials, κ is taken to be sufficiently large to minimize changes in volume. The expression of the Cauchy stress corresponding to the energy functions (3.58) and (3.59) is obtained using equation (3.28) with $W_2 = 0$. It has the form

$$\begin{aligned}\boldsymbol{\sigma} = {} & 2J^{-1}\left[\frac{\mu_{\text{iso}}}{2}\exp[\alpha(\bar{I}_1 - 3)]\text{dev}\,\bar{\mathbf{B}} + \mu_{\text{fib}}(I_4 - 1)\exp[k(\bar{I}_4 - 1)^2]\text{dev}\,(\bar{\mathbf{m}}\otimes\bar{\mathbf{m}})\right. \\ & + \left.\mu_{\text{fib}}(I_6 - 1)\exp[k(\bar{I}_6 - 1)^2]\text{dev}\,(\bar{\mathbf{m}}\otimes\bar{\mathbf{m}}) + \frac{1}{2}\text{dev}\,\bar{\boldsymbol{\Sigma}}\right] + \kappa(J-1)\mathbf{I}.\end{aligned} \tag{3.60}$$

In the residually stressed, unloaded reference configuration $\mathcal{B}_{\text{r}}$, using the penalty method to impose material incompressibility, $\mathbf{F} \approx \mathbf{I}$, i.e. the deformation gradient is not exactly the identity tensor due to the constrain violation of the penalty method in presence of residual stress. Hence,

$$\text{dev}\,\bar{\mathbf{B}} \approx \mathbf{0}, \quad \bar{I}_4 \approx 1, \quad \bar{I}_6 \approx 1, \quad \text{dev}\bar{\boldsymbol{\Sigma}} \approx \text{dev}\,\boldsymbol{\tau}, \quad J \approx 1. \tag{3.61}$$

From equation (3.60) it follows that the residual stress in $\mathcal{B}_{\mathrm{r}}$, denoted $\boldsymbol{\sigma}_{\mathrm{r}}$, is given by

$$\boldsymbol{\sigma}_{\mathrm{r}} = \mathrm{dev}\,\boldsymbol{\tau} + \kappa(J-1)\mathbf{I}, \tag{3.62}$$

where the first term on the right-hand side represents the deviatoric component of the residual stress and second term the equivalent hydrostatic pressure. From equilibrium of the residual stress in the reference configuration, where $\boldsymbol{\sigma}_{\mathrm{r}} = \boldsymbol{\tau}$, it follows that the hydrostatic pressure is equal $\frac{1}{3}\mathrm{tr}\,(\boldsymbol{\tau})$.

3.3.3 Estimation of residual stress

To the best of our knowledge, there are no available data that specify the magnitude and distribution of residual stress in human abdominal aortic aneurysms. Recent studies use different approaches to estimate these values. An analytical method is used by Pierce et al. [29] to estimate the residual stretches in the layered structure of a healthy arterial wall. The residual stretches are then used to numerically estimate the residual stress in the imaged, in vivo geometry of a patient specific AAA. Details of the corresponding equations, the data of the layer-specific residual deformation and geometric and traction compatibilities are given in [19]. An experimental study to evaluate AAA residual stress is summarized in [37]. The data are from an in vitro AAA model developed from an excised porcine aorta with elastase treatment. Tierney et al. [37] report a fourfold decrease in the opening angle measurement for the normal aorta and elastase treated rings directly indicating that the residual stress in AAA is much less than in a healthy aorta.

Any residual stress must satisfy the equilibrium equation (3.8) and the boundary condition (3.9). These conditions are used by Merodio and Ogden [21] to assume that the only nonzero components of the residual stress, for a circular cylindrical tube in terms of cylindrical polar coordinates, are τ_{RR} and $\tau_{\Theta\Theta}$. Specifically, the component in the radial direction has the form

$$\tau_{RR} = \alpha_{\mathrm{r}}(R-A)(R-B), \tag{3.63}$$

where α_{r} has the units of stress and defines the strength of the residual stress, R is the radius of a material point and A, B denote, respectively, the internal and external radii in the reference configuration $\mathcal{B}_{\mathrm{r}}$. The expression (3.63) satisfies the boundary condition

$$\tau_{RR} = 0 \quad \text{on} \quad R = A, B. \tag{3.64}$$

Using the radial component of the equilibrium equation (3.8) it follows that $\tau_{\Theta\Theta}$ has the form

$$\tau_{\Theta\Theta} = \alpha_{\mathrm{r}}[3R^2 - 2(A+B)R + AB]. \tag{3.65}$$

The geometry of patient specific AAAs is, in general, very irregular and cannot be approximated by a thick wall cylindrical tube with constant cross-section. In addition, limited and contradictory information on residual stresses is available [19, 37]. Therefore, we use a simplified approach to include residual stresses. Specifically, the components τ_{RR} and $\tau_{\Theta\Theta}$ are evaluated using constant values of $A = 10.7$ mm, $B = 12.7$ mm and $\alpha_{\mathrm{r}} = 0.9$, the latter chosen to approximate stress magnitudes reported in the literature [5, 19], see Figure 3.1. We assume that this represents the residual stress distribution in the AAA model analyzed next. A spatially varying residual stress distribution will be considered once corresponding data become available.

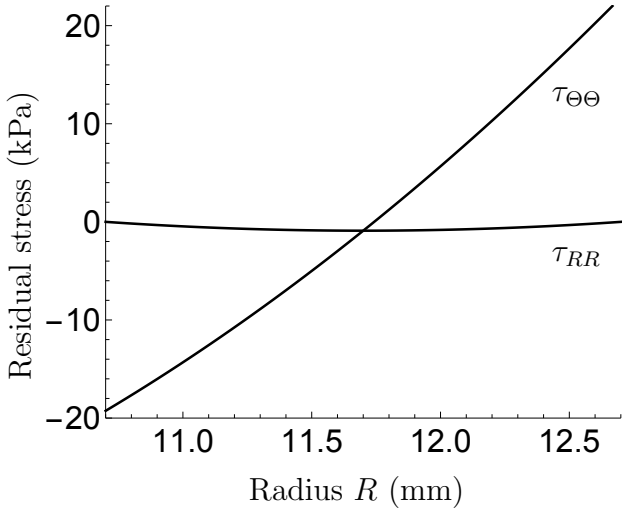

FIGURE 3.1: Distribution of the residual stress components τ_{RR} and $\tau_{\Theta\Theta}$ as a function of the radius R. The radial component satisfies the boundary conditions $\tau_{RR} = 0$ on the inner and outer surfaces located at $R = 10.7$ and 12.7 mm, respectively. $\tau_{\Theta\Theta}$ is in compression on the inner and in tension on the outer wall surface.

3.4 Patient based AAA model

The patient specific values of the material model parameters of a AAA are obtained from strain-controlled, planar biaxial tests of tissue samples resected during elective repair surgery [28]. For reference, cylindrical polar coordinates (r, θ, z), with unit basis vectors $\mathbf{e}_r, \mathbf{e}_\theta, \mathbf{e}_z$, are used to denoted the radial, circumferential and axial directions of the aortic wall. During each test, in situ axial stretch λ_z is held constant at physiologically realistic values while the specimen is subjected to five loading-unloading cycles in

the circumferential direction. The nonlinear iterative function *fmincon* of the commercial software package MATLAB [20] was used to determine the non-negative values of $\mu_{\text{iso}}, \alpha, \mu_{\text{fib}}, k, \varphi$ required to define the isochoric part of the energy function (3.58). The penalty parameter in the function (3.59) is taken as $\kappa = 20,000$ kPa. The magnitudes of all material parameters are shown in Table 3.1. Note that φ is the angle formed by the two families of oriented fibers and the circumferential direction $\mathbf{e}_\theta$. It follows that the preferred direction during biaxial extension, here denoted $\bar{\mathbf{M}}$ and $\bar{\mathbf{M}}'$, characterizing the structure of the material, are given by

$$\bar{\mathbf{M}} = \cos\varphi\,\mathbf{e}_\theta + \sin\varphi\,\mathbf{e}_z, \quad \bar{\mathbf{M}}' = \cos\varphi\,\mathbf{e}_\theta - \sin\varphi\,\mathbf{e}_z. \tag{3.66}$$

TABLE 3.1: The patient specific values of model parameters to define the isochoric energy function (3.58) and the penalty term (3.59). The values of μ_{iso}, μ_{fib} and κ are given in kPa, the angle φ in degrees.

Summary of model parameters					
μ_{iso}	α	μ_{fib}	k	φ	κ
46.987	21.071	33.922	37.287	6.744	20,000

A computational model of a patient-based AAA with a non-dilated inner diameter of 21.4 mm, maximum outer diameter of 56.5 mm and bulge length of 67 mm was used to validate the numerical implementation and to analyze the effect of the residual stress on the wall stress distribution. The wall thickness of the model was assumed to be uniform and was set at 2 mm and the outer diameter of the model entrance was set to 25.4 mm. The pressure distribution applied to the inner surface is obtained from measurements in a patient-based phantom cast at a series of physiologically relevant steady flow rates [13]. The data show that the wall pressure is 16.0 kPa at the phantom entrance, $x = 0$, where x is the axial position. At mid-bulge the pressure drops to it its minimum of 15.5 kPa ($x = 120 - 140$ mm) and recovers to 15.9 kPa at the bulge exit ($x = 215$ mm). Therefore, the wall pressure applied to the inner surface of the computation model was uniform in the circumferential direction and varied longitudinally.

3.4.1 Fiber orientation in the AAA model

The unit vectors $\bar{\mathbf{M}}$ and $\bar{\mathbf{M}}'$ specify the preferred direction during biaxial extension, equivalently during extension and inflation of a circular tube, i.e. a healthy aorta. To define the 'corresponding' orientations in the AAA model, we use the *projection* tensor $\mathbf{P}$ to generate images of $\bar{\mathbf{M}}$ and $\bar{\mathbf{M}}'$ projected onto the wall surface defined by the normal unit vector $\mathbf{n}$. This is accomplished by first identifying a 3D piecewise linear centerline

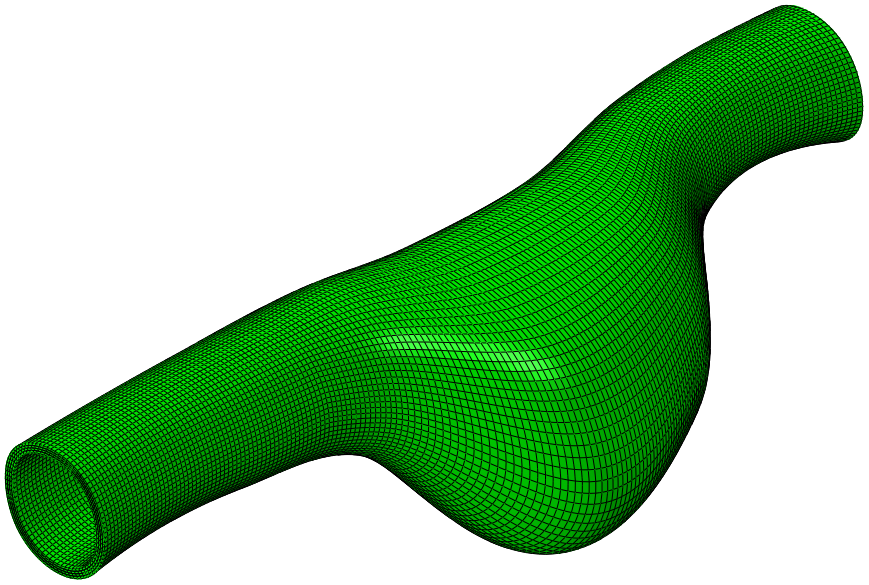

FIGURE 3.2: Geometric layout and element distribution of the computational AAA model used to evaluate the effect of residual stress. Four hexahedron elements are used through the wall thickness.

of the AAA. The line connecting the centroid of each element with the nearest linear section of the 3D centerline defines the local direction $\mathbf{e}_r$, the orientation of the centerline specifies $\mathbf{e}_z$ and their cross product provides $\mathbf{e}_\theta$, see Figure 3.3. The local orientation of the preferred directions are given by the unit vectors $\mathbf{M}$ and $\mathbf{M}'$ obtained by

$$\mathbf{M} = \frac{\mathbf{P}\bar{\mathbf{M}}}{|\mathbf{P}\bar{\mathbf{M}}|}, \quad \mathbf{M}' = \frac{\mathbf{P}\bar{\mathbf{M}}'}{|\mathbf{P}\bar{\mathbf{M}}'|}, \tag{3.67}$$

where the projection tensor $\mathbf{P}$ has the form

$$\mathbf{P} = \mathbf{I} - \mathbf{n} \otimes \mathbf{n}. \tag{3.68}$$

3.4.2 Results

To validate and verify the developments presented in the previous sections, we now summarize the numerical results of a nonlinear finite element analysis using a patient specific AAA geometry and patient based material parameters. We write a user specific material subroutine, called UMAT, of the constitutive formulations given in (3.58) and (3.59) and use ABAQUS [1] to solve the corresponding equations.

The undeformed, residually stressed reference configuration is used to visualize the von Mises stress distribution on the inner and outer surfaces of the AAA wall. We found

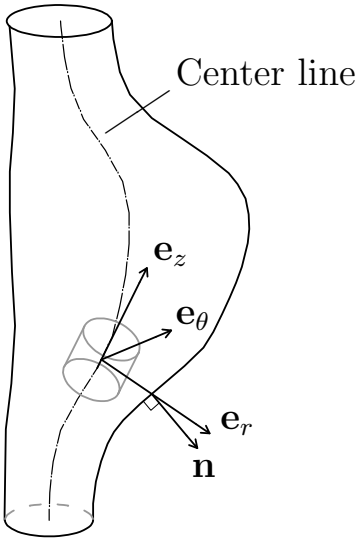

FIGURE 3.3: Location of the piecewise linear center line, which is used to define a local cylindrical coordinate system with unit basis vectors $\mathbf{e}_r, \mathbf{e}_\theta, \mathbf{e}_z$.

that the von Mises stress magnitudes, when residual stress is accounted for, are very similar to those without residual stress. Therefore, for the sake of space, only results of the former are included in this paper.

The von Mises stress distribution of AAA with physiological relevant pressure applied to the inner surface, accounting for residual stresses, is shown in Figure 3.4, where the images (a) and (b) depict the distribution on the inner surface and (c) and (d) on the outer surface of the AAA. For ease of reference we have added the orientation of the global coordinate system to each of the images.

As expected, the magnitude of the stress is non uniform and varies widely on the inner and outer surfaces. Not surprisingly, the magnitude on the inner surface is, in general, larger when compared to the values on the outer surface. We found that the maximum value of 460.85 kPa occurs on the inner surface on the posterior side of the AAA wall.

The absolute value of the displacements $||\mathbf{u}||$ on the inner and outer surfaces are shown on the four images in Figure 3.5. Similar to the von Mises stress distribution, the displacement results from analyses with and without residual stress are very similar and therefore only those including the residual stress are shown. The maximum displacement for an applied physiological pressure is given by $||\mathbf{u}|| = 16.89$ mm. For the analysis, where residual stress is not included, the magnitude is similar with a difference 0.03 mm at the same location.

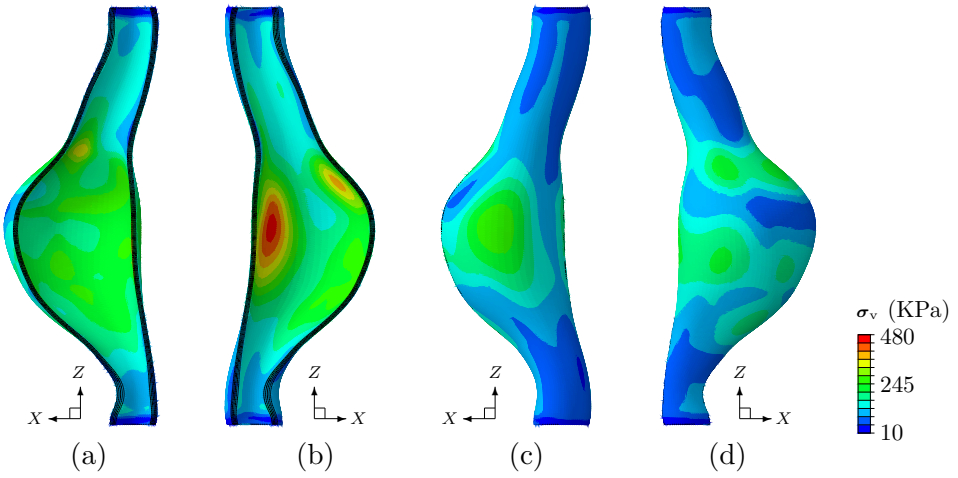

FIGURE 3.4: The von Mises stress distribution on the inner and outer surfaces of the AAA when a physiological relevant pressure is applied. The pressure applied to the inner surface is uniform in the circumferential direction but various longitudinally. The images (a) and (b) depict the distribution on the inner surface and (c) and (d) on the outer surface.

The variation of the von Mises stress across the wall thickness is presented in Figures 3.6 and 3.7. The path in Figure 3.6 is at the location where the von Mises stress on the inner surface assume its maximum value. The path in Figure 3.7 is at an arbitrarily location where the stress values are relatively small. For completeness, we have included the results for both analyses, with and without residual stress.

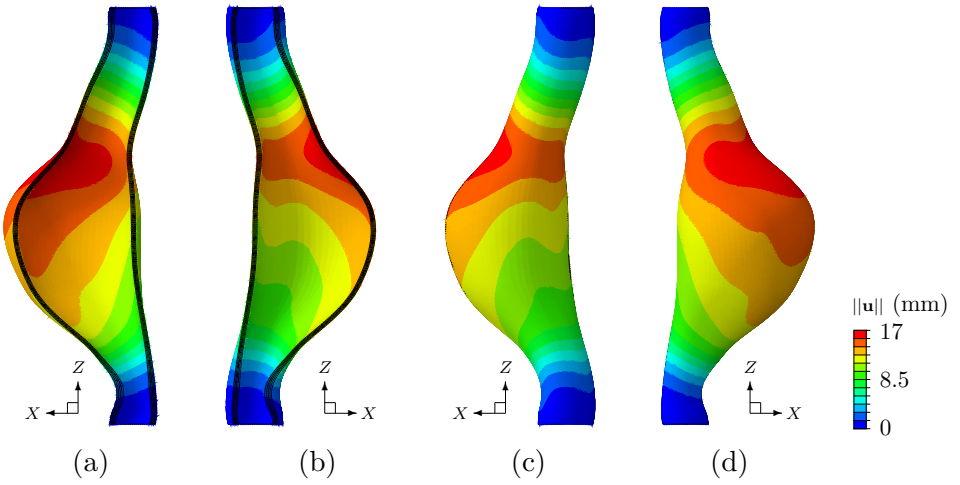

FIGURE 3.5: The absolute value of the displacements on the inner and outer surfaces of the AAA model subject to an internal pressure. The imposed boundary condition at the proximal and distal end of the AAA are unrealistic and created stress concentration but do not influence the results in the zone of interest.

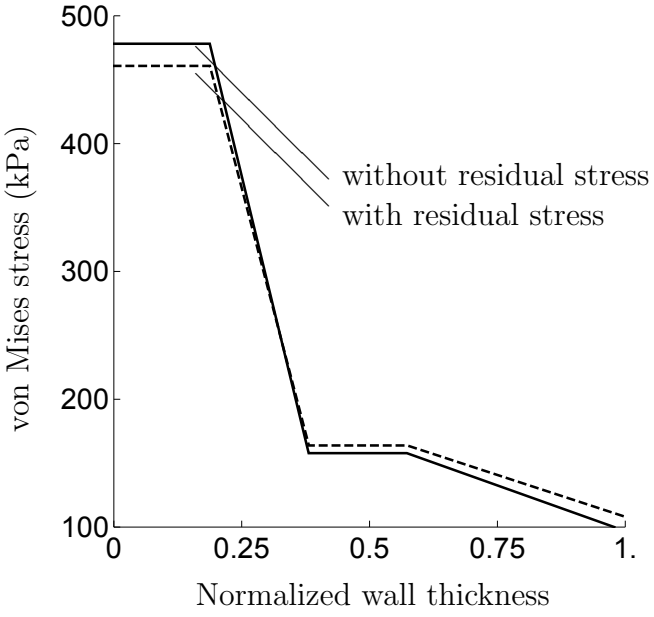

FIGURE 3.6: The variation of the von Mises stress across the wall thickness at the location where the von Mises stress on the inner surface assume its maximum value. Solid lines indicates values with residual stress not included, dashed line show results with residual stress included.

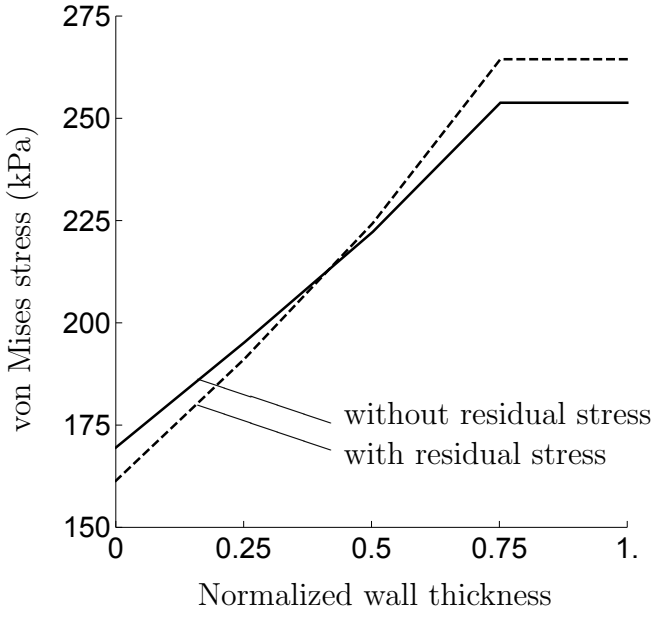

FIGURE 3.7: The variation of the von Mises stress across the wall thickness at an arbitrary location. Solid lines indicates values with residual stress not included, dashed line show results with residual stress included.

3.5 Discussion and concluding remarks

A numerical method for incorporating a three-dimensional residual stress state in a hyperelastic constitutive formulation is presented. The energy function is expressed in terms of invariants of an isotropic base matrix, two sets of preferred fiber directions and the residual stress tensor and, for numerical purposes, is decomposed into isochoric and volumetric parts. The isochoric part contains exponential terms related to the isotropic matrix, to the behavior of the oriented fibers and an additional term related to the residual stress. The volumetric part is a penalty function to enforce the incompressibility constraint. The corresponding fourth-order elasticity tensors are derived by linearizing the expression of internal virtual work and are given explicitly.

No reliable data exit that describe the three-dimensional residual stress state in AAAs. Therefore, for this study we use the expressions suggested by Merodio and Ogden [21], which satisfy the zero traction boundary conditions. The corresponding model parameters are determined to obtain residual stress magnitudes similar in to those given in [4, 19]. Finally, a new algorithm is proposed that projects the two oriented fiber orientations along a tubular configuration onto the irregular geometry of the AAA.

To verify and validate the formulation we summarize the main results of a finite element analysis using a patient specific AAA geometry. These show, when the effect of residual stress is neglected, a maximum von Mises stress of 478.14 kPa, which reduces to 460.85 kPa when the residual stress is included. This finding is consistent with the now accepted understanding that residual stress in tissue optimize the mechanical performance by homogenizing stress levels. The publications by Delfino et al. [10], Holzapfel et al. [18], Pierce et al. [29], Vaishnav and Vossoughi [38] report similar findings to further strengthen this understanding. Although, the inclusion of residual stress lowers the magnitude of the maximum stress, we also note that influence is minimal for the results here reported. Other authors, for example, Alastrué et al. [3], Delfino et al. [10], Pierce et al. [29], report significant reductions when residual stress is considered. Holzapfel et al. [18] report small and large changes in stress values in arteries of humans and other species. Holzapfel et al. [18] find that the influence of residual stress is minor when the wall thickness to diameter ratio is small. For the simulation in the paper, the wall thickness to diameter ratio is much smaller than that reported by Delfino et al. [10], Alastrué et al. [3], which validates the findings reported here.

The magnitudes of the displacement field, with and without residual stress, show minor changes similar to the the stress field. Alastrué et al. [3] show signifiant changes of the displacement field when the residual stress is accounted for. However, Alastrué et al. [3] consider a carotid brunch, which has a very complex geometry. Thus the

influence of residual stress might be magnified by the geometric layout and would require further investigation. Our results show that the applied pressure generates a maximum displacement magnitude of $||\mathbf{u}|| = 16.89$ mm. This large value is due to the rigid body motion of the bulge region and is thus related to the specific geometry of the AAA.

The von Mises stress values across the wall thickness where stresses have the larges value are presented in Figure 3.6. The graphs show that accounting of the residual stress homogenize the stress level across the thickness by reducing the stress gradient, consistent with the understanding reported in the literature. Note that the results in Figure 3.7 are different, but the stress level at this location is lower compared to the stress level shown in Figure 3.6.

In conclusion, we presented a numerical method for incorporating a three-dimensional residual stress state in a constitutive formulation that is very general and can be used in combination with any hyperelastic material law. A patient specific AAA geometry, subject to internal pressure, is used to evaluate the wall stress distribution with and without the influence of residual stress.

Acknowledgement

This research was supported by the National Science Foundation [Grant number CMMI-1031366] and by a Faculty Research Award provided by Tufts University.

Bibliography

[1] ABAQUS, 2013. Theory Manual. Dassault Systèmes Simulia, Providence, RI, USA.

[2] Adler, J. H., Dorfmann, L., Han, D., MacLachlan, S., Peatsch, C., 2014. Mathematical and computational models of incompressible materials subject to shear. IMA J. Appl. Math. 79, 889–914.

[3] Alastrué, V., Garía, A., Peña, E., Rodríguez, J. F., Martínez, M. A., Doblaré, M., 2009. Numerical framework for patient-specific computational modelling of vascular tissue. Int. J. Numer. Meth. Biomed. Engng. 26, 35–51.

[4] Alford, P. W., Feinberg, A. W., Sheehy, S. P., Parker, K. K., 2010. Biohybrid thin films for measuring contractility in engineered cardiovascular muscle. Biomaterials 31, 3613–3621.

[5] Alford, P. W., Humphrey, J. D., Taber, L. A., 2008. Growth and remodeling in a thick-walled artery model: Effects of spatial variations in wall constituents. Biomech. Model. Mechanobiol. 7, 245–262.

[6] Ambrosi, D., Guillou, A., Di Martino, E., 2008. Stress-modulated remodeling of a non-homogeneous body. Biomech. Model. Mechanobiol. 7, 63–76.

[7] Bose, K., Dorfmann, A., 2009. Computational aspects of a pseudo-elastic constitutive model for muscle properties in a soft-bodied arthropod. Int. J. Solids Struct. 44, 42–50.

[8] Chuong, C. J., Fung, Y. C., 1986. On residual stresses in arteries. J. Biomech. Eng. 108, 189–192.

[9] Costa, K. D., May-Newman, K., Farr, D., O'Dell, W. G., McCulloch, A. D., Omens, J. H., 1997. Three-dimensional residual strain in midanterior canine left ventricle. Am. J. Physiol.-Heart C. 273, H1968–H1976.

[10] Delfino, A., Stergiopulos, N., Moore, J. E., Meister, J. J., 1997. Residual strain effects on the stress field in a thick wall finite element model of the human carotid bifurcation. J. Biomech. 30, 777 – 786.

[11] Demiray, H., 1972. Elasticity of soft biological tissues. J. Biomech. 5, 309–311.

[12] Dorfmann, A., Ogden, R. W., 2014. Nonlineaer Theory of Electroelastic and Magnetoelastic Interactions. Springer.

[13] Dorfmann, A., Wilson, C., Edgar, E. S., Peattie, R. A., 2010. Evaluating patient-specific abdominal aortic aneurysm wall stress based on flow-induced loading. Biomech. Model. Mechanobiol. 9, 127–139.

[14] Flory, P. J., 1961. Thermodynamic relations for highly elastic materials. Trans. Faraday Soc. 57, 829–838.

[15] Fung, Y. C., 1983. On the foundations of biomechanics. J. Appl. Mech. 50, 1003–1009.

[16] Hoger, A., 1985. On the residual stress possible in an elastic body with material symmetry. Arch. Rat. Mech. Anal. 88, 271–290.

[17] Holzapfel, G. A., 2000. Nonlinear Solid Mechanics: A Continuum Approach for Engineering. John Wiley & Sons, Chichester.

[18] Holzapfel, G. A., Gasser, T. C., Ogden, R. W., 2000. A new constitutive framework for arterial wall mechanics and a comparative study of material models. J. Elasticity 61, 1–48.

[19] Holzapfel, G. A., Ogden, R. W., 2010. Modelling the layer-specific three-dimensional residual stresses in arteries, with an application to the human aorta. J. R. Soc. Interface 7, 787–799.

[20] MATLAB, 2014. The MathWorks Inc. Natick, MA, USA.

[21] Merodio, J., Ogden, R. W., 2015. Extension, inflation and torsion of a residually stressed circular cylindrical tube. Continnum Mech. Thermodyn. (In press), DOI 10.1007/s00161–015–0411–z.

[22] Nienhaus, U., Aegerter-Wilmsen, T., Aegerter, C. M., 2009. Determination of mechanical stress distribution in Drosophila wing discs using photoelasticity. Mech. Develop. 126, 942 – 949.

[23] Ogden, R. W., 1976. Volume changes associated with the deformation of rubber-like solids. J. Mech. Phys. Solids 24, 323–338.

[24] Ogden, R. W., 1978. Nearly isochoric elastic deformations: application to rubberlike solids. J. Mech. Phys. Solids 26, 37–57.

[25] Ogden, R. W., 2001. Elements of the theory of finite elasticity. In: Fu, Y. B., Ogden, R. W. (Eds.), Nonlinear Elasticity: Theory and Applications. Cambridge University Press, pp. 1–58.

[26] Ogden, R. W., 2014. Nonlinear elasticity with application to soft fibre-reinforced materials. In: CISM Course on Nonlinear Mechanics of Soft Fibrous Materials. Vol. 559. Springer, Wien, pp. 1–48.

[27] Olsson, T., Klarbring, A., 2008. Residual stresses in soft tissue as a consequence of growth and remodeling: application to an arterial geometry. Eur. J. Mech. A-Solid 27, 959–974.

[28] Pancheri, F. Q., 2014. Experimental and analytical aspects of biological and engineering materials subject to planar biaxial loading. Ph.D. thesis, Tufts University.

[29] Pierce, D. M., Fastl, T. E., Rodriguez-Vila, B., Verbrugghe, P., Fourneau, I., Maleux, G., Herijgers, P., Gomez, E. J., Holzapfel, G. A., 2015. A method for incorporating three-dimensional residual stretches/stresses into patient-specific finite element simulations of arteries. J. Mech. Behav. Biomed. 47, 147–164.

[30] Polzer, S., Bursa, J., Gasser, T. C., Staffa, R., Vlachovsky, R., 2013. A numerical implementation to predict residual strains from the homogeneous stress hypothesis with application to abdominal aortic aneurysms. Ann. Biomed. Eng. 41, 1516–1527.

[31] Prot, V. E., Skallerud, B. H., 2009. Nonlinear solid finite element analysis of mitral valves with heterogeneous leaflet layers. Comput. Mech. 43, 353–368.

[32] Shams, M., Destrade, M., Ogden, R. W., 2011. Initial stresses in elastic solids: Constitutive laws and acoustoelasticity. Wave Motion 48, 552–567.

[33] Skalak, R., Zargaryan, S., Jain, R. K., Netti, P. A., Hoger, A., 1996. Compatibility and the genesis of residual stress by volumetric growth. J. Math. Biol. 34, 889–914.

[34] Spencer, A. J. M., 1971. Theory of Invariants. In: Eringen, A. C. (Ed.), Continuum Physics. Vol. 1. Academic Press, New York, pp. 239–353.

[35] Spencer, A. J. M., Rivlin, R. S., 1959. Finite integrity bases for five or fewer symmetric 3x3 matrices. Arch. Rat. Mech. Anal. 2, 435–446.

[36] Taber, L. A., 1995. Biomechanics of growth, remodeling and morphogenesis. App. Mech. Rev. 48, 487–545.

[37] Tierney, A. P., Dumont, D. M., Callanan, A., Trahey, G. E., McGloughlin, T. M., 2010. Acoustic radiation force impulse imaging on ex vivo abdominal aortic aneurysm model. Ultrasound in Med. & Biol. 36, 821–832.

[38] Vaishnav, R. N., Vossoughi, J., 1987. Residual stress and strain in aortic segments. J. Biomech. 20, 235–239.

[39] Vandiver, R., Goriely, A., 2009. Differential growth and residual stress in cylindrical elastic structures. Phil. Trans. R. Soc. A 367, 3607–3630.

[40] Wang, H. M., Luo, X. Y., Gao, H., Ogden, R. W., Griffith, B. E., Berry, C., Wang, T. J., 2014. A modified Holzapfel-Ogden law for a residually stressed finite strain model of the human left ventricle in diastole. Biomech. Model. Mechanobiol. 13, 99–113.

[41] Wang, R., Raykin, J., Gleason, R. L., Ethier, C. R., 2015. Residual deformations in ocular tissues. J. R. Soc. Interface 12.

[42] Wells, S. M., Walter, E. J., 2010. Changes in the mechanical properties and residual strain of elastic tissue in the developing fetal aorta. Ann. Biomed. Eng. 38, 345–356.

[43] Yeni, Y. N., Schaffler, M. B., Gibson, G., Fyhrie, D. P., 2002. Prestress due to dimensional changes caused by demineralization: A potential mechanism for microcracking in bone. Ann. 30, 217–225.

Chapter 4

Conclusion

Constitutive material modeling and framework for incorporating three-dimensional residual stress in analysis for soft materials and structures are presented.

Proposed constitutive model is very general, which can model rate-independent and rate-dependent responses including the stress relaxation and recovery phenomena of passive skeletal muscle. Robust, strongly objective numerical integration algorithm is used in solving nonlinear evolution equation regarding the presented model. Comparison of numerical simulation results with corresponding experimental data shows model's ability to capture time-dependent responses of muscle tissue.

Framework for accounting residual stresses to predict accurate response of soft materials and structures is presented. The formulation has the generality to adopt any hyperelastic material law in combination with estimated residual stress. Details derivations of tensor quantities are included for numerical implementation of the method into finite-element codes. The framework is validated and verified by implementing, into ABAQUS using UMAT subroutine, and analyzing patient specific AAA wall stress. Analysis results are in agreement with the results in the literature and consistent with the accepted understanding regarding the influence of residual stress.

Appendix A

Derivation

Appendix A contain derivations of mathematical quantities used in Modeling of residually stressed materials with application to AAA. For convenience all the mathematical quantities are drived in index notation. Following the same index convention in the report, Roman indices are associated with the current configuration and Greek indices with the reference configuration.

$$\begin{aligned}
\frac{\partial \bar{\mathrm{F}}_{j\beta}}{\partial \mathrm{F}_{i\alpha}} &= \frac{\partial}{\partial \mathrm{F}_{i\alpha}}(J^{-1/3}\mathrm{F}_{j\beta}) \\
&= \frac{\partial J^{-1/3}}{\partial \mathrm{F}_{i\alpha}}\mathrm{F}_{j\beta} + J^{-1/3}\frac{\partial \mathrm{F}_{j\beta}}{\partial \mathrm{F}_{i\alpha}} \\
&= -\frac{1}{3}J^{-4/3}J\mathrm{F}^{-1}_{\alpha i}\mathrm{F}_{j\beta} + J^{-1/3}\delta_{ij}\delta_{\alpha\beta} \\
&= -\frac{1}{3}J^{-1/3}(\mathrm{F}^{-1}_{\alpha i})\mathrm{F}_{j\beta} + J^{-1/3}\delta_{ij}\delta_{\alpha\beta} \\
&= -\frac{1}{3}J^{-1/3}(J^{-1/3}\bar{\mathrm{F}}^{-1}_{\alpha i})\mathrm{F}_{j\beta} + J^{-1/3}\delta_{ij}\delta_{\alpha\beta} \\
&= -\frac{1}{3}J^{-1/3}\bar{\mathrm{F}}^{-1}_{\alpha i}\bar{\mathrm{F}}_{j\beta} + J^{-1/3}\delta_{ij}\delta_{\alpha\beta}
\end{aligned} \tag{A.1}$$

$$\begin{aligned}
\frac{\partial \bar{\mathrm{B}}_{jk}}{\partial \mathrm{F}_{i\alpha}} &= \frac{\partial}{\partial \mathrm{F}_{i\alpha}}(\bar{\mathrm{F}}_{j\beta}\bar{\mathrm{F}}_{k\beta}) \\
&= \frac{\partial \bar{\mathrm{F}}_{j\beta}}{\partial \mathrm{F}_{i\alpha}}\bar{\mathrm{F}}_{k\beta} + \bar{\mathrm{F}}_{j\beta}\frac{\partial \bar{\mathrm{F}}_{k\beta}}{\partial \mathrm{F}_{i\alpha}} \\
&= (-\frac{1}{3}J^{-1/3}\bar{\mathrm{F}}^{-1}_{\alpha i}\bar{\mathrm{F}}_{j\beta} + J^{-1/3}\delta_{ij}\delta_{\alpha\beta})\bar{\mathrm{F}}_{k\beta} + \bar{\mathrm{F}}_{j\beta}(-\frac{1}{3}J^{-1/3}\bar{\mathrm{F}}^{-1}_{\alpha i}\bar{\mathrm{F}}_{k\beta} + J^{-1/3}\delta_{ik}\delta_{\alpha\beta}) \\
&= -\frac{1}{3}J^{-1/3}\bar{\mathrm{F}}^{-1}_{\alpha i}\bar{\mathrm{B}}_{jk} + J^{-1/3}\delta_{ij}\bar{\mathrm{F}}_{k\alpha} - \frac{1}{3}J^{-1/3}\bar{\mathrm{F}}^{-1}_{\alpha i}\bar{\mathrm{B}}_{jk} + J^{-1/3}\delta_{ik}\bar{\mathrm{F}}_{j\alpha} \\
&= J^{-1/3}\delta_{ij}\bar{\mathrm{F}}_{k\alpha} + J^{-1/3}\delta_{ik}\bar{\mathrm{F}}_{j\alpha} - \frac{2}{3}J^{-1/3}\bar{\mathrm{F}}^{-1}_{\alpha i}\bar{\mathrm{B}}_{jk} \\
&= J^{-1/3}\left[\delta_{ij}\bar{\mathrm{F}}_{k\alpha} + \delta_{ik}\bar{\mathrm{F}}_{j\alpha} - \frac{2}{3}\bar{\mathrm{F}}^{-1}_{\alpha i}\bar{\mathrm{B}}_{jk}\right]
\end{aligned} \tag{A.2}$$

$$
\begin{aligned}
\frac{\partial \bar{\mathrm{C}}_{\beta\gamma}}{\partial \mathrm{F}_{i\alpha}} &= \frac{\partial}{\partial \mathrm{F}_{i\alpha}}(\bar{\mathrm{F}}_{j\beta}\bar{\mathrm{F}}_{j\gamma}) \\
&= \frac{\partial \bar{\mathrm{F}}_{j\beta}}{\partial \mathrm{F}_{i\alpha}}\bar{\mathrm{F}}_{j\gamma} + \bar{\mathrm{F}}_{j\beta}\frac{\partial \bar{\mathrm{F}}_{j\gamma}}{\partial \mathrm{F}_{i\alpha}} \\
&= (-\frac{1}{3}J^{-1/3}\bar{\mathrm{F}}^{-1}_{\alpha i}\bar{\mathrm{F}}_{j\beta} + J^{-1/3}\delta_{ij}\delta_{\alpha\beta})\bar{\mathrm{F}}_{j\gamma} + \bar{\mathrm{F}}_{j\beta}(-\frac{1}{3}J^{-1/3}\bar{\mathrm{F}}^{-1}_{\alpha i}\bar{\mathrm{F}}_{j\gamma} + J^{-1/3}\delta_{ij}\delta_{\alpha\gamma}) \\
&= -\frac{1}{3}J^{-1/3}\bar{\mathrm{F}}^{-1}_{\alpha i}\bar{\mathrm{C}}_{\beta\gamma} + J^{-1/3}\delta_{\alpha\beta}\bar{\mathrm{F}}_{i\gamma} - \frac{1}{3}J^{-1/3}\bar{\mathrm{F}}^{-1}_{\alpha i}\bar{\mathrm{C}}_{\beta\gamma} + J^{-1/3}\delta_{\alpha\gamma}\bar{\mathrm{F}}_{i\beta} \\
&= J^{-1/3}\delta_{\alpha\beta}\bar{\mathrm{F}}_{i\gamma} + J^{-1/3}\delta_{\alpha\gamma}\bar{\mathrm{F}}_{i\beta} - \frac{2}{3}J^{-1/3}\bar{\mathrm{F}}^{-1}_{\alpha i}\bar{\mathrm{C}}_{\beta\gamma} \\
&= J^{-1/3}\left[\delta_{\alpha\beta}\bar{\mathrm{F}}_{i\gamma} + \delta_{\alpha\gamma}\bar{\mathrm{F}}_{i\beta} - \frac{2}{3}\bar{\mathrm{F}}^{-1}_{\alpha i}\bar{\mathrm{C}}_{\beta\gamma}\right]
\end{aligned}
\tag{A.3}
$$

$$
\begin{aligned}
\frac{\partial \bar{I}_1}{\partial \mathrm{F}_{i\alpha}} &= \frac{\partial \bar{\mathrm{B}}_{jj}}{\partial \mathrm{F}_{i\alpha}} \\
&= \frac{\partial}{\partial \mathrm{F}_{i\alpha}}(\bar{\mathrm{F}}_{j\beta}\bar{\mathrm{F}}_{j\beta}) \\
&= \frac{\partial \bar{\mathrm{F}}_{j\beta}}{\partial \mathrm{F}_{i\alpha}}\bar{\mathrm{F}}_{j\beta} + \bar{\mathrm{F}}_{j\beta}\frac{\partial \bar{\mathrm{F}}_{j\beta}}{\partial \mathrm{F}_{i\alpha}} \\
&= 2\frac{\partial \bar{\mathrm{F}}_{j\beta}}{\partial \mathrm{F}_{i\alpha}}\bar{\mathrm{F}}_{j\beta} \\
&= -\frac{2}{3}J^{-1/3}\bar{\mathrm{F}}^{-1}_{\alpha i}\bar{\mathrm{F}}_{j\beta}\bar{\mathrm{F}}_{j\beta} + 2J^{-1/3}\delta_{ij}\delta_{\alpha\beta}\bar{\mathrm{F}}_{j\beta} \\
&= -\frac{2}{3}J^{-1/3}\bar{\mathrm{F}}^{-1}_{\alpha i}\bar{I}_1 + 2J^{-1/3}\bar{\mathrm{F}}_{i\alpha} \\
&= 2J^{-1/3}\left[\bar{\mathrm{F}}_{i\alpha} - \frac{1}{3}\bar{I}_1\bar{\mathrm{F}}^{-1}_{\alpha i}\right]
\end{aligned}
\tag{A.4}
$$

$$
\begin{aligned}
\frac{\partial \bar{I}_2}{\partial \mathrm{F}_{i\alpha}} &= \frac{\partial}{\partial \mathrm{F}_{i\alpha}}(\frac{1}{2}\left[\bar{I}_1^2 - \bar{\mathrm{B}}_{jk}\bar{\mathrm{B}}_{kj}\right]) \\
&= \frac{1}{2}\left[\frac{\partial \bar{I}_1^2}{\partial \mathrm{F}_{i\alpha}} - \frac{\partial \bar{\mathrm{B}}_{jk}}{\partial \mathrm{F}_{i\alpha}}\bar{\mathrm{B}}_{kj} - \bar{\mathrm{B}}_{jk}\frac{\partial \bar{\mathrm{B}}_{kj}}{\partial \mathrm{F}_{i\alpha}}\right] \\
&= 2\bar{I}_1 J^{-1/3}\left[\bar{\mathrm{F}}_{i\alpha} - \frac{1}{3}\bar{I}_1\bar{\mathrm{F}}^{-1}_{\alpha i}\right] - J^{-1/3}\frac{1}{2}\left[\delta_{ij}\bar{\mathrm{F}}_{k\alpha} + \delta_{ik}\bar{\mathrm{F}}_{j\alpha} - \frac{2}{3}\bar{\mathrm{F}}^{-1}_{\alpha i}\bar{\mathrm{B}}_{jk}\right]\bar{\mathrm{B}}_{kj} \\
&\quad - J^{-1/3}\frac{1}{2}\bar{\mathrm{B}}_{jk}\left[\delta_{ik}\bar{\mathrm{F}}_{j\alpha} + \delta_{ij}\bar{\mathrm{F}}_{k\alpha} - \frac{2}{3}\bar{\mathrm{F}}^{-1}_{\alpha i}\bar{\mathrm{B}}_{kj}\right] \\
&= J^{-1/3}\left[2\bar{I}_1\bar{\mathrm{F}}_{i\alpha} - \frac{2}{3}\bar{I}_1^2\bar{\mathrm{F}}^{-1}_{\alpha i} - \frac{1}{2}\bar{\mathrm{F}}_{k\alpha}\bar{\mathrm{B}}_{ki} - \frac{1}{2}\bar{\mathrm{F}}_{j\alpha}\bar{\mathrm{B}}_{ij}\right. \\
&\quad \left. + \frac{1}{3}\bar{\mathrm{F}}^{-1}_{\alpha i}\bar{\mathrm{B}}_{jk}\bar{\mathrm{B}}_{kj} - \frac{1}{2}\bar{\mathrm{B}}_{ji}\bar{\mathrm{F}}_{j\alpha} - \frac{1}{2}\bar{\mathrm{B}}_{ik}\bar{\mathrm{F}}_{k\alpha} + \frac{1}{3}\bar{\mathrm{F}}^{-1}_{\alpha i}\bar{\mathrm{B}}_{jk}\bar{\mathrm{B}}_{kj}\right] \\
&= J^{-1/3}\left[2\bar{I}_1\bar{\mathrm{F}}_{i\alpha} - \frac{2}{3}\bar{I}_1^2\bar{\mathrm{F}}^{-1}_{\alpha i} - 2\bar{\mathrm{B}}_{ji}\bar{\mathrm{F}}_{j\alpha} + \frac{2}{3}\bar{\mathrm{F}}^{-1}_{\alpha i}\bar{\mathrm{B}}_{jk}\bar{\mathrm{B}}_{kj}\right] \\
&= 2J^{-1/3}\left[\bar{I}_1\bar{\mathrm{F}}_{i\alpha} - \bar{\mathrm{B}}_{ji}\bar{\mathrm{F}}_{j\alpha} - \frac{1}{3}\left(\bar{I}_1^2 - \bar{\mathrm{B}}_{jk}\bar{\mathrm{B}}_{kj}\right)\bar{\mathrm{F}}^{-1}_{\alpha i}\right] \\
&= 2J^{-1/3}\left[\bar{I}_1\bar{\mathrm{F}}_{i\alpha} - \bar{\mathrm{B}}_{ij}\bar{\mathrm{F}}_{j\alpha} - \frac{2}{3}\bar{I}_2\bar{\mathrm{F}}^{-1}_{\alpha i}\right]
\end{aligned}
\tag{A.5}
$$

$$
\begin{aligned}
\frac{\partial \bar{I}_4}{\partial \mathrm{F}_{i\alpha}} &= \frac{\partial}{\partial \mathrm{F}_{i\alpha}} \left(\mathrm{M}_{1\beta} \bar{\mathrm{C}}_{\beta\gamma} \mathrm{M}_{1\gamma} \right) \\
&= \mathrm{M}_{1\beta} \frac{\partial \bar{\mathrm{C}}_{\beta\gamma}}{\partial \mathrm{F}_{i\alpha}} \mathrm{M}_{1\gamma} \\
&= J^{-1/3} \left[\mathrm{M}_{1\beta} \delta_{\alpha\beta} \bar{\mathrm{F}}_{i\gamma} \mathrm{M}_{1\gamma} + \mathrm{M}_{1\beta} \delta_{\alpha\gamma} \bar{\mathrm{F}}_{i\beta} \mathrm{M}_{1\gamma} - \frac{2}{3} \mathrm{M}_{1\beta} \bar{\mathrm{F}}^{-1}_{\alpha i} \bar{\mathrm{C}}_{\beta\gamma} \mathrm{M}_{1\gamma} \right] \\
&= J^{-1/3} \left[\mathrm{M}_{1\alpha} \bar{\mathrm{F}}_{i\gamma} \mathrm{M}_{1\gamma} + \mathrm{M}_{1\beta} \bar{\mathrm{F}}_{i\beta} \mathrm{M}_{1\alpha} - \frac{2}{3} \bar{I}_4 \bar{\mathrm{F}}^{-1}_{\alpha i} \right] \\
&= J^{-1/3} \left[\mathrm{M}_{1\alpha} \bar{\mathrm{F}}_{i\beta} \mathrm{M}_{1\beta} + \mathrm{M}_{1\alpha} \bar{\mathrm{F}}_{i\beta} \mathrm{M}_{1\beta} - \frac{2}{3} \bar{I}_4 \bar{\mathrm{F}}^{-1}_{\alpha i} \right] \\
&= J^{-1/3} \left[2\mathrm{M}_{1\alpha} \bar{\mathrm{F}}_{i\beta} \mathrm{M}_{1\beta} - \frac{2}{3} \bar{I}_4 \bar{\mathrm{F}}^{-1}_{\alpha i} \right] \\
&= 2J^{-1/3} \left[\mathrm{M}_{1\alpha} \bar{\mathrm{F}}_{i\beta} \mathrm{M}_{1\beta} - \frac{1}{3} \bar{I}_4 \bar{\mathrm{F}}^{-1}_{\alpha i} \right]
\end{aligned}
\tag{A.6}
$$

$$
\begin{aligned}
\frac{\partial \bar{I}_6}{\partial \mathrm{F}_{i\alpha}} &= \frac{\partial}{\partial \mathrm{F}_{i\alpha}} \left(\mathrm{M}_{2\beta} \bar{\mathrm{C}}_{\beta\gamma} \mathrm{M}_{2\gamma} \right) \\
&= \mathrm{M}_{2\beta} \frac{\partial \bar{\mathrm{C}}_{\beta\gamma}}{\partial \mathrm{F}_{i\alpha}} \mathrm{M}_{2\gamma} \\
&= J^{-1/3} \left[\mathrm{M}_{2\beta} \delta_{\alpha\beta} \bar{\mathrm{F}}_{i\gamma} \mathrm{M}_{2\gamma} + \mathrm{M}_{2\beta} \delta_{\alpha\gamma} \bar{\mathrm{F}}_{i\beta} \mathrm{M}_{2\gamma} - \frac{2}{3} \mathrm{M}_{2\beta} \bar{\mathrm{F}}^{-1}_{\alpha i} \bar{\mathrm{C}}_{\beta\gamma} \mathrm{M}_{2\gamma} \right] \\
&= J^{-1/3} \left[\mathrm{M}_{2\alpha} \bar{\mathrm{F}}_{i\gamma} \mathrm{M}_{2\gamma} + \mathrm{M}_{2\beta} \bar{\mathrm{F}}_{i\beta} \mathrm{M}_{2\alpha} - \frac{2}{3} \bar{I}_6 \bar{\mathrm{F}}^{-1}_{\alpha i} \right] \\
&= J^{-1/3} \left[\mathrm{M}_{2\alpha} \bar{\mathrm{F}}_{i\beta} \mathrm{M}_{2\beta} + \mathrm{M}_{2\alpha} \bar{\mathrm{F}}_{i\beta} \mathrm{M}_{2\beta} - \frac{2}{3} \bar{I}_6 \bar{\mathrm{F}}^{-1}_{\alpha i} \right] \\
&= J^{-1/3} \left[2\mathrm{M}_{2\alpha} \bar{\mathrm{F}}_{i\beta} \mathrm{M}_{2\beta} - \frac{2}{3} \bar{I}_6 \bar{\mathrm{F}}^{-1}_{\alpha i} \right] \\
&= 2J^{-1/3} \left[\mathrm{M}_{2\alpha} \bar{\mathrm{F}}_{i\beta} \mathrm{M}_{2\beta} - \frac{1}{3} \bar{I}_6 \bar{\mathrm{F}}^{-1}_{\alpha i} \right]
\end{aligned}
\tag{A.7}
$$

$$
\begin{aligned}
\frac{\partial \bar{I}_8}{\partial \mathrm{F}_{i\alpha}} &= \frac{\partial}{\partial \mathrm{F}_{i\alpha}} \left(\tau_{\beta\gamma} \bar{\mathrm{C}}_{\gamma\beta} \right) \\
&= \tau_{\beta\gamma} \frac{\partial \bar{\mathrm{C}}_{\gamma\beta}}{\partial \mathrm{F}_{i\alpha}} \\
&= J^{-1/3} \left[\tau_{\beta\gamma} \delta_{\alpha\gamma} \bar{\mathrm{F}}_{i\beta} + \tau_{\beta\gamma} \delta_{\alpha\beta} \bar{\mathrm{F}}_{i\gamma} - \frac{2}{3} \tau_{\beta\gamma} \bar{\mathrm{F}}^{-1}_{\alpha i} \bar{\mathrm{C}}_{\gamma\beta} \right] \\
&= J^{-1/3} \left[\tau_{\beta\alpha} \bar{\mathrm{F}}_{i\beta} + \tau_{\alpha\gamma} \bar{\mathrm{F}}_{i\gamma} - \frac{2}{3} \tau_{\beta\gamma} \bar{\mathrm{C}}_{\gamma\beta} \bar{\mathrm{F}}^{-1}_{\alpha i} \right] \\
&= J^{-1/3} \left[\tau_{\alpha\beta} \bar{\mathrm{F}}_{i\beta} + \tau_{\alpha\beta} \bar{\mathrm{F}}_{i\beta} - \frac{2}{3} \bar{I}_8 \bar{\mathrm{F}}^{-1}_{\alpha i} \right] \\
&= J^{-1/3} \left[2\tau_{\alpha\beta} \bar{\mathrm{F}}_{i\beta} - \frac{2}{3} \bar{I}_8 \bar{\mathrm{F}}^{-1}_{\alpha i} \right] \\
&= 2J^{-1/3} \left[\tau_{\alpha\beta} \bar{\mathrm{F}}_{i\beta} - \frac{1}{3} \bar{I}_8 \bar{\mathrm{F}}^{-1}_{\alpha i} \right]
\end{aligned}
\tag{A.8}
$$

$$\begin{aligned} \mathrm{d}F_{i\alpha} &= \mathrm{d}\frac{\partial u_i}{\partial X_\alpha} \\ &= \mathrm{d}\frac{\partial u_i}{\partial x_j}\frac{\partial x_j}{\partial X_\alpha} \\ &= \mathrm{d}\frac{\partial u_i}{\partial x_j}\frac{\partial x_j}{\partial X_\alpha} \\ &= \mathrm{d}l_{ij}F_{j\alpha} \end{aligned} \tag{A.9}$$

$$\begin{aligned} \mathrm{d}J &= \frac{\partial J}{\partial F_{i\alpha}}\mathrm{d}F_{i\alpha} \\ &= JF^{-1}_{\alpha i}\mathrm{d}l_{ij}F_{j\alpha} \\ &= J\mathrm{d}l_{ij}\delta_{ij} \\ &= J\mathrm{d}l_{ii} \end{aligned} \tag{A.10}$$

$$\begin{aligned} \mathrm{d}\bar{F}_{i\alpha} &= \mathrm{d}\left(J^{-1/3}F_{i\alpha}\right) \\ &= \mathrm{d}J^{-1/3}F_{i\alpha} + J^{-1/3}\mathrm{d}F_{i\alpha} \\ &= -\frac{1}{3}J^{-1/3}J^{-1}J\mathrm{d}l_{jj}F_{i\alpha} + J^{-1/3}\mathrm{d}l_{ij}F_{j\alpha} \\ &= -\frac{1}{3}\mathrm{d}l_{jj}\bar{F}_{i\alpha} + \mathrm{d}l_{ij}\bar{F}_{j\alpha} \\ &= \mathrm{d}l_{ij}\bar{F}_{j\alpha} - \frac{1}{3}\mathrm{d}l_{jj}\bar{F}_{i\alpha} \end{aligned} \tag{A.11}$$

$$
\begin{aligned}
\mathrm{d}\bar{B}_{ij} &= \mathrm{d}\left(\bar{F}_{i\alpha}\bar{F}_{j\alpha}\right) \\
&= \mathrm{d}\bar{F}_{i\alpha}\bar{F}_{j\alpha} + \bar{F}_{i\alpha}\mathrm{d}\bar{F}_{j\alpha} \\
&= \left(\mathrm{d}l_{ik}\bar{F}_{k\alpha} - \frac{1}{3}\mathrm{d}l_{kk}\bar{F}_{i\alpha}\right)\bar{F}_{j\alpha} + \bar{F}_{i\alpha}\left(\mathrm{d}l_{jk}\bar{F}_{k\alpha} - \frac{1}{3}\mathrm{d}l_{kk}\bar{F}_{j\alpha}\right) \\
&= \mathrm{d}l_{ik}\bar{B}_{kj} - \frac{1}{3}\mathrm{d}l_{kk}\bar{B}_{ij} + \bar{B}_{ik}\mathrm{d}l_{jk} - \frac{1}{3}\mathrm{d}l_{kk}\bar{B}_{ij} \\
&= (\mathrm{d}d_{ik} + \mathrm{d}w_{ik})\bar{B}_{kj} - \frac{1}{3}\mathrm{d}l_{kk}\bar{B}_{ij} + \bar{B}_{ik}(\mathrm{d}d_{kj} - \mathrm{d}w_{kj}) - \frac{1}{3}\mathrm{d}l_{kk}\bar{B}_{ij} \\
&= \mathrm{d}d_{ik}\bar{B}_{kj} + \mathrm{d}w_{ik}\bar{B}_{kj} - \frac{1}{3}\mathrm{d}l_{kk}\bar{B}_{ij} + \bar{B}_{ik}\mathrm{d}d_{kj} - \bar{B}_{ik}\mathrm{d}w_{kj} - \frac{1}{3}\mathrm{d}l_{kk}\bar{B}_{ij} \\
&= \mathrm{d}d_{ik}\bar{B}_{kj} - \frac{1}{3}\mathrm{d}l_{kk}\bar{B}_{ij} + \bar{B}_{ik}\mathrm{d}d_{kj} - \frac{1}{3}\mathrm{d}l_{kk}\bar{B}_{ij} + \mathrm{d}w_{ik}\bar{B}_{kj} - \bar{B}_{ik}\mathrm{d}w_{kj} \\
&= \mathrm{d}d_{ik}\bar{B}_{kj} - \frac{1}{3}\mathrm{d}d_{kk}\bar{B}_{ij} + \bar{B}_{ik}\mathrm{d}d_{kj} - \frac{1}{3}\mathrm{d}d_{kk}\bar{B}_{ij} + \mathrm{d}w_{ik}\bar{B}_{kj} - \bar{B}_{ik}\mathrm{d}w_{kj} \\
&= \frac{1}{2}\left(\mathrm{d}d_{ik}\bar{B}_{kj} + \mathrm{d}d_{ik}\bar{B}_{kj}\right) + \frac{1}{2}\left(\bar{B}_{ik}\mathrm{d}d_{kj} + \bar{B}_{ik}\mathrm{d}d_{kj}\right) \\
&\quad - \frac{1}{2}\left(\frac{1}{3}\mathrm{d}d_{kk}\bar{B}_{ij} + \frac{1}{3}\mathrm{d}d_{kk}\bar{B}_{ij} + \frac{1}{3}\mathrm{d}d_{kk}\bar{B}_{ij} + \frac{1}{3}\mathrm{d}d_{kk}\bar{B}_{ij}\right) \\
&\quad + \mathrm{d}w_{ik}\bar{B}_{kj} - \bar{B}_{ik}\mathrm{d}w_{kj} \\
&= \frac{1}{2}\left(\delta_{il}\mathrm{d}d_{lk}\bar{B}_{kj} + \delta_{il}\mathrm{d}d_{lk}\bar{B}_{kj}\right) + \frac{1}{2}\left(\bar{B}_{ik}\mathrm{d}d_{kl}\delta_{lj} + \bar{B}_{ik}\mathrm{d}d_{kl}\delta_{lj}\right) \\
&\quad - \frac{1}{2}\left(\frac{1}{3}\mathrm{d}d_{mm}\bar{B}_{ij} + \frac{1}{3}\mathrm{d}d_{mm}\bar{B}_{ij} + \frac{1}{3}\mathrm{d}d_{mm}\bar{B}_{ij} + \frac{1}{3}\mathrm{d}d_{mm}\bar{B}_{ij}\right) \\
&\quad + \mathrm{d}w_{ik}\bar{B}_{kj} - \bar{B}_{ik}\mathrm{d}w_{kj} \\
&= \frac{1}{2}\left(\delta_{il}\mathrm{d}d_{lk}\bar{B}_{kj} + \delta_{il}\mathrm{d}d_{lk}\bar{B}_{kj}\right) + \frac{1}{2}\left(\bar{B}_{ik}\delta_{jl}\mathrm{d}d_{lk} + \bar{B}_{ik}\delta_{jl}\mathrm{d}d_{lk}\right) \\
&\quad - \frac{1}{2}\left(\frac{1}{3}\mathrm{d}d_{mm}\bar{B}_{ij} + \frac{1}{3}\mathrm{d}d_{mm}\bar{B}_{ij} + \frac{1}{3}\mathrm{d}d_{mm}\bar{B}_{ij} + \frac{1}{3}\mathrm{d}d_{mm}\bar{B}_{ij}\right) \\
&\quad + \mathrm{d}w_{ik}\bar{B}_{kj} - \bar{B}_{ik}\mathrm{d}w_{kj} \\
&= \frac{1}{2}\left(\delta_{il}\bar{B}_{kj} + \delta_{il}\bar{B}_{kj} + \bar{B}_{ik}\delta_{jl} + \bar{B}_{ik}\delta_{jl}\right)\mathrm{d}d_{lk} \\
&\quad - \frac{1}{2}\left(\bar{B}_{ij} + \bar{B}_{ij} + \bar{B}_{ij} + \bar{B}_{ij}\right)\frac{1}{3}\mathrm{d}d_{mm} + \mathrm{d}w_{ik}\bar{B}_{kj} - \bar{B}_{ik}\mathrm{d}w_{kj} \\
&= \frac{1}{2}\left(\delta_{il}\bar{B}_{jk} + \delta_{ik}\bar{B}_{jl} + \bar{B}_{ik}\delta_{jl} + \bar{B}_{il}\delta_{jk}\right)\mathrm{d}d_{kl} \\
&\quad - \frac{1}{2}\left(\delta_{kl}\delta_{il}\bar{B}_{jk} + \delta_{kl}\delta_{ik}\bar{B}_{jl} + \bar{B}_{ik}\delta_{jl}\delta_{kl} + \bar{B}_{il}\delta_{jk}\delta_{kl}\right)\frac{1}{3}\mathrm{d}d_{mm} \\
&\quad + \mathrm{d}w_{ik}\bar{B}_{kj} - \bar{B}_{ik}\mathrm{d}w_{kj} \\
&= \frac{1}{2}\left(\delta_{il}\bar{B}_{jk} + \bar{B}_{il}\delta_{jk} + \delta_{ik}\bar{B}_{jl} + \bar{B}_{ik}\delta_{jl}\right)\mathrm{d}d_{kl} \\
&\quad - \frac{1}{2}\left(\delta_{il}\bar{B}_{jk} + \bar{B}_{il}\delta_{jk} + \delta_{ik}\bar{B}_{jl} + \bar{B}_{ik}\delta_{jl}\right)\frac{1}{3}\mathrm{d}d_{mm}\delta_{kl} + \mathrm{d}w_{ik}\bar{B}_{kj} - \bar{B}_{ik}\mathrm{d}w_{kj} \\
&= \mathbb{H}_{ijkl}\mathrm{d}d_{kl} - \mathbb{H}_{ijkl}\frac{1}{3}\mathrm{d}d_{mm}\delta_{kl} + \mathrm{d}w_{ik}\bar{B}_{kj} - \bar{B}_{ik}\mathrm{d}w_{kj} \\
&= \mathbb{H}_{ijkl}\left(\mathrm{d}d_{kl} - \frac{1}{3}\mathrm{d}d_{mm}\delta_{kl}\right) + \mathrm{d}w_{ik}\bar{B}_{kj} - \bar{B}_{ik}\mathrm{d}w_{kj}
\end{aligned}
\tag{A.12}
$$

$$
\begin{aligned}
\mathrm{d}\bar{I}_1 &= \frac{\partial \bar{I}_1}{\partial F_{i\alpha}} \mathrm{d}F_{i\alpha} \\
&= 2J^{-1/3} \left[\bar{F}_{i\alpha} - \frac{1}{3} \bar{I}_1 \bar{F}^{-1}_{\alpha i} \right] \mathrm{d}l_{ij} F_{j\alpha} \\
&= 2 \left[\bar{F}_{i\alpha} - \frac{1}{3} \bar{I}_1 \bar{F}^{-1}_{\alpha i} \right] \mathrm{d}l_{ij} \bar{F}_{j\alpha} \\
&= 2 \left[\bar{B}_{ij} - \frac{1}{3} \bar{I}_1 \delta_{ij} \right] \mathrm{d}l_{ij} \\
&= 2 \left[\bar{B}_{ij} - \frac{1}{3} \bar{I}_1 \delta_{ij} \right] \mathrm{d}d_{ij}
\end{aligned}
\tag{A.13}
$$

$$
\begin{aligned}
\mathrm{d}\bar{I}_2 &= \frac{\partial \bar{I}_2}{\partial F_{i\alpha}} \mathrm{d}F_{i\alpha} \\
&= 2J^{-1/3} \left[\bar{I}_1 \bar{F}_{i\alpha} - \bar{B}_{ik} \bar{F}_{k\alpha} - \frac{2}{3} \bar{I}_2 \bar{F}^{-1}_{\alpha i} \right] \mathrm{d}l_{ij} F_{j\alpha} \\
&= 2 \left[\bar{I}_1 \bar{F}_{i\alpha} - \bar{B}_{ik} \bar{F}_{k\alpha} - \frac{2}{3} \bar{I}_2 \bar{F}^{-1}_{\alpha i} \right] \mathrm{d}l_{ij} \bar{F}_{j\alpha} \\
&= 2 \left[\bar{I}_1 \bar{B}_{ij} - \bar{B}_{ik} \bar{B}_{kj} - \frac{2}{3} \bar{I}_2 \delta_{ij} \right] \mathrm{d}l_{ij} \\
&= 2 \left[\bar{I}_1 \bar{B}_{ij} - \bar{B}_{ik} \bar{B}_{kj} - \frac{2}{3} \bar{I}_2 \delta_{ij} \right] \mathrm{d}d_{ij}
\end{aligned}
\tag{A.14}
$$

$$
\begin{aligned}
\mathrm{d}\bar{I}_4 &= \frac{\partial \bar{I}_4}{\partial F_{i\alpha}} \mathrm{d}F_{i\alpha} \\
&= 2J^{-1/3} \left[M_{1\alpha} \bar{F}_{i\beta} M_{1\beta} - \frac{1}{3} \bar{I}_4 \bar{F}^{-1}_{\alpha i} \right] \mathrm{d}l_{ij} F_{j\alpha} \\
&= 2 \left[M_{1\alpha} \bar{F}_{i\beta} M_{1\beta} - \frac{1}{3} \bar{I}_4 \bar{F}^{-1}_{\alpha i} \right] \mathrm{d}l_{ij} \bar{F}_{j\alpha} \\
&= 2 \left[\bar{F}_{j\alpha} M_{1\alpha} \bar{F}_{i\beta} M_{1\beta} - \frac{1}{3} \bar{I}_4 \delta_{ij} \right] \mathrm{d}l_{ij} \\
&= 2 \left[m_{1i} m_{1j} - \frac{1}{3} \bar{I}_4 \delta_{ij} \right] \mathrm{d}l_{ij} \\
&= 2 \left[m_{1i} m_{1j} - \frac{1}{3} \bar{I}_4 \delta_{ij} \right] \mathrm{d}d_{ij}
\end{aligned}
\tag{A.15}
$$

$$
\begin{aligned}
\mathrm{d}\bar{I}_6 &= \frac{\partial \bar{I}_6}{\partial F_{i\alpha}} \mathrm{d}F_{i\alpha} \\
&= 2J^{-1/3} \left[M_{2\alpha} \bar{F}_{i\beta} M_{2\beta} - \frac{1}{3} \bar{I}_4 \bar{F}^{-1}_{\alpha i} \right] \mathrm{d}l_{ij} F_{j\alpha} \\
&= 2 \left[M_{2\alpha} \bar{F}_{i\beta} M_{2\beta} - \frac{1}{3} \bar{I}_6 \bar{F}^{-1}_{\alpha i} \right] \mathrm{d}l_{ij} \bar{F}_{j\alpha} \\
&= 2 \left[\bar{F}_{j\alpha} M_{2\alpha} \bar{F}_{i\beta} M_{2\beta} - \frac{1}{3} \bar{I}_6 \delta_{ij} \right] \mathrm{d}l_{ij} \\
&= 2 \left[m_{2i} m_{2j} - \frac{1}{3} \bar{I}_4 \delta_{ij} \right] \mathrm{d}l_{ij} \\
&= 2 \left[m_{2i} m_{2j} - \frac{1}{3} \bar{I}_4 \delta_{ij} \right] \mathrm{d}d_{ij}
\end{aligned}
\tag{A.16}
$$

$$
\begin{aligned}
\mathrm{d}\bar{I}_8 &= \frac{\partial \bar{I}_8}{\partial F_{i\alpha}} \mathrm{d}F_{i\alpha} \\
&= 2J^{-1/3}\left[\tau_{\alpha\beta}\bar{F}_{i\beta} - \frac{1}{3}\bar{I}_8\bar{F}^{-1}_{\alpha i}\right]\mathrm{d}l_{ij}F_{j\alpha} \\
&= 2\left[\tau_{\alpha\beta}\bar{F}_{i\beta} - \frac{1}{3}\bar{I}_8\bar{F}^{-1}_{\alpha i}\right]\mathrm{d}l_{ij}\bar{F}_{j\alpha} \\
&= 2\left[\bar{F}_{j\alpha}\tau_{\alpha\beta}\bar{F}_{i\beta} - \frac{1}{3}\bar{I}_8\delta_{ij}\right]\mathrm{d}l_{ij} \\
&= 2\left[\bar{F}_{i\alpha}\tau_{\alpha\beta}\bar{F}_{j\beta} - \frac{1}{3}\bar{I}_8\delta_{ij}\right]\mathrm{d}l_{ij} \\
&= 2\left[\Sigma_{ij} - \frac{1}{3}\bar{I}_8\delta_{ij}\right]\mathrm{d}l_{ij} \\
&= 2\left[\Sigma_{ij} - \frac{1}{3}\bar{I}_8\delta_{ij}\right]\mathrm{d}d_{ij}
\end{aligned}
\tag{A.17}
$$

$$
\begin{aligned}
\mathbb{H}_{ijmm} &= \frac{1}{2}\left(\delta_{im}\bar{B}_{jm} + \bar{B}_{im}\delta_{jm} + \delta_{im}\bar{B}_{jm} + \bar{B}_{im}\delta_{jm}\right) \\
&= 2\bar{B}_{ij}
\end{aligned}
\tag{A.18}
$$

$$
\begin{aligned}
\mathrm{d}(\mathrm{div}\,\bar{B}_{ij}) &= \mathrm{d}\left(\bar{B}_{ij} - \frac{1}{3}\bar{I}_1\delta_{ij}\right) \\
&= \mathrm{d}\bar{B}_{ij} - \frac{1}{3}\,\mathrm{d}\bar{I}_1\delta_{ij} \\
&= \mathbb{H}_{ijkl}\left(\mathrm{d}d_{kl} - \frac{1}{3}\mathrm{d}d_{mm}\delta_{kl}\right) + \mathrm{d}w_{ik}\bar{B}_{kj} - \bar{B}_{ik}\mathrm{d}w_{kj} \\
&\quad - \frac{2}{3}\left[\bar{B}_{kl} - \frac{1}{3}\bar{I}_1\delta_{kl}\right]\mathrm{d}d_{kl}\delta_{ij} \\
&= \mathbb{H}_{ijkl}\left(\mathrm{d}d_{kl} - \frac{1}{3}\mathrm{d}d_{mm}\delta_{kl}\right) + \mathrm{d}w_{ik}\bar{B}_{kj} - \bar{B}_{ik}\mathrm{d}w_{kj} \\
&\quad - \frac{2}{3}\left(\delta_{ij}\bar{B}_{kl} - \frac{1}{3}\bar{I}_1\delta_{ij}\delta_{kl}\right)\mathrm{d}d_{kl} \\
&= \mathbb{H}_{ijkl}\mathrm{d}d_{kl} - \frac{1}{3}\mathbb{H}_{ijmm}\delta_{kl}\mathrm{d}d_{kl} + \mathrm{d}w_{ik}\bar{B}_{kj} - \bar{B}_{ik}\mathrm{d}w_{kj} \\
&\quad - \frac{2}{3}\left(\delta_{ij}\bar{B}_{kl} - \frac{1}{3}\bar{I}_1\delta_{ij}\delta_{kl}\right)\mathrm{d}d_{kl} \\
&= \mathbb{H}_{ijkl}\mathrm{d}d_{kl} - \frac{2}{3}\bar{B}_{ij}\delta_{kl}\mathrm{d}d_{kl} + \mathrm{d}w_{ik}\bar{B}_{kj} - \bar{B}_{ik}\mathrm{d}w_{kj} \\
&\quad - \frac{2}{3}\left(\delta_{ij}\bar{B}_{kl} - \frac{1}{3}\bar{I}_1\delta_{ij}\delta_{kl}\right)\mathrm{d}d_{kl} \\
&= \left[\mathbb{H}_{ijkl} - \frac{2}{3}\bar{B}_{ij}\delta_{kl} - \frac{2}{3}\delta_{ij}\bar{B}_{kl} - \frac{2}{9}\bar{I}_1\delta_{ij}\delta_{kl}\right]\mathrm{d}d_{kl} \\
&\quad + \mathrm{d}w_{ik}\bar{B}_{kj} - \bar{B}_{ik}\mathrm{d}w_{kj} \\
&= \left[\mathbb{H}_{ijkl} - \frac{2}{3}\left(\bar{B}_{ij}\delta_{kl} + \delta_{ij}\bar{B}_{kl}\right) - \frac{2}{9}\bar{I}_1\delta_{ij}\delta_{kl}\right]\mathrm{d}d_{kl} \\
&\quad + \mathrm{d}w_{ik}\bar{B}_{kj} - \bar{B}_{ik}\mathrm{d}w_{kj}
\end{aligned}
\tag{A.19}
$$

$$
\begin{aligned}
\mathrm{d}\bar{\Sigma}_{ij} &= \mathrm{d}\left(\bar{F}_{i\alpha}\tau_{\alpha\beta}\bar{F}_{j\beta}\right)\\
&= \mathrm{d}\bar{F}_{i\alpha}\tau_{\alpha\beta}\bar{F}_{j\beta} + \bar{F}_{i\alpha}\tau_{\alpha\beta}\mathrm{d}\bar{F}_{j\beta}\\
&= \left(\mathrm{d}l_{ik}\bar{F}_{k\alpha} - \frac{1}{3}\mathrm{d}l_{kk}\bar{F}_{i\alpha}\right)\tau_{\alpha\beta}\bar{F}_{j\beta} + \bar{F}_{i\alpha}\tau_{\alpha\beta}\left(\mathrm{d}l_{jk}\bar{F}_{k\beta} - \frac{1}{3}\mathrm{d}l_{kk}\bar{F}_{j\beta}\right)\\
&= \mathrm{d}l_{ik}\bar{\tau}_{kj} - \frac{1}{3}\mathrm{d}l_{kk}\bar{\tau}_{ij} + \bar{\tau}_{ik}\mathrm{d}l_{jk} - \frac{1}{3}\mathrm{d}l_{kk}\bar{\tau}_{ij}\\
&= (\mathrm{d}d_{ik} + \mathrm{d}w_{ik})\bar{\tau}_{kj} - \frac{1}{3}\mathrm{d}l_{kk}\bar{\tau}_{ij} + \bar{\tau}_{ik}(\mathrm{d}d_{kj} - \mathrm{d}w_{kj}) - \frac{1}{3}\mathrm{d}l_{kk}\bar{\tau}_{ij}\\
&= \mathrm{d}d_{ik}\bar{\tau}_{kj} + \mathrm{d}w_{ik}\bar{\tau}_{kj} - \frac{1}{3}\mathrm{d}l_{kk}\bar{\tau}_{ij} + \bar{\tau}_{ik}\mathrm{d}d_{kj} - \bar{\tau}_{ik}\mathrm{d}w_{kj} - \frac{1}{3}\mathrm{d}l_{kk}\bar{\tau}_{ij}\\
&= \mathrm{d}d_{ik}\bar{\tau}_{kj} - \frac{1}{3}\mathrm{d}l_{kk}\bar{\tau}_{ij} + \bar{\tau}_{ik}\mathrm{d}d_{kj} - \frac{1}{3}\mathrm{d}l_{kk}\bar{\tau}_{ij} + \mathrm{d}w_{ik}\bar{\tau}_{kj} - \bar{\tau}_{ik}\mathrm{d}w_{kj}\\
&= \mathrm{d}d_{ik}\bar{\tau}_{kj} - \frac{1}{3}\mathrm{d}d_{kk}\bar{\tau}_{ij} + \bar{\tau}_{ik}\mathrm{d}d_{kj} - \frac{1}{3}\mathrm{d}d_{kk}\bar{\tau}_{ij} + \mathrm{d}w_{ik}\bar{\tau}_{kj} - \bar{\tau}_{ik}\mathrm{d}w_{kj}\\
&= \frac{1}{2}\left(\mathrm{d}d_{ik}\bar{\tau}_{kj} + \mathrm{d}d_{ik}\bar{\tau}_{kj}\right) + \frac{1}{2}\left(\bar{\tau}_{ik}\mathrm{d}d_{kj} + \bar{\tau}_{ik}\mathrm{d}d_{kj}\right)\\
&\quad - \frac{1}{2}\left(\frac{1}{3}\mathrm{d}d_{kk}\bar{\tau}_{ij} + \frac{1}{3}\mathrm{d}d_{kk}\bar{\tau}_{ij} + \frac{1}{3}\mathrm{d}d_{kk}\bar{\tau}_{ij} + \frac{1}{3}\mathrm{d}d_{kk}\bar{\tau}_{ij}\right)\\
&\quad + \mathrm{d}w_{ik}\bar{\tau}_{kj} - \bar{\tau}_{ik}\mathrm{d}w_{kj}\\
&= \frac{1}{2}\left(\delta_{il}\mathrm{d}d_{lk}\bar{\tau}_{kj} + \delta_{il}\mathrm{d}d_{lk}\bar{\tau}_{kj}\right) + \frac{1}{2}\left(\bar{\tau}_{ik}\mathrm{d}d_{kl}\delta_{lj} + \bar{\tau}_{ik}\mathrm{d}d_{kl}\delta_{lj}\right)\\
&\quad - \frac{1}{2}\left(\frac{1}{3}\mathrm{d}d_{mm}\bar{\tau}_{ij} + \frac{1}{3}\mathrm{d}d_{mm}\bar{\tau}_{ij} + \frac{1}{3}\mathrm{d}d_{mm}\bar{\tau}_{ij} + \frac{1}{3}\mathrm{d}d_{mm}\bar{\tau}_{ij}\right)\\
&\quad + \mathrm{d}w_{ik}\bar{\tau}_{kj} - \bar{\tau}_{ik}\mathrm{d}w_{kj}\\
&= \frac{1}{2}\left(\delta_{il}\mathrm{d}d_{lk}\bar{\tau}_{kj} + \delta_{il}\mathrm{d}d_{lk}\bar{\tau}_{kj}\right) + \frac{1}{2}\left(\bar{\tau}_{ik}\delta_{jl}\mathrm{d}d_{lk} + \bar{\tau}_{ik}\delta_{jl}\mathrm{d}d_{lk}\right)\\
&\quad - \frac{1}{2}\left(\frac{1}{3}\mathrm{d}d_{mm}\bar{\tau}_{ij} + \frac{1}{3}\mathrm{d}d_{mm}\bar{\tau}_{ij} + \frac{1}{3}\mathrm{d}d_{mm}\bar{\tau}_{ij} + \frac{1}{3}\mathrm{d}d_{mm}\bar{\tau}_{ij}\right)\\
&\quad + \mathrm{d}w_{ik}\bar{\tau}_{kj} - \bar{\tau}_{ik}\mathrm{d}w_{kj}\\
&= \frac{1}{2}\left(\delta_{il}\bar{\tau}_{kj} + \delta_{il}\bar{\tau}_{kj} + \bar{\tau}_{ik}\delta_{jl} + \bar{\tau}_{ik}\delta_{jl}\right)\mathrm{d}d_{lk}\\
&\quad - \frac{1}{2}\left(\bar{\tau}_{ij} + \bar{\tau}_{ij} + \bar{\tau}_{ij} + \bar{\tau}_{ij}\right)\frac{1}{3}\mathrm{d}d_{mm} + \mathrm{d}w_{ik}\bar{\tau}_{kj} - \bar{\tau}_{ik}\mathrm{d}w_{kj}\\
&= \frac{1}{2}\left(\delta_{il}\bar{\tau}_{jk} + \delta_{ik}\bar{\tau}_{jl} + \bar{\tau}_{ik}\delta_{jl} + \bar{\tau}_{il}\delta_{jk}\right)\mathrm{d}d_{kl}\\
&\quad - \frac{1}{2}\left(\delta_{kl}\delta_{il}\bar{\tau}_{jk} + \delta_{kl}\delta_{ik}\bar{\tau}_{jl} + \bar{\tau}_{ik}\delta_{jl}\delta_{kl} + \bar{\tau}_{il}\delta_{jk}\delta_{kl}\right)\frac{1}{3}\mathrm{d}d_{mm}\\
&\quad + \mathrm{d}w_{ik}\bar{\tau}_{kj} - \bar{\tau}_{ik}\mathrm{d}w_{kj}\\
&= \frac{1}{2}\left(\delta_{il}\bar{\tau}_{jk} + \bar{\tau}_{il}\delta_{jk} + \delta_{ik}\bar{\tau}_{jl} + \bar{\tau}_{ik}\delta_{jl}\right)\mathrm{d}d_{kl}\\
&\quad - \frac{1}{2}\left(\delta_{il}\bar{\tau}_{jk} + \bar{\tau}_{il}\delta_{jk} + \delta_{ik}\bar{\tau}_{jl} + \bar{\tau}_{ik}\delta_{jl}\right)\frac{1}{3}\mathrm{d}d_{mm}\delta_{kl} + \mathrm{d}w_{ik}\bar{\tau}_{kj} - \bar{\tau}_{ik}\mathrm{d}w_{kj}\\
&= \mathbb{A}_{3ijkl}\mathrm{d}d_{kl} - \mathbb{A}_{3ijkl}\frac{1}{3}\mathrm{d}d_{mm}\delta_{kl} + \mathrm{d}w_{ik}\bar{\tau}_{kj} - \bar{\tau}_{ik}\mathrm{d}w_{kj}\\
&= \mathbb{A}_{3ijkl}\left(\mathrm{d}d_{kl} - \frac{1}{3}\mathrm{d}d_{mm}\delta_{kl}\right) + \mathrm{d}w_{ik}\bar{\tau}_{kj} - \bar{\tau}_{ik}\mathrm{d}w_{kj}
\end{aligned}
\tag{A.20}
$$

$$
\begin{aligned}
\mathbb{A}_{3ijmm} &= \frac{1}{2}\left(\delta_{im}\bar{\tau}_{jm} + \bar{\tau}_{im}\delta_{jm} + \delta_{im}\bar{\tau}_{jm} + \bar{\tau}_{im}\delta_{jm}\right)\\
&= 2\bar{\tau}_{ij}
\end{aligned}
\tag{A.21}
$$

$$
\begin{aligned}
\mathrm{d}(\operatorname{div}\bar{\tau}_{ij}) &= \mathrm{d}\left(\bar{\tau}_{ij} - \frac{1}{3}\bar{I}_8\delta_{ij}\right) \\
&= \mathrm{d}\bar{\tau}_{ij} - \frac{1}{3}\,\mathrm{d}\bar{I}_8\delta_{ij} \\
&= \mathbb{A}_{3ijkl}\left(\mathrm{d}d_{kl} - \frac{1}{3}\mathrm{d}d_{mm}\delta_{kl}\right) + \mathrm{d}w_{ik}\bar{\tau}_{kj} - \bar{\tau}_{ik}\mathrm{d}w_{kj} \\
&\quad - \frac{2}{3}\left[\bar{\tau}_{kl} - \frac{1}{3}\bar{I}_8\delta_{kl}\right]\mathrm{d}d_{kl}\delta_{ij} \\
&= \mathbb{A}_{3ijkl}\left(\mathrm{d}d_{kl} - \frac{1}{3}\mathrm{d}d_{mm}\delta_{kl}\right) + \mathrm{d}w_{ik}\bar{\tau}_{kj} - \bar{\tau}_{ik}\mathrm{d}w_{kj} \\
&\quad - \frac{2}{3}\left(\delta_{ij}\bar{\tau}_{kl} - \frac{1}{3}\bar{I}_8\delta_{ij}\delta_{kl}\right)\mathrm{d}d_{kl} \\
&= \mathbb{A}_{3ijkl}\mathrm{d}d_{kl} - \frac{1}{3}\mathbb{A}_{3ijmm}\delta_{kl}\mathrm{d}d_{kl} + \mathrm{d}w_{ik}\bar{\tau}_{kj} - \bar{\tau}_{ik}\mathrm{d}w_{kj} \\
&\quad - \frac{2}{3}\left(\delta_{ij}\bar{\tau}_{kl} - \frac{1}{3}\bar{I}_8\delta_{ij}\delta_{kl}\right)\mathrm{d}d_{kl} \\
&= \mathbb{A}_{3ijkl}\mathrm{d}d_{kl} - \frac{2}{3}\bar{\tau}_{ij}\delta_{kl}\mathrm{d}d_{kl} + \mathrm{d}w_{ik}\bar{\tau}_{kj} - \bar{\tau}_{ik}\mathrm{d}w_{kj} \\
&\quad - \frac{2}{3}\left(\delta_{ij}\bar{\tau}_{kl} - \frac{1}{3}\bar{I}_8\delta_{ij}\delta_{kl}\right)\mathrm{d}d_{kl} \\
&= \left[\mathbb{A}_{3ijkl} - \frac{2}{3}\bar{\tau}_{ij}\delta_{kl} - \frac{2}{3}\delta_{ij}\bar{\tau}_{kl} - \frac{2}{9}\bar{I}_8\delta_{ij}\delta_{kl}\right]\mathrm{d}d_{kl} \\
&\quad + \mathrm{d}w_{ik}\bar{\tau}_{kj} - \bar{\tau}_{ik}\mathrm{d}w_{kj} \\
&= \left[\mathbb{A}_{3ijkl} - \frac{2}{3}\left(\bar{\tau}_{ij}\delta_{kl} + \delta_{ij}\bar{\tau}_{kl}\right) - \frac{2}{9}\bar{I}_8\delta_{ij}\delta_{kl}\right]\mathrm{d}d_{kl} \\
&\quad + \mathrm{d}w_{ik}\bar{\tau}_{kj} - \bar{\tau}_{ik}\mathrm{d}w_{kj}
\end{aligned}
\tag{A.22}
$$

$$
\begin{aligned}
\mathrm{d}\left(\bar{m}_{1i}\bar{m}_{1j}\right) &= \mathrm{d}\left(\bar{F}_{i\alpha}M_{1\alpha}\bar{F}_{j\beta}M_{1\beta}\right)\\
&= \mathrm{d}\bar{F}_{i\alpha}M_{1\alpha}\bar{F}_{j\beta}M_{1\beta} + \bar{F}_{i\alpha}M_{1\alpha}\mathrm{d}\bar{F}_{j\beta}M_{1\beta}\\
&= \left(\mathrm{d}l_{ik}\bar{F}_{k\alpha} - \frac{1}{3}\mathrm{d}l_{kk}\bar{F}_{i\alpha}\right)M_{1\alpha}\bar{F}_{j\beta}M_{1\beta} + \bar{F}_{i\alpha}M_{1\alpha}\left(\mathrm{d}l_{jk}\bar{F}_{k\beta} - \frac{1}{3}\mathrm{d}l_{kk}\bar{F}_{j\beta}\right)M_{1\beta}\\
&= \mathrm{d}l_{ik}\bar{m}_{1k}\bar{m}_{1j} - \frac{1}{3}\mathrm{d}l_{kk}\bar{m}_{1i}\bar{m}_{1j} + \bar{m}_{1i}\bar{m}_{1k}\mathrm{d}l_{jk} - \frac{1}{3}\mathrm{d}l_{kk}\bar{m}_{1i}\bar{m}_{1j}\\
&= (\mathrm{d}d_{ik} + \mathrm{d}w_{ik})\bar{m}_{1k}\bar{m}_{1j} - \frac{1}{3}\mathrm{d}l_{kk}\bar{m}_{1i}\bar{m}_{1j} + \bar{m}_{1i}\bar{m}_{1k}(\mathrm{d}d_{kj} - \mathrm{d}w_{kj}) - \frac{1}{3}\mathrm{d}l_{kk}\bar{m}_{1i}\bar{m}_{1j}\\
&= \mathrm{d}d_{ik}\bar{m}_{1k}\bar{m}_{1j} + \mathrm{d}w_{ik}\bar{m}_{1k}\bar{m}_{1j} - \frac{1}{3}\mathrm{d}l_{kk}\bar{m}_{1i}\bar{m}_{1j} + \bar{m}_{1i}\bar{m}_{1k}\mathrm{d}d_{kj}\\
&\quad - \bar{m}_{1i}\bar{m}_{1k}\mathrm{d}w_{kj} - \frac{1}{3}\mathrm{d}l_{kk}\bar{m}_{1i}\bar{m}_{1j}\\
&= \mathrm{d}d_{ik}\bar{m}_{1k}\bar{m}_{1j} - \frac{1}{3}\mathrm{d}l_{kk}\bar{m}_{1i}\bar{m}_{1j} + \bar{m}_{1i}\bar{m}_{1k}\mathrm{d}d_{kj} - \frac{1}{3}\mathrm{d}l_{kk}\bar{m}_{1i}\bar{m}_{1j}\\
&\quad + \mathrm{d}w_{ik}\bar{m}_{1k}\bar{m}_{1j} - \bar{m}_{1i}\bar{m}_{1k}\mathrm{d}w_{kj}\\
&= \mathrm{d}d_{ik}\bar{m}_{1k}\bar{m}_{1j} - \frac{1}{3}\mathrm{d}d_{kk}\bar{m}_{1i}\bar{m}_{1j} + \bar{m}_{1i}\bar{m}_{1k}\mathrm{d}d_{kj} - \frac{1}{3}\mathrm{d}d_{kk}\bar{m}_{1i}\bar{m}_{1j}\\
&\quad + \mathrm{d}w_{ik}\bar{m}_{1k}\bar{m}_{1j} - \bar{m}_{1i}\bar{m}_{1k}\mathrm{d}w_{kj}\\
&= \frac{1}{2}\left(\mathrm{d}d_{ik}\bar{m}_{1k}\bar{m}_{1j} + \mathrm{d}d_{ik}\bar{m}_{1k}\bar{m}_{1j}\right) + \frac{1}{2}\left(\bar{m}_{1i}\bar{m}_{1k}\mathrm{d}d_{kj} + \bar{m}_{1i}\bar{m}_{1k}\mathrm{d}d_{kj}\right)\\
&\quad - \frac{1}{2}\left(\frac{1}{3}\mathrm{d}d_{kk}\bar{m}_{1i}\bar{m}_{1j} + \frac{1}{3}\mathrm{d}d_{kk}\bar{m}_{1i}\bar{m}_{1j} + \frac{1}{3}\mathrm{d}d_{kk}\bar{m}_{1i}\bar{m}_{1j} + \frac{1}{3}\mathrm{d}d_{kk}\bar{m}_{1i}\bar{m}_{1j}\right)\\
&\quad + \mathrm{d}w_{ik}\bar{m}_{1k}\bar{m}_{1j} - \bar{m}_{1i}\bar{m}_{1k}\mathrm{d}w_{kj}\\
&= \frac{1}{2}\left(\delta_{il}\mathrm{d}d_{lk}\bar{m}_{1k}\bar{m}_{1j} + \delta_{il}\mathrm{d}d_{lk}\bar{m}_{1k}\bar{m}_{1j}\right) + \frac{1}{2}\left(\bar{m}_{1i}\bar{m}_{1k}\mathrm{d}d_{kl}\delta_{lj} + \bar{m}_{1i}\bar{m}_{1k}\mathrm{d}d_{kl}\delta_{lj}\right)\\
&\quad - \frac{1}{2}\left(\frac{1}{3}\mathrm{d}d_{mm}\bar{m}_{1i}\bar{m}_{1j} + \frac{1}{3}\mathrm{d}d_{mm}\bar{m}_{1i}\bar{m}_{1j} + \frac{1}{3}\mathrm{d}d_{mm}\bar{m}_{1i}\bar{m}_{1j} + \frac{1}{3}\mathrm{d}d_{mm}\bar{m}_{1i}\bar{m}_{1j}\right)\\
&\quad + \mathrm{d}w_{ik}\bar{m}_{1k}\bar{m}_{1j} - \bar{m}_{1i}\bar{m}_{1k}\mathrm{d}w_{kj}\\
&= \frac{1}{2}\left(\delta_{il}\mathrm{d}d_{lk}\bar{m}_{1k}\bar{m}_{1j} + \delta_{il}\mathrm{d}d_{lk}\bar{m}_{1k}\bar{m}_{1j}\right) + \frac{1}{2}\left(\bar{m}_{1i}\bar{m}_{1k}\delta_{jl}\mathrm{d}d_{lk} + \bar{m}_{1i}\bar{m}_{1k}\delta_{jl}\mathrm{d}d_{lk}\right)\\
&\quad - \frac{1}{2}\left(\frac{1}{3}\mathrm{d}d_{mm}\bar{m}_{1i}\bar{m}_{1j} + \frac{1}{3}\mathrm{d}d_{mm}\bar{m}_{1i}\bar{m}_{1j} + \frac{1}{3}\mathrm{d}d_{mm}\bar{m}_{1i}\bar{m}_{1j} + \frac{1}{3}\mathrm{d}d_{mm}\bar{m}_{1i}\bar{m}_{1j}\right)\\
&\quad + \mathrm{d}w_{ik}\bar{m}_{1k}\bar{m}_{1j} - \bar{m}_{1i}\bar{m}_{1k}\mathrm{d}w_{kj}\\
&= \frac{1}{2}\left(\delta_{il}\bar{m}_{1k}\bar{m}_{1j} + \delta_{il}\bar{m}_{1k}\bar{m}_{1j} + \bar{m}_{1i}\bar{m}_{1k}\delta_{jl} + \bar{m}_{1i}\bar{m}_{1k}\delta_{jl}\right)\mathrm{d}d_{lk}\\
&\quad - \frac{1}{2}\left(\bar{m}_{1i}\bar{m}_{1j} + \bar{m}_{1i}\bar{m}_{1j} + \bar{m}_{1i}\bar{m}_{1j} + \bar{m}_{1i}\bar{m}_{1j}\right)\frac{1}{3}\mathrm{d}d_{mm} + \mathrm{d}w_{ik}\bar{m}_{1k}\bar{m}_{1j} - \bar{m}_{1i}\bar{m}_{1k}\mathrm{d}w_{kj}\\
&= \frac{1}{2}\left(\delta_{il}\bar{m}_{1k}\bar{m}_{1j} + \delta_{ik}\bar{m}_{1j}\bar{m}_{1l} + \bar{m}_{1i}\bar{m}_{1k}\delta_{jl} + \bar{m}_{1i}\bar{m}_{1l}\delta_{jk}\right)\mathrm{d}d_{kl}\\
&\quad - \frac{1}{2}\left(\delta_{kl}\delta_{il}\bar{m}_{1i}\bar{m}_{1k} + \delta_{kl}\delta_{ik}\bar{m}_{1j}\bar{m}_{1l} + \bar{m}_{1i}\bar{m}_{1k}\delta_{jl}\delta_{kl} + \bar{m}_{1i}\bar{m}_{1l}\delta_{jk}\delta_{kl}\right)\frac{1}{3}\mathrm{d}d_{mm}\\
&\quad + \mathrm{d}w_{ik}\bar{m}_{1k}\bar{m}_{1j} - \bar{m}_{1i}\bar{m}_{1k}\mathrm{d}w_{kj}\\
&= \frac{1}{2}\left(\delta_{il}\bar{m}_{1k}\bar{m}_{1j} + \bar{m}_{1i}\bar{m}_{1l}\delta_{jk} + \delta_{ik}\bar{m}_{1j}\bar{m}_{1l} + \bar{m}_{1i}\bar{m}_{1k}\delta_{jl}\right)\mathrm{d}d_{kl}\\
&\quad - \frac{1}{2}\left(\delta_{il}\bar{m}_{1j}\bar{m}_{1k} + \bar{m}_{1i}\bar{m}_{1l}\delta_{jk} + \delta_{ik}\bar{m}_{1j}\bar{m}_{1l} + \bar{m}_{1i}\bar{m}_{1k}\delta_{jl}\right)\frac{1}{3}\mathrm{d}d_{mm}\delta_{kl}\\
&\quad + \mathrm{d}w_{ik}\bar{m}_{1k}\bar{m}_{1j} - \bar{m}_{1i}\bar{m}_{1k}\mathrm{d}w_{kj}\\
&= \mathbb{A}_{1ijkl}\mathrm{d}d_{kl} - \mathbb{A}_{1ijkl}\frac{1}{3}\mathrm{d}d_{mm}\delta_{kl} + \mathrm{d}w_{ik}\bar{m}_{1k}\bar{m}_{1j} - \bar{m}_{1i}\bar{m}_{1k}\mathrm{d}w_{kj}\\
&= \mathbb{A}_{1ijkl}\left(\mathrm{d}d_{kl} - \frac{1}{3}\mathrm{d}d_{mm}\delta_{kl}\right) + \mathrm{d}w_{ik}\bar{m}_{1k}\bar{m}_{1j} - \bar{m}_{1i}\bar{m}_{1k}\mathrm{d}w_{kj}
\end{aligned}
\tag{A.23}
$$

$$\begin{aligned}\mathbb{A}_{1ijmm} &= \frac{1}{2}\left(\delta_{im}\bar{m}_{1j}\bar{m}_{1m} + \bar{m}_{1i}\bar{m}_{1m}\delta_{jm} + \delta_{im}\bar{m}_{1j}\bar{m}_{1m} + \bar{m}_{1i}\bar{m}_{1m}\delta_{jm}\right)\\ &= 2\bar{m}_{1i}\bar{m}_{1j}\end{aligned} \tag{A.24}$$

$$\begin{aligned}\mathrm{d}(\mathrm{div}\,\bar{m}_{1i}\bar{m}_{1j}) &= \mathrm{d}\left(\bar{m}_{1i}\bar{m}_{1j} - \frac{1}{3}\bar{I}_4\delta_{ij}\right)\\ &= \mathrm{d}\bar{m}_{1i}\bar{m}_{1j} - \frac{1}{3}\,\mathrm{d}\bar{I}_4\delta_{ij}\\ &= \mathbb{A}_{1ijkl}\left(\mathrm{d}d_{kl} - \frac{1}{3}\mathrm{d}d_{mm}\delta_{kl}\right) + \mathrm{d}w_{ik}\bar{m}_{1k}\bar{m}_{1j} - \bar{m}_{1i}\bar{m}_{1k}\mathrm{d}w_{kj}\\ &\quad - \frac{2}{3}\left[\bar{m}_{1k}\bar{m}_{1l} - \frac{1}{3}\bar{I}_4\delta_{kl}\right]\mathrm{d}d_{kl}\delta_{ij}\\ &= \mathbb{A}_{1ijkl}\left(\mathrm{d}d_{kl} - \frac{1}{3}\mathrm{d}d_{mm}\delta_{kl}\right) + \mathrm{d}w_{ik}\bar{m}_{1k}\bar{m}_{1j} - \bar{m}_{1i}\bar{m}_{1k}\mathrm{d}w_{kj}\\ &\quad - \frac{2}{3}\left(\delta_{ij}\bar{m}_{1k}\bar{m}_{1l} - \frac{1}{3}\bar{I}_4\delta_{ij}\delta_{kl}\right)\mathrm{d}d_{kl}\\ &= \mathbb{A}_{1ijkl}\mathrm{d}d_{kl} - \frac{1}{3}\mathbb{A}_{1ijmm}\delta_{kl}\mathrm{d}d_{kl} + \mathrm{d}w_{ik}\bar{m}_{1k}\bar{m}_{1j} - \bar{m}_{1i}\bar{m}_{1k}\mathrm{d}w_{kj}\\ &\quad - \frac{2}{3}\left(\delta_{ij}\bar{m}_{1k}\bar{m}_{1l} - \frac{1}{3}\bar{I}_4\delta_{ij}\delta_{kl}\right)\mathrm{d}d_{kl}\\ &= \mathbb{A}_{1ijkl}\mathrm{d}d_{kl} - \frac{2}{3}\bar{m}_{1i}\bar{m}_{1j}\delta_{kl}\mathrm{d}d_{kl} + \mathrm{d}w_{ik}\bar{m}_{1k}\bar{m}_{1j} - \bar{m}_{1i}\bar{m}_{1k}\mathrm{d}w_{kj}\\ &\quad - \frac{2}{3}\left(\delta_{ij}\bar{m}_{1k}\bar{m}_{1l} - \frac{1}{3}\bar{I}_4\delta_{ij}\delta_{kl}\right)\mathrm{d}d_{kl}\\ &= \left[\mathbb{A}_{1ijkl} - \frac{2}{3}\bar{m}_{1i}\bar{m}_{1j}\delta_{kl} - \frac{2}{3}\delta_{ij}\bar{m}_{1k}\bar{m}_{1l} - \frac{2}{9}\bar{I}_4\delta_{ij}\delta_{kl}\right]\mathrm{d}d_{kl}\\ &\quad + \mathrm{d}w_{ik}\bar{m}_{1k}\bar{m}_{1j} - \bar{m}_{1i}\bar{m}_{1k}\mathrm{d}w_{kj}\\ &= \left[\mathbb{A}_{1ijkl} - \frac{2}{3}\left(\bar{m}_{1i}\bar{m}_{1j}\delta_{kl} + \delta_{ij}\bar{m}_{1k}\bar{m}_{1l}\right) - \frac{2}{9}\bar{I}_4\delta_{ij}\delta_{kl}\right]\mathrm{d}d_{kl}\\ &\quad + \mathrm{d}w_{ik}\bar{m}_{1k}\bar{m}_{1j} - \bar{m}_{1i}\bar{m}_{1k}\mathrm{d}w_{kj}\end{aligned} \tag{A.25}$$

$$\begin{aligned}\mathrm{d}(\mathrm{div}\,\bar{m}_{2i}\bar{m}_{2j}) &= \left[\mathbb{A}_{2ijkl} - \frac{2}{3}\left(\bar{m}_{2i}\bar{m}_{2j}\delta_{kl} + \delta_{ij}\bar{m}_{2k}\bar{m}_{2l}\right) - \frac{2}{9}\bar{I}_6\delta_{ij}\delta_{kl}\right]\mathrm{d}d_{kl}\\ &\quad + \mathrm{d}w_{ik}\bar{m}_{2k}\bar{m}_{2j} - \bar{m}_{2i}\bar{m}_{2k}\mathrm{d}w_{kj}\end{aligned} \tag{A.26}$$

Appendix B

UMAT

The UMAT subroutine, to be used with ABAQUS, for residually stressed material with two preferred directions used in analysis of patient specific AAA is given below. Where preferred directions and residual stresses are defined as state variables for the UMAT.

```
C-----------------------------------------------------------------------
C----------------------------------UMAT---------------------------------
C-----------------------------------------------------------------------
      SUBROUTINE UMAT(STRESS, STATEV, DDSDDE, SSE, SPD, SCD, RPL,
     1 DDSDDT, DRPLDE, DRPLDT, STRAN, DSTRAN, TIME, DTIME, TEMP, DTEMP,
     2 PREDEF, DPRED, CMNAME, NDI, NSHR, NTENS, NSTATV, PROPS, NPROPS,
     3 COORDS, DROT, PNEWDT, CELENT, DFGRD0, DFGRD1, NOEL, NPT, LAYER,
     4 KSPT, KSTEP, KINC)
C
      INCLUDE 'ABA_PARAM.INC'
C
      CHARACTER*20 CMNAME
C
      DIMENSION STRESS(NTENS), STATEV(NSTATV), DDSDDE(NTENS, NTENS),
     1 DDSDDT(NTENS), DRPLDE(NTENS), STRAN(NTENS), DSTRAN(NTENS),
     2 PREDEF(1), DPRED(1), PROPS(NPROPS), COORDS(3), DROT(3, 3),
     3 DFGRD0(3, 3), DFGRD1(3, 3)
C
C-----------------------------------------------------------------
C    LOCAL ARRAY DESCRIPTION
C-----------------------------------------------------------------
C    BBAR = UNIMODULAR LEFT GREEN CAUCHY TENSOR
```

```
C    BBARD = DEV(BBAR)
C    DISTGR = UNIMDULAR DFORMATION GRADIANT
C    FR1 = FIBER 1 DIRECTION (REFERENCE)
C    FR2 = FIBER 2 DIRECTION (REFERENCE)
C    FC1 = FIBER 1 DIRECTION (CURRENT)
C    FC2 = FIBER 2 DIRECTION (CURRENT)
C    F1CF1 = FC1 TENSOR CROSS PRODUCT FC1 (FC1 X FC1)
C    F1CF1D = DEV(F1CF1)
C    F2CF2 = FC2 TENSOR CROSS PRODUCT FC2 (FC2 X FC2)
C    F2CF2D = DEV(FC2FC)
C    CI4 = I4 INVARIANT
C    CI6 = I6 INVRIANT
C    CI8 = I8 INVRIANT
C    H = FOURTH ORDER H TENSOR
C    A1 = FOURTH ORDER TENSOR FOR FIBER SET 1
C    A2 = FOURTH ORDER TENSOR FOR FIBER SET 2
C    A3 = FOURTH ORDER TENSOR FOR RESIDUAL STRESS
C-----------------------------------------------------------------
C
C    LOCAL ARRAY
C
      DIMENSION  FR1(3), FR2(3), DISTGR(3,3), FC1(3),
     1  FC2(3), F1CF1(6), F1CF1D(6), F2CF2(6), F2CF2D(6),
     2  BBAR(6), BBARD(6), CBAR(6), DEL(6), H(6,6), A1(6,6),
     3  A2(6,6), A3(6,6), TAU(6), SBAR(6), SBARD(6)
C
C
      PARAMETER(ZERO=0.D0, ONE=1.D0, TWO=2.D0, THREE=3.D0, FOUR=4.D0,
     1         SIX=6.D0, CNINE=9.D0, PI=3.141592653D0)
C
C -----------------------------------------------------------------
C    UMAT FOR  HYPERELASTICITY. CANNOT BE USED FOR PLANE STRESS
C    DESCRIPTION OF REQUIRED INPUT PARAMETERS ARE GIVEN BELOW.
C    FIBERS DIRECTION AND RESIDUAL STRESS MUST BE DEFINED USING
C    TWELVE STATE VARIABLES IN GLOBAL COORDINATES; FIRST THREE
C    FOR FIBER-1, FOUTH TO SIXTH FOR FIBER-2 AND LAST SIX FOR
C         RESIDUAL STRESS
C -----------------------------------------------------------------
C    PROPS(1) - ALPHA
```

```
C     PROPS(2) - EMU
C     PROPS(3) - ALPHA1
C     PROPS(4) - EMU1
C     PROPS(5) - FIBER1 ANGEL IN DEGREE (NOT USED HERE)
C     PROPS(6) - ALPHA2
C     PROPS(7) - EMU2
C     PROPS(8) - FIBER1 ANGEL IN DEGREE (NOT USED HERE)
C     PROPS(9) - D1 PARAMETER (SEE ABAQUS THEOTY MANUAL)
C -----------------------------------------------------------------
C
C     ELASTIC MATERIAL PROPERTIES
C
       ALPHA=PROPS(1)
       EMU=PROPS(2)
       ALPHA1 = PROPS(3)
       EMU1 = PROPS(4)
       F1ANG = PROPS(5)*PI/180.D0
       ALPHA2 = PROPS(6)
       EMU2 = PROPS(7)
       F2ANG = PROPS(8)*PI/180.D0
       D1=PROPS(9)
C
C     DEFINING FIBER-1 DIRECTION
C
       FR1(1) = STATEV(1)
       FR1(2) = STATEV(2)
       FR1(3) = STATEV(3)
C
C     DEFINING FIBER-2 DIRECTION
C
       FR2(1) = STATEV(4)
       FR2(2) = STATEV(5)
       FR2(3) = STATEV(6)
C
C     DEFINING RESIDUAL STRESS AND STORING IN FIRST INCREMENT (GLOBAL)
C
       TAU(1) = STATEV(7)
       TAU(2) = STATEV(8)
       TAU(3) = STATEV(9)
```

```
101       TAU(4) = STATEV(10)
102       TAU(5) = STATEV(11)
103       TAU(6) = STATEV(12)
104   C
105   C     JACOBIAN AND DISTORTION TENSOR
106   C
107       DET=DFGRD1(1, 1)*DFGRD1(2, 2)*DFGRD1(3, 3)
108      1 -DFGRD1(1, 2)*DFGRD1(2, 1)*DFGRD1(3, 3)
109       IF(NSHR.EQ.3) THEN
110         DET=DET+DFGRD1(1, 2)*DFGRD1(2, 3)*DFGRD1(3, 1)
111      1         +DFGRD1(1, 3)*DFGRD1(3, 2)*DFGRD1(2, 1)
112      2         -DFGRD1(1, 3)*DFGRD1(3, 1)*DFGRD1(2, 2)
113      3         -DFGRD1(2, 3)*DFGRD1(3, 2)*DFGRD1(1, 1)
114       END IF
115       SCALE=DET**(-ONE/THREE)
116       DO K1=1, 3
117         DO K2=1, 3
118           DISTGR(K2, K1)=SCALE*DFGRD1(K2, K1)
119         END DO
120       END DO
121   C
122   C     FIBER IN CURRENT DIRRECTION (FBAR-FC1) & (FBAR-FC2)
123   C
124       FC1(1) = DISTGR(1,1)*FR1(1) + DISTGR(1,2)*FR1(2)
125      1         + DISTGR(1,3)*FR1(3)
126       FC1(2) = DISTGR(2,1)*FR1(1) + DISTGR(2,2)*FR1(2)
127      1         + DISTGR(2,3)*FR1(3)
128       FC1(3) = DISTGR(3,1)*FR1(1) + DISTGR(3,2)*FR1(2)
129      1         + DISTGR(3,3)*FR1(3)
130       FC2(1) = DISTGR(1,1)*FR2(1) + DISTGR(1,2)*FR2(2)
131      1         + DISTGR(1,3)*FR2(3)
132       FC2(2) = DISTGR(2,1)*FR2(1) + DISTGR(2,2)*FR2(2)
133      1         + DISTGR(2,3)*FR2(3)
134       FC2(3) = DISTGR(3,1)*FR2(1) + DISTGR(3,2)*FR2(2)
135      1         + DISTGR(3,3)*FR2(3)
136   C
137   C     DEFINING F1CF1 TENSOR
138   C
139       F1CF1(1) = FC1(1)**2
```

```
      F1CF1(2) = FC1(2)**2
      F1CF1(3) = FC1(3)**2
      F1CF1(4) = FC1(1)*FC1(2)
      F1CF1(5) = FC1(1)*FC1(3)
      F1CF1(6) = FC1(2)*FC1(3)
C
C    DEFINING F1CF1D TENSOR  (DEVIATORIC)
C
      TF1CF1 = F1CF1(1)+F1CF1(2)+F1CF1(3)
      F1CF1D(1) = F1CF1(1)-TF1CF1/THREE
      F1CF1D(2) = F1CF1(2)-TF1CF1/THREE
      F1CF1D(3) = F1CF1(3)-TF1CF1/THREE
      F1CF1D(4) = F1CF1(4)
      F1CF1D(5) = F1CF1(5)
      F1CF1D(6) = F1CF1(6)
C
C    DEFINING F2CF2 TENSOR
C
      F2CF2(1) = FC2(1)**2
      F2CF2(2) = FC2(2)**2
      F2CF2(3) = FC2(3)**2
      F2CF2(4) = FC2(1)*FC2(2)
      F2CF2(5) = FC2(1)*FC2(3)
      F2CF2(6) = FC2(2)*FC2(3)
C
C    DEFINING F2CF2D TENSOR (DEVIATORIC)
C
      TF2CF2 = F2CF2(1)+F2CF2(2)+F2CF2(3)
      F2CF2D(1) = F2CF2(1)-TF2CF2/THREE
      F2CF2D(2) = F2CF2(2)-TF2CF2/THREE
      F2CF2D(3) = F2CF2(3)-TF2CF2/THREE
      F2CF2D(4) = F2CF2(4)
      F2CF2D(5) = F2CF2(5)
      F2CF2D(6) = F2CF2(6)
C
C    CALCULATE ISO LEFT CAUCHY-GREEN DEFORMATION TENSOR
C
      BBAR(1)=DISTGR(1, 1)**2+DISTGR(1, 2)**2+DISTGR(1, 3)**2
      BBAR(2)=DISTGR(2, 1)**2+DISTGR(2, 2)**2+DISTGR(2, 3)**2
```

```
      BBAR(3)=DISTGR(3, 3)**2+DISTGR(3, 1)**2+DISTGR(3, 2)**2
      BBAR(4)=DISTGR(1, 1)*DISTGR(2, 1)+DISTGR(1, 2)*DISTGR(2, 2)
     1       +DISTGR(1, 3)*DISTGR(2, 3)
      IF(NSHR.EQ.3) THEN
        BBAR(5)=DISTGR(1, 1)*DISTGR(3, 1)+DISTGR(1, 2)*DISTGR(3, 2)
     1         +DISTGR(1, 3)*DISTGR(3, 3)
        BBAR(6)=DISTGR(2, 1)*DISTGR(3, 1)+DISTGR(2, 2)*DISTGR(3, 2)
     1         +DISTGR(2, 3)*DISTGR(3, 3)
      END IF
C
C    DEFINING BBARD = DEV(BBAR)  (DEVIATORIC)
C
      TRBBAR=(BBAR(1)+BBAR(2)+BBAR(3))
      BBARD(1)= BBAR(1)-TRBBAR/THREE
      BBARD(2)= BBAR(2)-TRBBAR/THREE
      BBARD(3)= BBAR(3)-TRBBAR/THREE
      BBARD(4)= BBAR(4)
      BBARD(5)= BBAR(5)
      BBARD(6)= BBAR(6)
C
C    CALCULATE ISO RIGHT CAUCHY-GREEN DEFORMATION TENSOR
C
      CBAR(1)=DISTGR(1, 1)**2+DISTGR(2, 1)**2+DISTGR(3, 1)**2
      CBAR(2)=DISTGR(1, 2)**2+DISTGR(2, 2)**2+DISTGR(3, 2)**2
      CBAR(3)=DISTGR(3, 3)**2+DISTGR(1, 3)**2+DISTGR(2, 3)**2
      CBAR(4)=DISTGR(1, 1)*DISTGR(1, 2)+DISTGR(2, 1)*DISTGR(2, 2)
     1       +DISTGR(3, 1)*DISTGR(3, 2)
      IF(NSHR.EQ.3) THEN
        CBAR(5)=DISTGR(1, 1)*DISTGR(1, 3)+DISTGR(2, 1)*DISTGR(2, 3)
     1         +DISTGR(3, 1)*DISTGR(3, 3)
        CBAR(6)=DISTGR(1, 2)*DISTGR(1, 3)+DISTGR(2, 2)*DISTGR(2, 3)
     1         +DISTGR(3, 2)*DISTGR(3, 3)
      END IF
C
C    SBAR (RESIDUAL STRESS FBAR-TAU-FBART)
C
      SBAR(1) = DISTGR(1, 1)*(DISTGR(1, 1)*TAU(1)+DISTGR(1, 2)*TAU(4)
     1        + DISTGR(1, 3)*TAU(5))
     2        + DISTGR(1, 2)*(DISTGR(1, 1)*TAU(4)+DISTGR(1, 2)*TAU(2)
```

```
     3        + DISTGR(1, 3)*TAU(6))
     4        + DISTGR(1, 3)*(DISTGR(1, 1)*TAU(5)+DISTGR(1, 2)*TAU(6)
     5        + DISTGR(1, 3)*TAU(3))
      SBAR(2) = DISTGR(2, 1)*(DISTGR(2, 1)*TAU(1)+DISTGR(2, 2)*TAU(4)
     1        + DISTGR(2, 3)*TAU(5))
     2        + DISTGR(2, 2)*(DISTGR(2, 1)*TAU(4)+DISTGR(2, 2)*TAU(2)
     3        + DISTGR(2, 3)*TAU(6))
     4        + DISTGR(2, 3)*(DISTGR(2, 1)*TAU(5)+DISTGR(2, 2)*TAU(6)
     5        + DISTGR(2, 3)*TAU(3))
      SBAR(3) = DISTGR(3, 1)*(DISTGR(3, 1)*TAU(1)+DISTGR(3, 2)*TAU(4)
     1        + DISTGR(3, 3)*TAU(5))
     2        + DISTGR(3, 2)*(DISTGR(3, 1)*TAU(4)+DISTGR(3, 2)*TAU(2)
     3        + DISTGR(3, 3)*TAU(6))
     4        + DISTGR(3, 3)*(DISTGR(3, 1)*TAU(5)+DISTGR(3, 2)*TAU(6)
     5        + DISTGR(3, 3)*TAU(3))
      SBAR(4) = DISTGR(2, 1)*(DISTGR(1, 1)*TAU(1)+DISTGR(1, 2)*TAU(4)
     1        + DISTGR(1, 3)*TAU(5))
     2        + DISTGR(2, 2)*(DISTGR(1, 1)*TAU(4)+DISTGR(1, 2)*TAU(2)
     3        + DISTGR(1, 3)*TAU(6))
     4        + DISTGR(2, 3)*(DISTGR(1, 1)*TAU(5)+DISTGR(1, 2)*TAU(6)
     5        + DISTGR(1, 3)*TAU(3))
      SBAR(5) = DISTGR(3, 1)*(DISTGR(1, 1)*TAU(1)+DISTGR(1, 2)*TAU(4)
     1        + DISTGR(1, 3)*TAU(5))
     2        + DISTGR(3, 2)*(DISTGR(1, 1)*TAU(4)+DISTGR(1, 2)*TAU(2)
     3        + DISTGR(1, 3)*TAU(6))
     4        + DISTGR(3, 3)*(DISTGR(1, 1)*TAU(5)+DISTGR(1, 2)*TAU(6)
     5        + DISTGR(1, 3)*TAU(3))
      SBAR(6) = DISTGR(3, 1)*(DISTGR(2, 1)*TAU(1)+DISTGR(2, 2)*TAU(4)
     1        + DISTGR(2, 3)*TAU(5))
     2        + DISTGR(3, 2)*(DISTGR(2, 1)*TAU(4)+DISTGR(2, 2)*TAU(2)
     3        + DISTGR(2, 3)*TAU(6))
     4        + DISTGR(3, 3)*(DISTGR(2, 1)*TAU(5)+DISTGR(2, 2)*TAU(6)
     5        + DISTGR(2, 3)*TAU(3))
C
C    SBARD (DEVIATORIC OF SBAR)
C
      TSBAR = SBAR(1)+SBAR(2)+SBAR(3)
      SBARD(1) = SBAR(1)-TSBAR/THREE
      SBARD(2) = SBAR(2)-TSBAR/THREE
```

```
257       SBARD(3) = SBAR(3)-TSBAR/THREE
258       SBARD(4) = SBAR(4)
259       SBARD(5) = SBAR(5)
260       SBARD(6) = SBAR(6)
261   C
262   C    INVARIANT I4
263   C
264       CI4 = FR1(1)*(CBAR(1)*FR1(1)+CBAR(4)*FR1(2)+CBAR(5)*FR1(3))
265      1     +FR1(2)*(CBAR(4)*FR1(1)+CBAR(2)*FR1(2)+CBAR(6)*FR1(3))
266      2     +FR1(3)*(CBAR(5)*FR1(1)+CBAR(6)*FR1(2)+CBAR(3)*FR1(3))
267
268   C    FIBER CANNOT GO IN COMPRESSION
269       IF(CI4 .LT. ONE) CI4=ONE
270   C
271   C    INVARIANT I6
272   C
273       CI6 = FR2(1)*(CBAR(1)*FR2(1)+CBAR(4)*FR2(2)+CBAR(5)*FR2(3))
274      1     +FR2(2)*(CBAR(4)*FR2(1)+CBAR(2)*FR2(2)+CBAR(6)*FR2(3))
275      2     +FR2(3)*(CBAR(5)*FR2(1)+CBAR(6)*FR2(2)+CBAR(3)*FR2(3))
276   C
277   C    FIBER CANNOT GO IN COMPRESSION
278       IF(CI6 .LT. ONE) CI6=ONE
279   C
280   C    INVARIANT I8
281   C
282       CI8 = CBAR(1)*TAU(1)+CBAR(2)*TAU(2)+CBAR(3)*TAU(3)
283      1     +TWO*(CBAR(4)*TAU(4)+CBAR(5)*TAU(5)+CBAR(6)*TAU(6))
284   C
285   C    CALCULATE THE STRESS
286   C
287   C    W1J = PARTIAL DERIVATIVES OF W RESPECT TO I1, OVER J
288   C    W11J = PARTIAL DERIVATIVES OF W1 RESPECT TO I1, OVER J
289
290   C    USE ONLY ONE BASE MATRIX MODEL (EXPONENTIAL/NEOHOOKEAN)
291   C    TURN OF OTHER BY COMMENTING OUT
292
293   C    EXPONENTIAL BASE MATRIX MODEL
294       W1J=EMU*EXP(ALPHA*(TRBBAR-THREE))/(TWO*DET)
295       W11J=EMU*ALPHA*EXP(ALPHA*(TRBBAR-THREE))/(TWO*DET)
```

```
C
C    NEOHOOKEAN BASE MATRIX MODEL
C      W1J = EMU/(TWO*DET)
C      W11J = ZERO

       W4J=EMU1*(CI4-ONE)*EXP(ALPHA1*(CI4-ONE)**2)/DET
       W44J=(TWO*EMU1*ALPHA1*(CI4-ONE)**2*EXP(ALPHA1*(CI4-ONE)**2)
     1      +EMU1*EXP(ALPHA1*(CI4-ONE)**2))/DET
       W6J=EMU2*(CI6-ONE)*EXP(ALPHA2*(CI6-ONE)**2)/DET
       W66J=(TWO*EMU2*ALPHA2*(CI6-ONE)**2*EXP(ALPHA2*(CI6-ONE)**2)
     1     +EMU2*EXP(ALPHA2*(CI6-ONE)**2))/DET
       W8J = ONE/(TWO*DET)
       EK=TWO/D1*(TWO*DET-ONE)
       PR=TWO*(DET-ONE)/D1
C        EK = TWO*DET/D1
C        PR = (DET-ONE/DET)/D1
       DO K1=1,NDI
         STRESS(K1)=TWO*(W1J*BBARD(K1)+W4J*F1CF1D(K1)
     1             +W6J*F2CF2D(K1)+W8J*SBARD(K1))+PR
       END DO
       DO K1=NDI+1,NDI+NSHR
         STRESS(K1)=TWO*(W1J*BBARD(K1)+W4J*F1CF1D(K1)
     1             +W6J*F2CF2D(K1)+W8J*SBARD(K1))
       END DO
C
C    DEFINING A UNIT TENSOR DEL
C
       DEL(1) = ONE
       DEL(2) = ONE
       DEL(3) = ONE
       DEL(4) = ZERO
       DEL(5) = ZERO
       DEL(6) = ZERO
C
C    CALCULATION OF FORTH ORDER H TENSOR
C

       DO K1 = 1,3
         DO K2 = 1,3
```

```
335           DO K3 = 1,3
336             DO K4 = 1,3
337                IF (K1 .EQ. K2) THEN
338                  K5 = K1
339                ELSE
340                  K5 = K1+K2+1
341                END IF
342                IF (K3 .EQ. K4) THEN
343                  K6 = K3
344                ELSE
345                  K6 = K3+K4+1
346                END IF
347                IF (K1 .EQ. K3) THEN
348                  K7 = K1
349                ELSE
350                  K7 = K1+K3+1
351                END IF
352                IF (K2 .EQ. K4) THEN
353                  K8 = K2
354                ELSE
355                  K8 = K2+K4+1
356                END IF
357                IF (K1 .EQ. K4) THEN
358                  K9 = K1
359                ELSE
360                  K9 = K1+K4+1
361                END IF
362                IF (K2 .EQ. K3) THEN
363                  K10 = K2
364                ELSE
365                  K10 = K2+K3+1
366                END IF
367
368                   H(K5,K6) = (DEL(K7)*BBAR(K8)+DEL(K8)*BBAR(K7)
369       1             +DEL(K9)*BBAR(K10)+DEL(K10)*BBAR(K9))/TWO
370             END DO
371           END DO
372         END DO
373       END DO
```

```
C
C    CALCULATION OF FORTH ORDER A1 TENSOR FIBER SET ONE
C
      DO K1 = 1,3
        DO K2 = 1,3
          DO K3 = 1,3
            DO K4 = 1,3
               IF (K1 .EQ. K2) THEN
                 K5 = K1
               ELSE
                 K5 = K1+K2+1
               END IF
               IF (K3 .EQ. K4) THEN
                 K6 = K3
               ELSE
                 K6 = K3+K4+1
               END IF
               IF (K1 .EQ. K3) THEN
                 K7 = K1
               ELSE
                 K7 = K1+K3+1
               END IF
               IF (K2 .EQ. K4) THEN
                 K8 = K2
               ELSE
                 K8 = K2+K4+1
               END IF
               IF (K1 .EQ. K4) THEN
                 K9 = K1
               ELSE
                 K9 = K1+K4+1
               END IF
               IF (K2 .EQ. K3) THEN
                 K10 = K2
               ELSE
                 K10 = K2+K3+1
               END IF

                  A1(K5,K6) = (DEL(K7)*F1CF1(K8)+DEL(K8)*F1CF1(K7)
```

```
     1              +DEL(K9)*F1CF1(K10)+DEL(K10)*F1CF1(K9))/TWO
            END DO
          END DO
        END DO
       END DO
C
C    CALCULATION OF FORTH ORDER A2 TENSOR FIBER SET TWO
C
       DO K1 = 1,3
         DO K2 = 1,3
           DO K3 = 1,3
             DO K4 = 1,3
                IF (K1 .EQ. K2) THEN
                  K5 = K1
                ELSE
                  K5 = K1+K2+1
                END IF
                IF (K3 .EQ. K4) THEN
                  K6 = K3
                ELSE
                  K6 = K3+K4+1
                END IF
                IF (K1 .EQ. K3) THEN
                  K7 = K1
                ELSE
                  K7 = K1+K3+1
                END IF
                IF (K2 .EQ. K4) THEN
                  K8 = K2
                ELSE
                  K8 = K2+K4+1
                END IF
                IF (K1 .EQ. K4) THEN
                  K9 = K1
                ELSE
                  K9 = K1+K4+1
                END IF
                IF (K2 .EQ. K3) THEN
                  K10 = K2
```

```
452                ELSE
453                  K10 = K2+K3+1
454                END IF
455
456                   A2(K5,K6) = (DEL(K7)*F2CF2(K8)+DEL(K8)*F2CF2(K7)
457     1              +DEL(K9)*F2CF2(K10)+DEL(K10)*F2CF2(K9))/TWO
458              END DO
459            END DO
460          END DO
461        END DO
462
463 C
464 C    CALCULATION OF FORTH ORDER A3 TENSOR FOR RESIDUAL
465 C
466        DO K1 = 1,3
467          DO K2 = 1,3
468            DO K3 = 1,3
469              DO K4 = 1,3
470                IF (K1 .EQ. K2) THEN
471                  K5 = K1
472                ELSE
473                  K5 = K1+K2+1
474                END IF
475                IF (K3 .EQ. K4) THEN
476                  K6 = K3
477                ELSE
478                  K6 = K3+K4+1
479                END IF
480                IF (K1 .EQ. K3) THEN
481                  K7 = K1
482                ELSE
483                  K7 = K1+K3+1
484                END IF
485                IF (K2 .EQ. K4) THEN
486                  K8 = K2
487                ELSE
488                  K8 = K2+K4+1
489                END IF
490                IF (K1 .EQ. K4) THEN
```

```
                  K9 = K1
                ELSE
                  K9 = K1+K4+1
                END IF
                IF (K2 .EQ. K3) THEN
                  K10 = K2
                ELSE
                  K10 = K2+K3+1
                END IF

                   A3(K5,K6) = (DEL(K7)*SBAR(K8)+DEL(K8)*SBAR(K7)
     1             +DEL(K9)*SBAR(K10)+DEL(K10)*SBAR(K9))/TWO
            END DO
          END DO
        END DO
       END DO
C
C    CALCULATE THE STIFFNESS
C
C
C    CALCULATION OF FORTH ORDER DDSDDE TENSOR
C

       DO K1 = 1,3
         DO K2 = 1,3
           DO K3 = 1,3
             DO K4 = 1,3
                IF (K1 .EQ. K2) THEN
                  K5 = K1
                ELSE
                  K5 = K1+K2+1
                END IF
                IF (K3 .EQ. K4) THEN
                  K6 = K3
                ELSE
                  K6 = K3+K4+1
                END IF
                   DDSDDE(K5,K6) = FOUR*W11J*BBARD(K5)*BBARD(K6)+
     1             FOUR*W44J*F1CF1D(K5)*F1CF1D(K6)+
```

```
     2            FOUR*W66J*F2CF2D(K5)*F2CF2D(K6)+
     3            TWO*W1J*(H(K5,K6)-TWO*(DEL(K5)*BBAR(K6)+
     4              BBAR(K5)*DEL(K6))/THREE+
     5              TWO*TRBBAR*DEL(K5)*DEL(K6)/CNINE)+
     6            TWO*W4J*(A1(K5,K6)-TWO*(DEL(K5)*F1CF1(K6)+
     7              F1CF1(K5)*DEL(K6))/THREE+
     8              TWO*CI4*DEL(K5)*DEL(K6)/CNINE)+
     9            TWO*W6J*(A2(K5,K6)-TWO*(DEL(K5)*F2CF2(K6)+
     1              F2CF2(K5)*DEL(K6))/THREE+
     2              TWO*CI6*DEL(K5)*DEL(K6)/CNINE)+
     3            TWO*W8J*(A3(K5,K6)-TWO*(DEL(K5)*SBAR(K6)+
     4              SBAR(K5)*DEL(K6))/THREE+
     5              TWO*CI8*DEL(K5)*DEL(K6)/CNINE)

              IF (K5 .LT. 4 .AND. K6 .LT. 4) THEN
                 DDSDDE(K5,K6) = DDSDDE(K5,K6)+EK
              END IF
           END DO
         END DO
       END DO
     END DO

     RETURN
     END
```